TSO2020 Activity 2:
Stability Analysis of an International Electricity System connected to Regional and Local Sustainable Gas Systems

Final Report

dr.ir. José L. Rueda Torres
dr.ir. Bart W. Tuinema
dr.ir. M. Ebrahim Adabi
dr.ir. Zameer Ahmad
ir. Víctor García Suárez
ir. Patrick K.S. Ayivor
ir. N. Veera Kumar
ir. Lian Liu
ir. Arcadio Perilla
ir. Feras A. Alshehri
dr.ir. Marjan Popov
dr.ir. Alex Stefanov
prof.dr. Arno Smets
prof.dr. Peter Palensky
prof.ir. Mart A.M.M. van der Meijden

16 December 2019

Intelligent Electrical Power Grids
Department of Electrical Sustainable Energy
Faculty of Electrical Engineering, Mathematics and Computer Science
Delft University of Technology

This work has received funding from the European Union's Connecting Europe Facility (CEF) programme under the grant agreement No INEA/CEF/SYN/A2016/1336043 – TSO2020 Project (Electric "Transmission and Storage Options" along TEN-E and TEN-T corridors for 2020). This report reflects only the authors' views and the European Commission is not responsible for any use that may be made of the information it contains.

Executive Summary

In the transition of the electrical power system towards a more sustainable energy supply, conventional generation is gradually being replaced by Renewable Energy Sources (RES). The integration of RES leads to various challenges in the planning and operation of power systems. For example, when the amount of conventional generation decreases, the inertia of the power system reduces, making the power system more prone to frequency instability. In practice, operation of the power system is secured, in part, by the provision of electrical ancillary services like frequency balancing, voltage support and congestion management. As conventional generators traditionally are the main providers of these ancillary services, alternatives are currently being searched for.

A promising alternative can be found in Power-to-Gas (P2G) technology and electrolysers. In electrolysers, water is converted into hydrogen and oxygen by electrolysis, thereby converting electrical energy into chemical energy. Hydrogen can be converted back to electricity by fuels cells, but also offers the possibility to be used as fuel in the transport system and in industries. As electrolysers are able to vary their power consumption relatively fast, electrolysers can respond to electrical disturbances in the power system within a short time. TSO2020 considers the installation of a 1-MW pilot electrolyser in Veendam-Zuidwending and a theoretical 300-MW electrolyser in Eemshaven, together with the potential participation in ancillary services provision. Activity 2 of TSO2020 studies the impact of electrolysers on power system stability and the practical implementation of control approaches for the provision of ancillary services.

Activity 2 of TSO2020 started with an analysis of the current regulations for ancillary services provision. The work continued with the development of a model of a 1-MW electrolyser equipped with frequency and voltage controllers to support the stability of the local transmission network. The performance of this electrolyser in a power system was simulated and analysed by using a reduced size model of the electrical transmission network in Veendam-Zuidwending. The electrolyser model was then scaled up to represent a large 300-MW electrolyser. A test model of the northern part of the Dutch transmission network was developed and various simulations were performed to study the impact of a large-scale electrolyser in an interconnected power system. The study was completed by the development of control approaches that enable electrolysers to participate in the provision of electrical ancillary services.

The conclusions of this report can be summarised as follows:

- Due to their fast dynamics, electrolysers are a promising solution for frequency balancing. Electrolysers can prioritise in short-term frequency support like Frequency Containment Reserve (FCR), possibly followed by participation in mid-term frequency support like Automatic Frequency Restoration Reserve (aFRR). When installed in an area in need of voltage control or congestion management, electrolysers could also be deployed for these purposes as well. This followed from the electrical ancillary services market review described in Section 2.2.
- The developed electrolyser model is able to accurately replicate the behaviour of a real, MW-scale electrolyser, as comparison with literature data and field measurements of the 1-MW electrolyser located in Veendam-Zuidwending shows (Chapter 3).

- Simulations of the 300-MW electrolyser in the test model of the Northern Netherlands Network show that a large electrolyser can have a positive effect on frequency stability when participating in FCR, as electrolysers are able to ramp up/down their power consumption faster than conventional generators (Section 4.4.1). In order to ramp up or down its consumption when needed, an electrolyser should operate between a certain minimum (larger than 0) and maximum (smaller than rated) level. Frequency control by HVDC connections, in this study considering a hypothetical case with COBRAcable, also has a positive impact, but relatively smaller than the electrolyser. This can be attributed to the assumed smaller ramp rate of COBRAcable in the simulations.
- Although not the case in the studied test model of Northern Netherlands Network, electrolysers can improve local voltage stability in more remote areas with less voltage support by other facilities (Section 4.4.2 and Appendix D). A certain capacity of the converter must then be reserved for this purpose, which means either operation at a capacity smaller than rated or an over-dimensioned electrolyser converter.
- Although congestion issues are not foreseen in the studied test model of Northern Netherlands Network under the considered operational scenarios, electrolysers can possibly contribute to congestion management by varying their consumption (Section 4.4.3 and Appendix D). Electrolysers could also reduce the variability of renewable generation like offshore wind by absorbing short-term variations.
- It is expected that electrolysers can easily comply with the FCR prequalification tests because of their fast ramping capabilities. Electrolysers could even participate in faster frequency support ancillary services, like Enhanced Frequency Response (EFR) in the UK (Section 5.2).
- Three control approaches of Fast Active Power-frequency Regulation (FAPR) by electrolysers are proposed: droop-based control, combined derivative-droop-based control and Virtual Synchronous Power (VSP)-based control. Combined derivative-droop-based control is faster than droop-based control, as it also responds to the Rate-of-Change-of-Frequency (RoCoF), thereby anticipating possible large frequency deviations. VSP-based control compares the power required with the reference power available at a bus to determine how much the electrolyser should vary its active power consumption. In this way, frequency measurement ambiguities (e.g. an error in the frequency estimation) can be eliminated completely. Simulations show that VSP-based control results in the best frequency response of the three proposed control strategies (Section 5.3).

The studies described in this report generally show that electrolysers hold promising potential for participation in ancillary services in the future power system. This is mainly because of their fast ramping capabilities in comparison to conventional generators. Although electrolysers could contribute to local voltage stability and congestion management, the results provided in the study of this report show that their main potential is in the provision of frequency support, especially in the short term (e.g. FCR or EFR). When equipped with the appropriate controllers (like VSP-based FAPR), electrolysers are able to respond relatively quickly to disturbances of the power system frequency, thereby positively contributing to effectively reduce frequency excursions.

Contents

Abbreviations

AC	Alternating Current
AEM	Anion Exchange Membrane
aFRR	Automatic Frequency Restoration Reserve
AVR	Automatic Voltage Regulation
B2B	Back-to-Back
BESS	Battery Energy Storage System
BoP	Balance of Plant
BPMS	Battery Power Management System
CAPEX	Capital Expenditure
CBA	Cost-Benefit Analysis
CHIL	Control Hardware-in-the-Loop
CIPC	Circular Inter-Process Communication
DC	Direct Current
DSR	Demand Side Response
DUT	Device Under Test
EFR	Enhanced Frequency Response
EMT	Electromagnetic Transient
FACTS	Flexible AC Transmission Systems
FAPR	Fast Active Power-frequency Regulation
FCR	Frequency Containment Reserve
FEC	Front End Controller
HIL	Hardware-in-the-Loop
HVDC	High-Voltage Direct Current
IE	Inertia Emulation
IGCC	International Grid Control Cooperation
LCC	Line-Commutated Converter
mFRR	Manual Frequency Restoration Reserve
N3	Northern Netherlands Network
OCV	Open-Cell Voltage
OPEX	Operational Expenditure
P2G	Power to Gas
PCC	Point of Common Coupling
PE	Power Electronics
PEM	Proton Exchange Membrane (Polymer Electrolyte Membrane)
PHIL	Power Hardware-in-the-Loop
PTU	Programme Time Unit
PV	Photovoltaics
RES	Renewable Energy Source
RMS	Root Mean Square
RTDS	Real-Time Digital Simulator

RTT	Real Time Target
SOE	Solid Oxide Electrolyser
THD	Total Harmonic Distortion
TSO	Transmission System Operator
VSC	Voltage Source Converter
VSP	Virtual Synchronous Power

1 Introduction

1.1 Motivation

In the transition towards a more renewable energy supply, various new technologies are currently being investigated. In the generation of electricity, the share of offshore wind and solar photovoltaics is already increasing continuously. At the same time, industries, households and the transport system are searching for alternatives for fossil fuels like natural gas. In this context, a highly promising synergy between electric power systems and natural gas systems is created in the form of hydrogen. In electrolysers, water is converted into hydrogen and oxygen by electrolysis, thereby converting electrical energy into chemical energy. Hydrogen can be converted back to electricity by fuels cells, but also offers the possibility to be used as fuel in the transport system and in industries. Hydrogen can even be converted to syngas and be used by industries and households. As hydrogen can be stored for longer periods, electrolysis solves the issue of long-term electricity storage, which can effectively be applied to absorb excess electricity from fluctuating renewable sources like large-scale offshore wind.

Electrolysers also hold potential to support the operation of the power system by participating in electrical ancillary services. Electrical Transmission System Operators (TSOs) are challenged on a daily basis by various operational challenges like maintaining a stable system frequency and voltage. The transition towards a more renewable electricity supply even increases this challenge as conventional generators traditionally are the devices that control these variables. Support of the power system operation is organised in ancillary services like frequency and voltage support, in which (conventional and renewable) generators, but also large loads (Demand Side Response, DSR), can participate. Because of their fast ramping capability, electrolysers are a promising technology for the provision of ancillary services. From an electrolyser owner's point of view, participation in ancillary services could be an added value to the business case as revenues from hydrogen trade can be supplemented by the income from ancillary services participation.

In the context of the European Synergy Action TSO2020 project, a pilot 1-MW PEM electrolyser is installed in Veendam-Zuidwending (Groningen, Netherlands). It is assumed that a large-scale electrolyser plant of 300 MW will be installed within the same area at Eemshaven in the future. Integrating large-scale electrolysers requires good understanding of their interactions with the existing power system. This understanding can be facilitated with accurate models of electrolysers and power systems. The challenge is that models of large-scale (>1 MW) electrolysers are currently not available in literature, such that these models need to be developed specifically. By developing models and performing real-time simulations, the performance of electrolysers needs to be analysed and the capabilities of electrolysers to participate in ancillary services need to be investigated.

1.2 TSO2020 and the Scope of Activity 2

The European Synergy Action TSO2020 considers the interplay between electricity and gas systems. Part of the project is the installation of a 1-MW pilot electrolyser at Veendam (Groningen, Netherlands), which serves as a case study to analyse the performance of electrolysers in an electrical power system. A large-scale electrolyser of 300 MW is assumed to be installed in the Eemshaven region in the future. A Cost-Benefit Analysis (CBA) is performed to study the viability of this project. Electrical modelling and real-time simulation are performed to analyse the behaviour of the electrolysers in the power system. In addition, the possibilities of the electrolysers to participate in the provision of ancillary services are investigated.

TSO2020 is divided over several activities [1], as also illustrated in Figure 1.1:

- **Activity 1**: General coordination of the action;
- **Activity 2**: Stability study of international electricity systems;
- **Activity 3**: Cost-Benefit Analysis (CBA) modelling;
- **Activity 4**: Zuidwending Pilot and Delfzijl Hydrogen Hub;
- **Activity 5**: Analysis of scale-up to mass application (business plan);
- **Activity 6**: Dissemination and engagement.

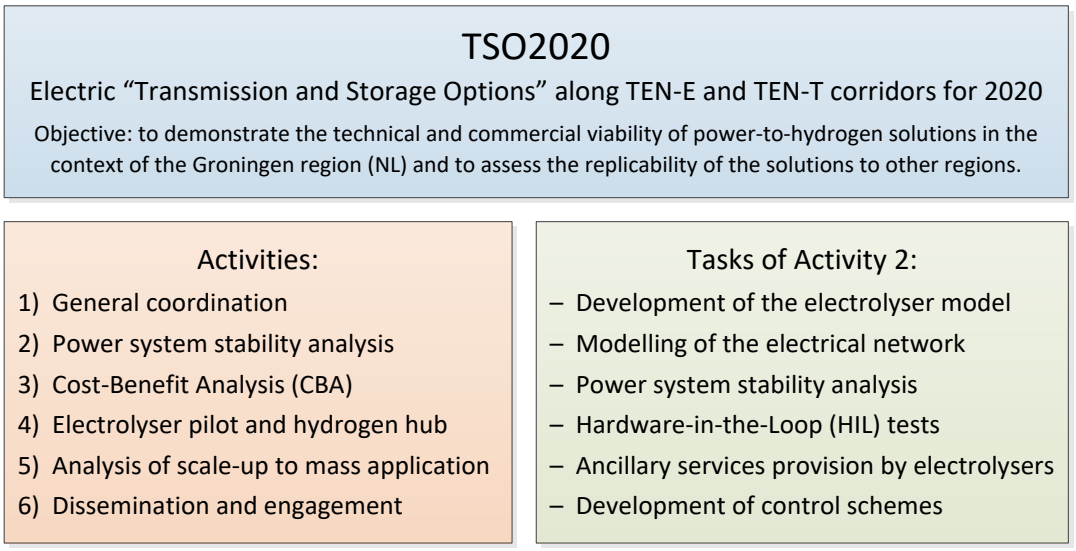

Figure 1.1: Activities of the TSO2020 project and tasks of Activity 2 (based on [1]).

Activity 2 of TSO2020 is performed by Delft University of Technology and considers the analysis of the performance of electrolysers in the electrical power system. Activity 2 thereby studies the dynamic interaction between international electrical transmission networks connected to regional and local sustainable gas systems and the large-scale demand side response associated to power-to-gas conversion. By electrical network modelling and real-time simulation, the impact of electrolysers on the stability of the power system is studied and the possibilities of supporting this power system stability by the provision of ancillary services are investigated.

The precise objective of Activity 2 within TSO2020 is to determine the impact on the stability of the electrical power grid of [1]: (i) the electrolyser and hydrogen storage system in Zuidwending and Eemshaven; and (ii) the dispatch of renewable power in relation to the cross-border exchange of electrical energy and ancillary services by COBRAcable and the electrolyser. Ancillary services refer to frequency control, voltage control, and reduction of congestion in the electrical grid. This creates an effective interconnection between the electricity and gas grid to support clean transport.

The work of Activity 2 is divided over several tasks [1], as also shown in Figure 1.1:

- analysing the impact of an electrolyser at the EnergyStock location in Zuidwending on the grid operation and stability of the Groningen region;
- analysing the impact of a larger electrolyser installation at Eemshaven on the grid operation and stability of the Groningen region and COBRAcable;
- power Hardware-in-the-Loop (HIL) tests by connecting real equipment (controller of electrolyser) to a Real-Time Digital Simulator (RTDS);
- investigation of the degree of flexibility and the volume of ancillary services that can be provided by the electrolyser/storage system in Zuidwending and Eemshaven;
- designing the necessary control schemes to enable the provision of ancillary services and providing recommendations for the exploitation of these ancillary services.

This report is the Deliverable of Activity 2 of TSO2020 and were presented in the workshop about the results of Activity 2 (i.e. Milestone 15), which took place at TU Delft on 11 December 2019.

1.3 Outline of this Report

This report starts with a discussion of ancillary services in Chapter 2. An overview is given of the various ancillary services that are applied to secure the operation of the power system. A review of the current and expected future regulations is made and the possibilities of electrolysers to participate in these ancillary services are discussed. Chapter 3 describes the case study of the 1-MW pilot electrolyser at Veendam-Zuidwending. The development of an electrolyser for real-time simulations is discussed, together with its validation against field measurements of the pilot electrolyser. The response of the electrolyser to various disturbances that affect the dynamic behaviour (i.e. stability) of the electrical network is analysed as well. Chapter 4 discusses the case study of a 300-MW electrolyser plant located at Eemshaven substation. This study includes the development of the network model of the Northern Netherlands for real-time simulation and a scale-up of the developed electrolyser model. The capabilities of this electrolyser to provide grid support are analysed as well. Chapter 5 discusses the development and implementation of control schemes for ancillary services provision by electrolysers. This provides valuable information for the design and qualification of future electrolysers. The main conclusions from this report, together with possible topics for future research, are discussed in Chapter 6.

2 Review of Electrical Ancillary Services Markets

Real-time power system operation is challenged by numerous disturbances such as faults, demand alterations and fluctuating renewable energy, which can induce undesired frequency, voltage or congestion issues in the grid. Ensuring an effective and reliable operation is handled by Transmission System Operators (TSOs), in part, through the procurement of ancillary services. As electrolysers could participate in these ancillary services in the future, the possibilities for this have been investigated in [2], [3]. This chapter presents a review of the electrical ancillary services market regulations and discusses how electrolysers could potentially participate. Because the available ancillary services are closely related to specific phenomena of power system stability, this chapter starts with a brief revisit of the main stability phenomena in Section 2.1.

After discussing the main stability phenomena, the market implementation of electrical ancillary services is considered in Section 2.2. Up until the last few years, the framework of ancillary services markets in European countries has been subjected to the specific rules of the corresponding national TSOs [4]. As the definition of the offered services, contracting methods, instructing procedures, remuneration settlement rules and prequalification requirements differ from one country to the other, it is hard to develop a joint analysis. This study therefore concentrates on the situation in the Netherlands, while also considering the possible development of the European market. General conclusions from this study are summarised in Section 2.3.

2.1 Power System Dynamics

When studying power system stability, the response of the power system to various events and disturbances is analysed. By definition, an electric power system is considered to be stable if it has the *"ability […], for a given initial operating condition, to regain a state of operating equilibrium after being subjected to a physical disturbance, with most system variables bounded so that practically the entire system remains intact"* [5]. Generally, rotor angle, voltage and frequency are regarded as the three principal power system variables considered in stability studies of electrical power systems. Rotor angle stability is defined as the ability of synchronous generators to remain in synchronism after disturbances; voltage stability deals with the ability of the power system to maintain admissible voltages throughout the grid; and frequency stability refers to the ability of the power system to maintain balance between generation and demand as to keep a steady system frequency. According to the power system stability classification shown in Figure 2.1, a distinction can be made depending on disturbance size (i.e. large or small) and time horizon (i.e. short or long term). Size has a stronger impact on the severity of the event, while duration determines the most suitable means to mitigate it.

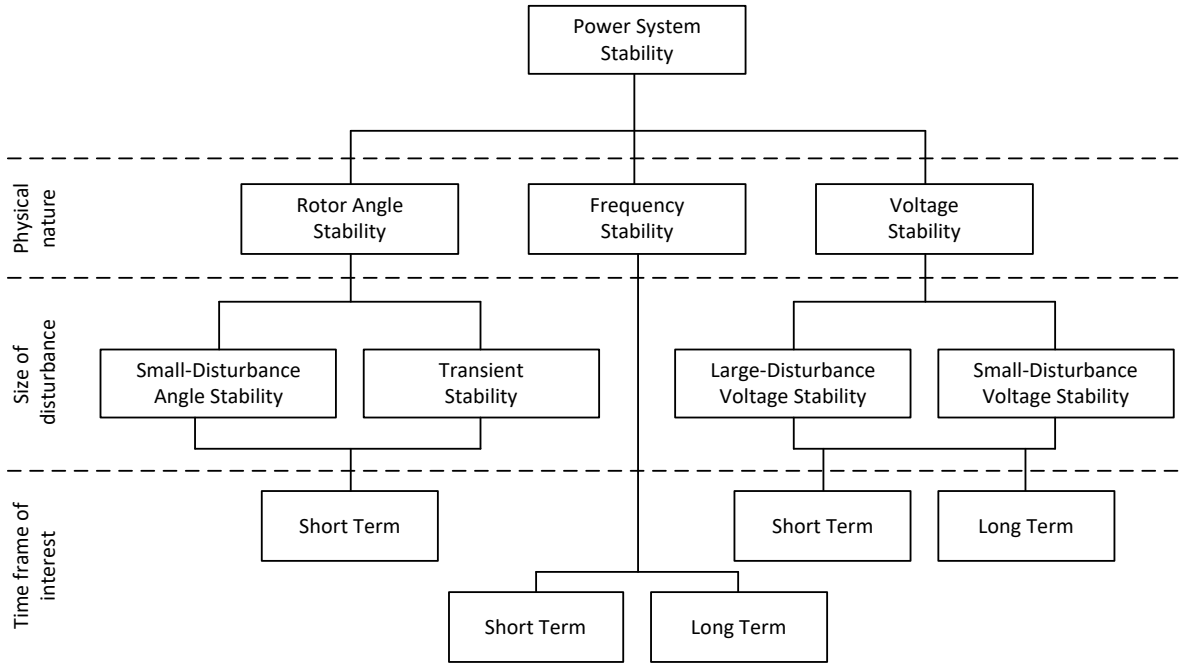

Figure 2.1: IEEE/CIGRE classification of power system stability [5].

Although the classification shown in Figure 2.1 lists the stability phenomena separately, disturbances in the power system often affect multiple phenomena in practice. Severe disturbances, such as the tripping of transmission lines or large generators, are related to transient stability, frequency stability and large-disturbance voltage stability. On the other hand, small-disturbance angle stability and small-disturbance voltage stability are related to small continuous disturbances, like load changes. Nevertheless, the classification can help understand the stability behaviour of the power system as particular situations often can be assigned to one (or some) of the specified phenomena.

The time frame of interest substantially depends on the time constants of the relevant facilities and control systems, as well as their interactions. This usually ranges from seconds to tens of seconds for short-term stability aspects and tens of seconds to tens of minutes for long-term stability aspects [5]. The various time frames can be associated with various disturbances [6]. For example, large time constants can be related to maintaining the power balance in the system. This includes the scheduling and optimisation of generation, but also long-term frequency control. Medium time constants are associated with the kinetic energy in the system. This kinetic energy is mainly stored in the large rotating machines (e.g. conventional generators) within the system. Typical related phenomena are power oscillations and the associated transient stability of the system. Short time constants are caused by the exchange of energy stored in the electric field and capacitances on the one hand and the magnetic field and inductances on the other hand. Typical phenomena are then switching transients, lightning and transient over-voltages.

In addition to the severity and duration of a disturbance, power system stability depends on the initial operating conditions before a disturbance occurs. Particularly highly loaded conditions are more prone to system collapse, as the network works closer to its stability limits [5]. For such reason, congestion management and hence the possibilities of generation redispatch and demand side response are worth to consider as well.

2.2 Market Implementation of the Electrical Ancillary Services[1]

As part of TSO2020 Activity 2, the present market implementation of electrical ancillary services has been analysed [2], [3]. Figure 2.2 gives an overview of the ancillary services considered in this study. Starting on the right, blackstart restoration plans are fixed action plans, mainly designed for traditional synchronous generators. Electrolysers could participate in these action plans as loads that are switched in at a certain moment. Voltage stability and network congestion are local issues and are addressed by local relief actions, determined by national TSOs. In contrast, frequency variations affect every control area in the power system and therefore, the development of a common European frequency balancing market is being pursued in the short term [7]. In such scenario, mitigation of renewable energy uncertainty will be more effective and at the same time, a harmonised market playing field across Europe is created. As shown in Figure 2.2, frequency balancing consists of three parts: Frequency Containment Reserve (FCR), Automatic Frequency Restoration Reserve (mFRR) and Manual Frequency Restoration Reserve (aFRR). The following sections present the detailed market implementation per ancillary service.

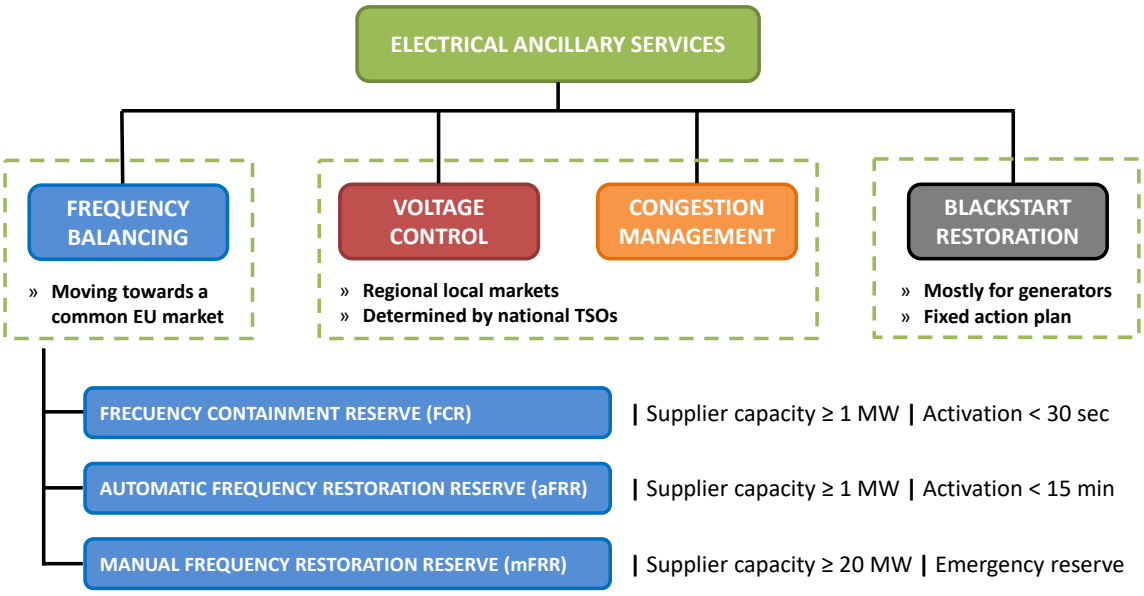

Figure 2.2: Organisation of electrical ancillary services.

2.2.1 Frequency Balancing

Frequency Containment Reserve

Frequency Containment Reserve (FCR), commonly known as primary frequency control, serves as the first barrier against active power imbalances. This service is designed to limit frequency excursions within the first 30 seconds after a disturbance. In the synchronous area of continental Europe, an overall capacity of ±3000 MW is allocated for FCR, further divided proportionally among the member states [8]. As of 2019, there is a shared European market with a total size of ±1470 MW, gathering TSOs from Germany, the Netherlands, Austria, Switzerland, Belgium and France. Denmark is involved

[1] This section is an updated version of the work as published in [2] and [3].

in the cooperation group and able to join the market anytime [9]. In the Dutch control area, the size of FCR was ±111 MW in 2019 [10]. Out of the overall FCR capacity, 30% is auctioned exclusively for Dutch providers (i.e. 34 MW), while the remaining 70% is auctioned in the shared market [10].

The FCR market is constructed around a symmetric capacity product. The minimum bid size is ±1 MW and the maximum bid size is the prequalified volume. The auction takes place once per working day (two days before actual procurement, i.e. D-2), and generators, loads and batteries are able to participate in it. The product resolution lasts for a single day, for which the providers must commit. Remuneration is based on a marginal pricing settlement rule, favouring the cheapest offers available [10]. Technically, FCR requests activation of the full bid within 30 seconds in case of a ±200-mHz frequency deviation. For providers without a limited energy supply, FCR support must persist for the entire deviation period. The control implementation is decentralised and follows a classic droop characteristic, such that the change in active power is proportional for smaller frequency deviations [11]. Figure 2.3 gives an overview of the framework of the joint FCR market.

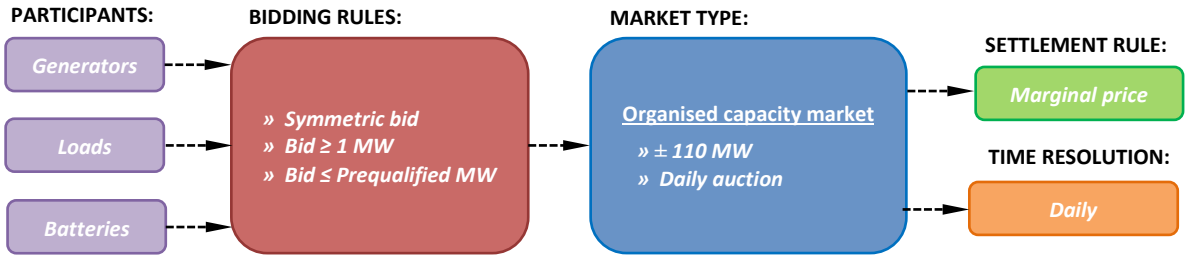

Figure 2.3: Current FCR market framework in the Netherlands.

By the end of 2020, the FCR product resolution will be shortened to 4 hours, according to the recommendations of the member TSOs [9]. The shortening of the resolution will benefit the operational flexibility of electrolysers, as this offers the opportunity to provide FCR support while also exploiting cheap electricity (e.g. at off-peak hours or at night). The implementation of asymmetric bidding would enable to bid exclusively for either upward or downward regulation, which allows further operational flexibility. Nevertheless, asymmetric bidding is not planned for the next years because of the increase in market complexity [12]. In line with the planned regulatory market changes, it is probable that the technical requirements will become more stringent, either by shortening the full activation time or by incentivising the participation of faster technologies. Several countries, like the UK and Ireland [13], [14], are already creating new products for fast frequency regulation purposes. The fast speed performance of electrolysers indicates notable ability to participate in FCR, as any variation of demand can be achieved within just 1 second.

Automatic Frequency Restoration Reserve

Automatic Frequency Restoration Reserve (aFRR), formerly known as secondary frequency control, acts right after FCR in order to restore the active power balance in each control area within 15 minutes after a disturbance. aFRR deployment is divided into Programme Time Units (PTUs) of 15 minutes each. Contrary to the FCR market, no common trading platform exists at the moment, making the framework disparity between countries more noticeable. In the Netherlands, a minimum of ±385 MW of aFRR capacity is required for late 2019, effectively guaranteed via bilateral contracts

of monthly or weekly duration [15]. The offered capacity must be symmetric with a minimum size of 1 MW and a maximum size of 999 MW [16]. Suppliers are remunerated on a pay-as-bid scheme [4]. For each PTU, all the contracted parties are obliged to bid their agreed capacity for upward and downward regulation. Additionally, non-contracted suppliers are allowed to send voluntary capacity bids, which in this case can be asymmetric and at least 1 MW in size. When all the bids have been received, they are inserted into a common bid ladder. In the event of an imbalance, the units are activated according to a merit order (i.e. cheapest bids first) [16], and the last participant unit sets the marginal price used to settle the energy usage in the PTU [4]. Power setpoints are realised in steps of 1 MW, a minimum ramp rate of 7% of the bid per minute must be provided, and full activation of the bid must be completed within 15 minutes [16]. The speed capabilities of electrolysers are well above the cited requirements, hence the provision of upward regulation aFRR by reducing consumption is a possibility. The structure of the complete aFRR market in the Netherlands is summarised in Figure 2.4.

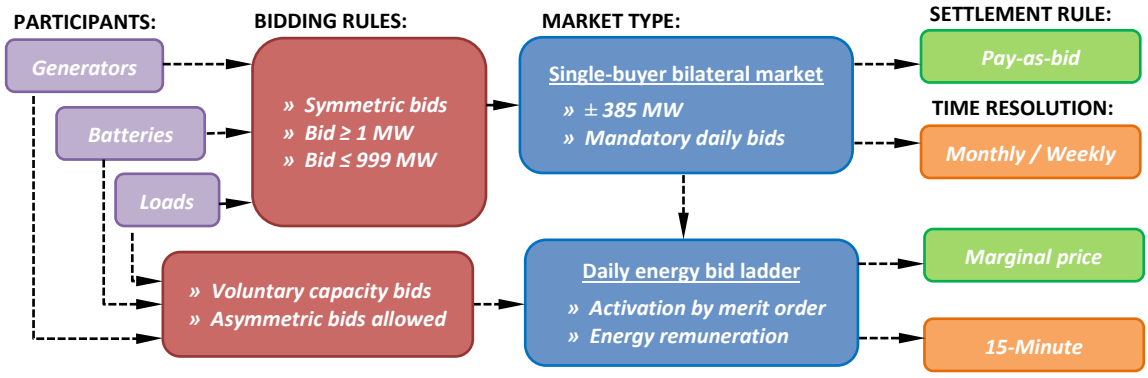

Figure 2.4: Current aFRR market framework in the Netherlands.

For the next years, the harmonisation and development of a joint European aFRR framework is being targeted [17]. In such scenario, a common cross-border merit list would determine the order of energy activation, while cross-border marginal pricing would ideally become the settlement rule. Another focal point is the mitigation of the uncertainty of renewable energy sources, which will be addressed by shifting the market gate closure time as close as possible to real time and by shortening the full bid activation time to 5-8 minutes. In the zone of central Europe, some degree of coordination is already implemented through International Grid Control Cooperation (IGCC) [18]. This initiative applies imbalance netting to avoid the simultaneous activation of aFRR in opposite directions among different control areas.

Manual Frequency Restoration Reserve

Manual Frequency Restoration Reserve (mFRR), formerly known as tertiary frequency control, is only activated when a severe outage occurs at a large power plant. Because it is rarely used, and due to large minimum size required to apply for the available capacity product [19], mFRR is judged as a low interest service for electrolysers.

2.2.2 Voltage Control

Voltage control is mainly performed by injection and absorption of reactive power. Grid codes usually demand voltage regulation capabilities of synchronous generators and power electronics-interfaced renewable energy sources connected to the transmission network. Transformers, FACTS (Flexible AC Transmission Systems), HVDC (High-Voltage Direct Current) links, battery storage and several industrial consumers are also able to support voltage control. The optimal use of the reactive power provided by these sources is defined by the national TSOs on the basis of optimisation programs, past experience and studies. Supplier remuneration relies on national legislation as well. In the Netherlands, these sources must act within 15 minutes when commanded [20]. For generators with installed capacity >5 MW, voltage control is mandatory and contracted [4]. A yearly tender is organised for external reactive power suppliers, where bilateral contracts for a specific agreed duration or situation are arranged. Remuneration is settled on a pay-as-bid rule, and depending on the contract, a yearly fixed fee or an hourly variable fee is agreed [20]. Since electrolysers are DC loads and limited reactive power is consumed by the other equipment, participation in voltage control can be achieved by varying the active power demand. Using the converter to manage reactive power is a more desirable solution, but an oversized converter would be required to operate at rated active power. For both options though, the response can be completed within 1 second.

2.2.3 Congestion Management

Congestion of the electrical network can be dealt with in different ways. Investing in grid infrastructure and using available cross-border capacity are strictly internal TSO relieving efforts. On the other hand, power redispatch or Demand Side Response (DSR) depend on external assets. In the Netherlands, enhancement of the grid infrastructure is the current action plan [21]. However, if a congestion issue is identified, a bilateral contract can be drawn with generators or industrial loads [20]. Electrolysers can contribute to the reduction of congestion by modulating their electricity demand. Furthermore, their fast ramping capability could help mitigate the fluctuations of renewable energy sources and lessen energy curtailment [22].

2.3 Conclusions

Electrolysers are a promising flexibility solution for future power systems as their fast dynamics can be exploited to improve the performance of the electrical power grid. Based on a review of recent literature of electrical ancillary services markets and participation of demand side response, it is concluded that electrolysers should prioritise involvement in FCR, followed by participation in aFRR. If electrolysers are installed in an area of the network in need of voltage control or congestion management, it could also be deployed for such purposes. The modifications of the framework of balancing markets to be introduced in the next years will allow broader operating flexibility for suppliers. For electrolysers, this offers the possibility to produce hydrogen during periods of inexpensive electricity price, while also providing frequency support.

3 Electrolyser Model and the Veendam-Zuidwending Case Study

In the context of TSO2020, a 1-MW pilot electrolyser has been installed in the northern part of the Netherlands in Veendam-Zuidwending (in the province of Groningen). The impact of this electrolyser on the local grid stability is considered in Activity 2 of the project. As practical models of large (>1 MW) electrolysers are not available in current literature yet [23], an electrical model has been developed in RSCAD specifically for the TSO2020 project [24], [25], [26], to be used in real-time simulations on the Real-Time Digital Simulator (RTDS). The dynamic performance of the developed electrolyser model has been analysed in various real-time simulations, which illustrate the possibilities of grid support by an electrolyser of this size at this location. The electrolyser model has been tuned and validated against field measurements of the 1-MW pilot electrolyser at Veendam-Zuidwending. A scaled-up version of the electrolyser model is used in the next chapter to study the impact of a 300-MW electrolyser plant in Eemshaven.

This chapter is organised as follows. First, in Section 3.1 the network topology of the Veendam-Zuidwending case study and the considered disturbances are presented. Then, in Section 3.2 the model of the electrolyser is presented. In Section 3.3, the performance of the electrolyser model is analysed for the selected disturbances to study the possibilities of grid support of a 1-MW electrolyser in this area. The performance of the electrolyser model is validated against field measurements of the pilot electrolyser in Section 3.4. Conclusions are then discussed in Section 3.5.

3.1 Network Topology and Disturbances

A simplified diagram of the electrical network at Veendam-Zuidwending is illustrated in Figure 3.1. As can be seen, a 5-km (double circuit) cable connects the 33-kV substation Veendam-Zuidwending to the 110-kV substation Meeden. At Veendam-Zuidwending, two 110/33-kV transformers are installed. The 33-kV substation contains two busbars and several bays, to which the compressors and other systems of the natural gas storage facility at this location are connected. The electrolyser has its own bay and is connected by a three-winding transformer. The electrolyser itself is linked to the secondary winding of the transformer, while auxiliary systems are connected to the tertiary winding. In the simulations in this chapter, the 110-kV substation Meeden is modelled as an infinite grid.

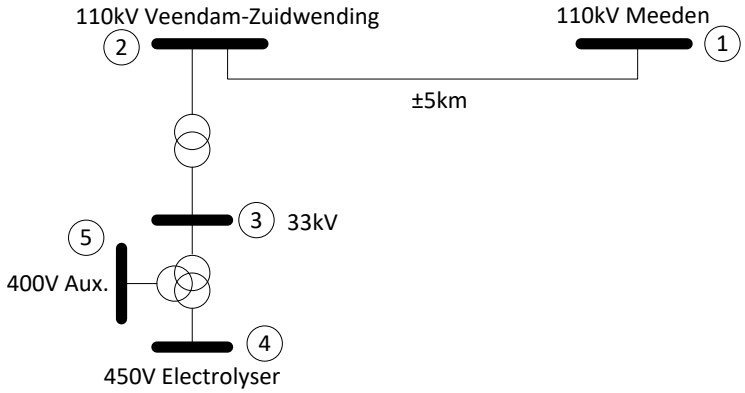

Figure 3.1: Simplified diagram of the electrolyser connection at Veendam-Zuidwending.

To investigate the possibilities of grid support by an electrolyser at this location, the electrolyser model's response and capabilities are demonstrated in several simulations. The selected cases are based on events and disturbances that are likely to occur in reality. The selected cases can be divided into three sets of simulations. In the first set, the response to basic step commands is simulated. The second set considers the response of the electrolyser to various power system disturbances, like frequency and voltage deviations. The third set studies the electrolyser's response to system faults. With these simulations, it is possible to compare the response of a electrolyser load that participates in grid support with that of an electrolyser that does not participate in grid support.

The complete list of disturbance cases considered in the simulations is as follows:

1. Basic Response:
   - **Test 1**: Step increase/decrease in hydrogen production (i.e. stack current)
2. Response to power system disturbances:
   - **Test 2**: Grid frequency disturbance
   - **Test 3**: Bus voltage disturbance (due to demand variation)
3. Response to faults:
   - **Test 4**: Single-line-to-ground fault
   - **Test 5**: Double-line-to-ground fault
   - **Test 6**: Symmetrical three-phase-ground fault

The response of the electrolyser model in these simulations will be discussed further in Section 3.3.

3.2 Modelling of the Electrolyser

In electrolysers, the electrochemical process of water electrolysis is performed, in which electricity is applied to split water into hydrogen and oxygen. There are mainly four types of electrolysers [28]: Polymer Electrolyte Membrane (PEM) electrolysers, alkaline electrolysers, Solid Oxide Electrolysers (SOE) and Anion Exchange Membrane (AEM) electrolysers. Currently, both PEM and alkaline electrolysers are commercially available. AEM electrolysis has a limited range of applications, whereas SOE technology is at its early stage of development. Among the cited technologies, alkaline electrolysis is the most mature, while PEM is in its initial commercial phase. Although alkaline technology is well suited for smaller applications, PEM electrolysis is a promising technology for future, large-scale applications [27], [30]. It holds the highest promise in the sense of lowest capital cost along with higher power densities, smaller footprint, larger dynamic range and a scalable design. The models developed in this study are therefore based on PEM electrolyser technology.

Figure 3.2 depicts the general PEM electrolyser system layout. This diagram is not a general standard, however it captures the relevant components and subsystems. An electrolysis system is made up of three layers [28]: (i) the PEM stack layer, which is the unit within which the chemical reaction takes place; (ii) the PEM module layer, which includes the stack as well as peripheral components to support stack operation (i.e. supply of reactants and removal of products); and (iii) the system layer, which comprises the module layer and other auxiliary subsystems that vary based on the installation site and application. Examples of auxiliary subsystems in the system layer are water purification systems, buffer gas reservoirs and hydrogen purification systems.

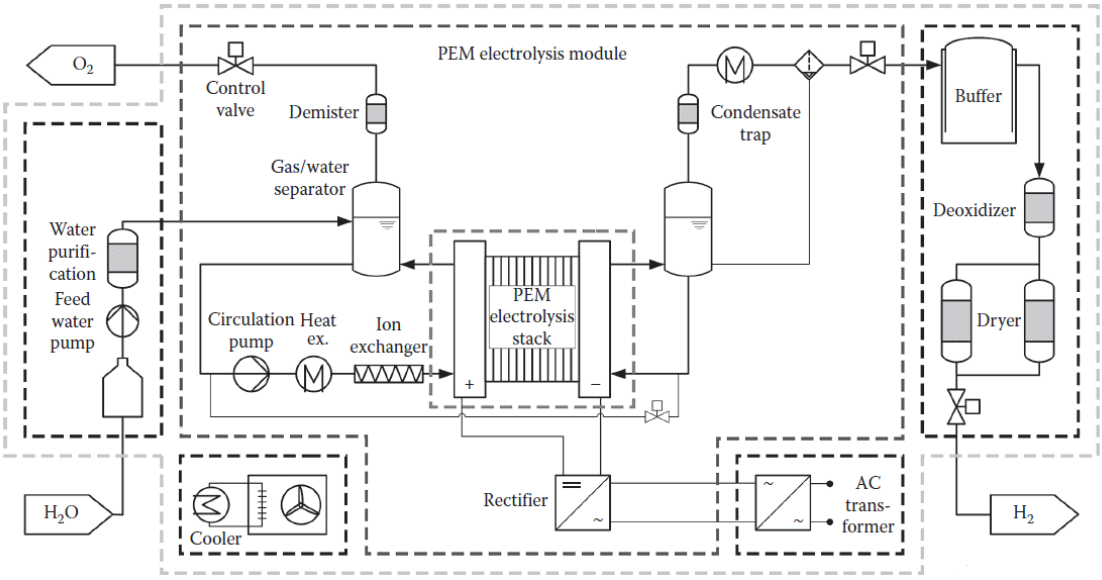

Figure 3.2: General system layout of an electrolyser showing the PEM stack and balance of plant components (controls not shown). Extracted from [31].

The PEM stack is the main component within which the production of hydrogen and oxygen takes place. It must be noted however that operation of the stack is only feasible with the support of other subsystems. The generic model developed in this study models the PEM system at the module layer, thus the Balance of Plant (BoP) components, which support the operation of the stack (such as feedwater and circulation pumps) are included, albeit simplified. The different characteristics of specific electrolyser installations make it difficult to capture the system layer in a generic model. The key components whose electrical response the generic RSCAD model emulates are: the PEM stack, the power conversion system (i.e. rectifier, DC/DC converter and main transformer) and the BoP components (i.e. the circulation pump, cooling system and electronic loads such as the control system). The chemical reaction within the PEM stack is not modelled.

Figure 3.3a shows the electrical connection of an electrolyser, as it is modelled in this study. The AC/DC and DC/DC converters are implemented in a number of ways by different manufacturers. In this study, the AC/DC conversion is implemented with a 3-phase active rectifier in series with three parallel DC/DC converters (for an increased current capacity). The BoP components are modelled by a constant load, as it can be assumed that most of these have a fixed power consumption.

Figure 3.3b shows the electrical equivalent of the PEM electrolyser stack. Electrolysis requires a DC (Direct Current) voltage that must overcome a reversible voltage in order to trigger the chemical reaction of water splitting into oxygen and hydrogen. Losses within the PEM stack increase the required voltage and are modelled as overpotentials. The representation by this electrical equivalent is widely used in current literature [29]. The reversible voltage is represented by a fixed DC voltage (OCV). Ract, Rmass and Rohm represent the activation, mass transport and ohmic losses, respectively. The double layer capacitance of the cell is represented by a capacitor. A further simplification of the model can be made by neglecting the activation and mass transport losses and the double layer capacitance. The electrical model then becomes a series connection of the open cell voltage and ohmic losses, which can be estimated from the slope of the I-V curve of the electrolyser stack.

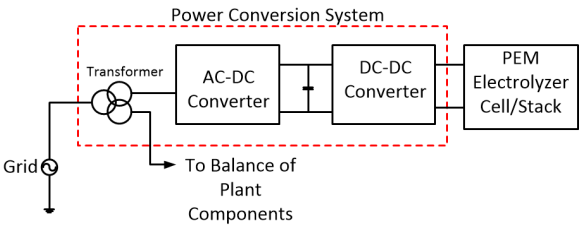

(a) components of the power conversion system

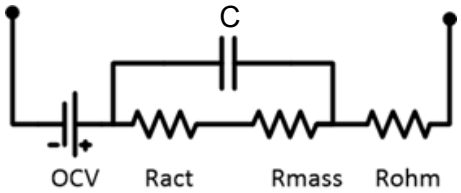

(b) electrical equivalent of the PEM cell

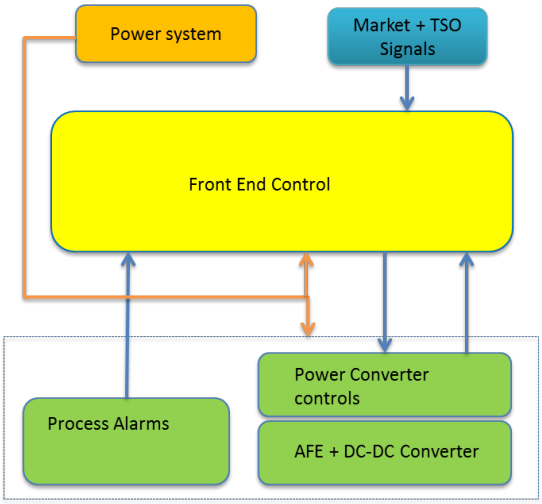

(c) implemented control of the electrolyser

Figure 3.3: Modelling of the electrolyser and its associated controls.

The electrolyser model developed in this project is equipped with a control system [24], [26], based on a generic architecture proposed in [32]. Control systems in commercially available electrolysers are primarily designed to support plant automation for the production of hydrogen gas. In order to optimise the electrolyser system to support additional objectives such as the provision of ancillary services, an additional control layer is required. The Front End Controller (FEC) is this additional high-level control and integrates with low-level controls to form a hierarchical control scheme with extended capabilities, such as the capability to simultaneously respond to market price signals, the condition of the power system and internal signals like electrolysis process alarms. Figure 3.3c shows the simplified structure of the high-level control. A detailed description of the high- and low-level controls of the electrolyser can be found in Appendix B and in [24], [26].

3.3 Electrolyser Model Performance

The electrolyser model's response and capabilities with and without the Front End Control (FEC) scheme are demonstrated in simulations of the disturbances as specified in Section 3.1. First, the model's response to basic step commands is simulated without the high-level controller in the loop. This is to verify the basic model's response. The augmented model with the FEC in the loop is then simulated for various types of power system disturbances and external control signals. The generic responses can be tuned to replicate the response of a real electrolyser. This provides a good level of visibility into the typical response of electrolysers based on the generic model and also the robustness of the implemented hierarchical control scheme.

3.3.1 Basic Response

Test 1: Step Increase/Decrease in Hydrogen Production (i.e. Stack Current)

An increase in hydrogen production requires upward adjustment of the current fed to the PEM stack. This leads to an increase in active power drawn from the power system. The opposite also holds, such that a decrease in hydrogen production is accomplished by reducing the stack current, which leads to less power consumption. The developed model is capable of emulating the response of an

electrolyser of which the stack current setpoint has been adjusted via a step command. The graphs in Figure 3.4 show the RSCAD model's response to step changes for a stack current increase and decrease, respectively. This command is typically initiated locally by a user from a control panel or remotely from a high-level controller such as the FEC or system control centre. An electrolyser can have the operating principle of storing excess generated electrical energy as hydrogen gas. Thus, electrolysers configured to increase demand and hydrogen output based on a signal from a high-level controller or dispatch centre must be able to ramp up demand within a certain time frame. In this case, the electrolyser responds by adjusting the current fed to the stack in less than 1 second.

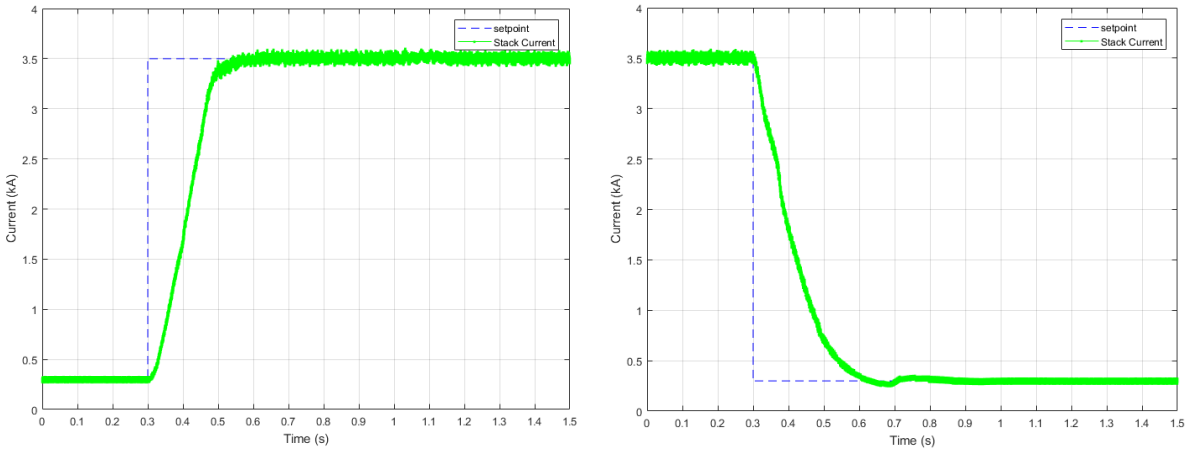

Figure 3.4: Response of the electrolyser model to load current setpoint increase (left) and decrease (right).

The response of the electrolyser model can be compared with the response of a real electrolyser from literature [22]. When comparing the response profile and settling time with that of a real electrolyser, as shown in the graphs of Figure 3.5, it can be concluded that the generic model replicates the real system fairly accurately. The response of the electrolyser model can be tuned to replicate the response of a specific electrolyser.

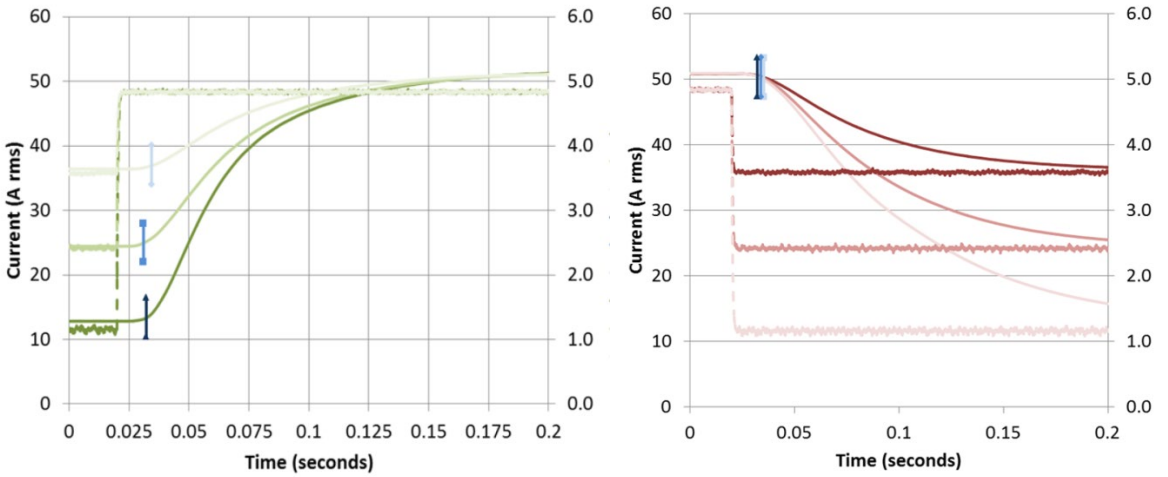

Figure 3.5: Load current response to setpoint increase (left) and decrease (right) for a real PEM electrolyser, extracted from [22].

The fast ramping capability of electrolysers is a feature that can be of interest for Frequency Containment Reserve (FCR) applications in future power systems, since electrolysers are known to have relatively faster ramping capabilities than conventional generators [22]. The fast response time also holds potential for improving the system frequency performance after a disturbance.

3.3.2 Response to Power System Disturbances

Test 2: Grid Frequency Disturbance

Participation in ancillary services requires the electrolyser to respond to external signals from the power system and the system operator. Frequency support is accomplished by varying the active power consumption and voltage support by adjusting the reactive power consumption. The electrolyser must therefore be able to vary its active and reactive power consumption independently when demanded. In the high-level controller of the electrolyser model, signals from external sources are translated into signals for the low-level controllers. In this way, the low-level control signals (e.g. the stack current) are determined based on high-level control signals (e.g. the active power setpoint).

The response of the electrolyser model to active power ramp up and ramp down commands is shown in Figure 3.6. This feature enables frequency control and congestion management capabilities. It can be seen that the electrolyser ramps up/down its active power consumption within one second after a command. There is only a small and temporary deviation of the reactive power consumption.

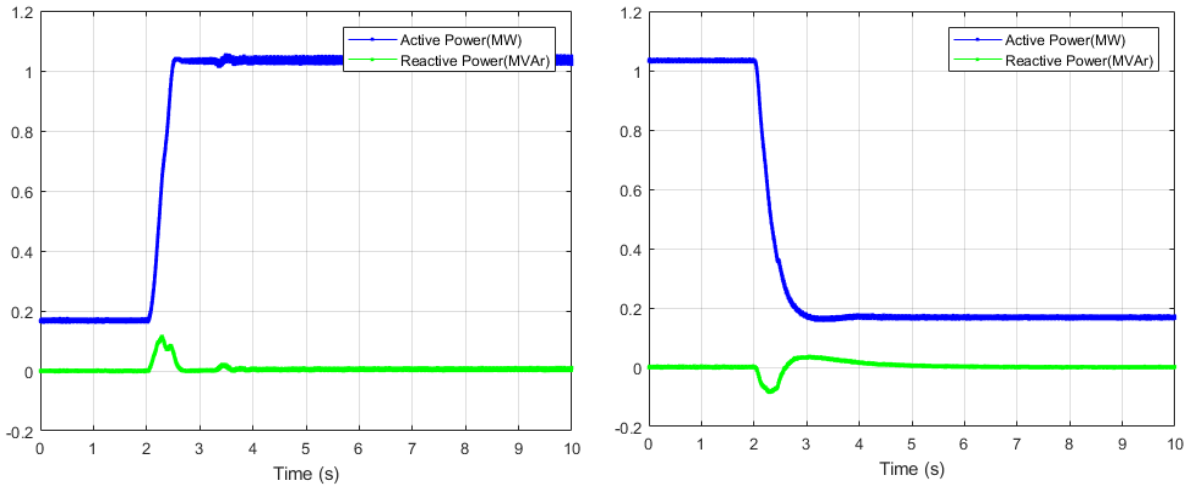

Figure 3.6: Electrolyser model response to active power ramp up (left) and ramp down (right) commands.

In order to implement frequency support, the electrolyser must be able to vary its active power consumption based on the frequency of the power system. In the case of a frequency smaller than normal, the electrolyser must decrease its consumption and in the case of a frequency higher than normal, the electrolyser must increase its consumption. This simulation studies how the electrolyser model responds to a drop in system frequency of 0.1 Hz. This scenario typically occurs when there is a sudden loss of generation capacity or a sudden increase in load in the system. In Figure 3.7, it can be observed that the electrolyser model ramps down its active power consumption when the frequency drop occurs. A similar response is obtained for an increase in frequency. The response of the electrolyser model to frequency deviations is implemented by a droop control. Depending on the ancillary service agreement, the capacity assigned to frequency support can be adjusted in practice.

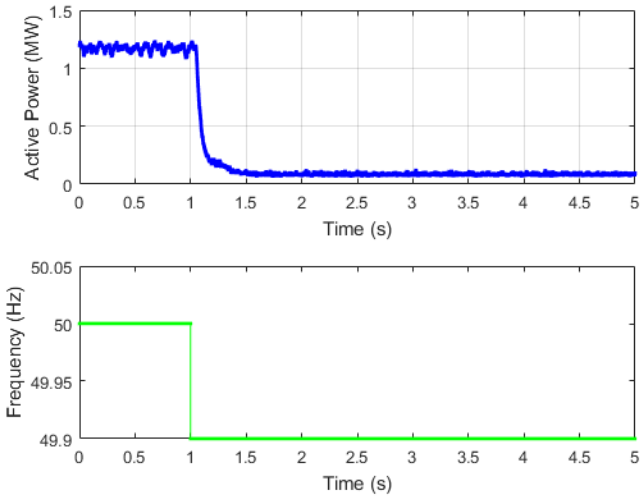

Figure 3.7: Response of the electrolyser model to 0.1 Hz change in power system frequency.

Test 3: Bus Voltage Disturbance (due to Load Variation)

Voltage support by electrolysers can be accomplished by adjusting the reactive power consumption of the electrolyser converter. The electrolyser must be able to vary its reactive power consumption independently from its active power consumption. The graphs in Figure 3.8 show the electrolyser model's response to a command from the system operator to inject or absorb reactive power. It can be seen that the electrolyser adjusts it reactive power consumption, while its active power consumption remain about the same. Changing the reactive power consumption influences the local voltage. Therefore, the graphs show an increase and decrease in voltage at the PCC (i.e. bus 3 in Figure 3.1), which is the 33-kV bus to which the electrolyser is connected.

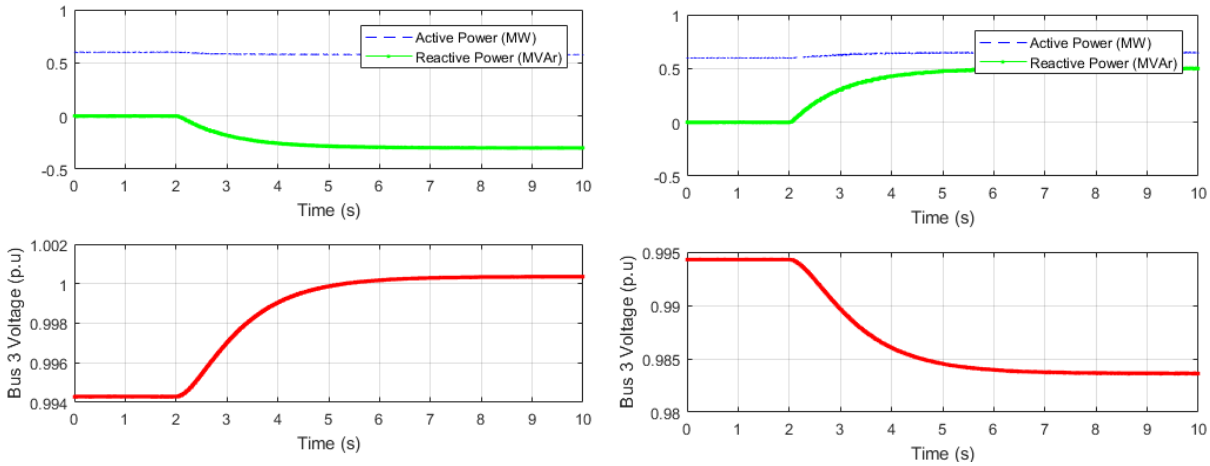

Figure 3.8: Electrolyser response to reactive power injection (left) and power absorption (right) commands.

In order to implement voltage support by an electrolyser, the electrolyser must be able to adjust its reactive power consumption based on the local voltage. The electrolyser model has been equipped with a controller that performs this task. To study its response, a simulation is performed considering a deviation in bus voltage at the PCC. During the simulation, a large load is connected to bus 2 by closing a circuit breaker. The increased current flowing through the transmission line results in a

larger voltage drop across it. As a result, the voltage at bus 2 reduces. The response of the electrolyser model with and without voltage support is shown in Figure 3.9. When voltage support is inactive, the bus voltage does not recover while the load is connected. However, if voltage support is activated, the bus voltage improves. The improvement is due to the increased injection of reactive power by the converter. In order to have this feature functional, the converter must have extra capacity above what is required for active power transfer. This means that the converter must be over-dimensioned or that the electrolyser is operating at a capacity smaller than rated. This can limit the possibilities for voltage support.

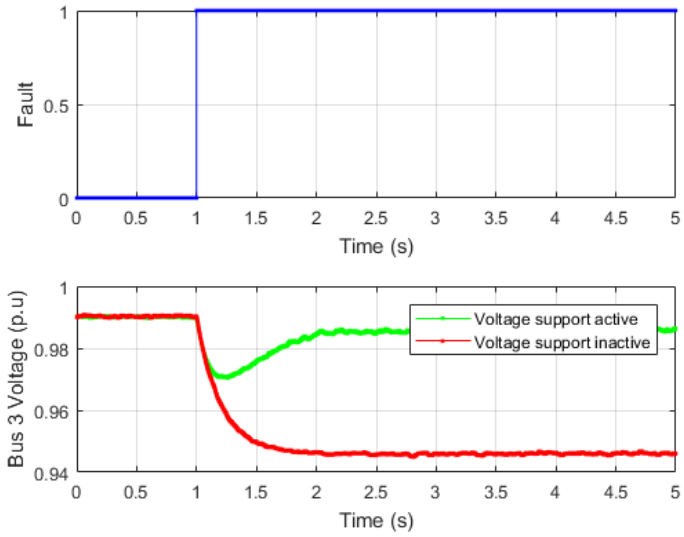

Figure 3.9: Response of the electrolyser model to bus voltage disturbance with and without voltage support.

3.3.3 Response to Faults

A fault in a power system is any failure which interferes with the normal flow of current. Most faults in transmission lines are caused by lightning, which results in the flash-over of insulators [33]. The high voltage between the conductors and the grounded tower causes ionisation, which creates a path to ground for the charge induced by lightning. Other causes of faults in transmission lines are flashovers between tree branches and conductors and flashovers between two conductors. Faults are categorised based on how many phases (of 3) are involved in the fault, such as single-line-to-ground faults, double-line-to-ground faults and symmetrical three-phase-ground faults.

Test 4: Single-line-to-ground Fault

Unsymmetrical faults are very common in power systems. According to [33], about 70–80% of the faults are single-line-to-ground faults. It is therefore useful to study how the electrolyser model behaves under these faults. The simulation performed here involves creating a fault on phase A at bus 1 in Figure 3.1. The fault impedance is 0.1 Ohm and the fault is cleared in 100 ms, which is the standard fault clearing time in simulations of the Dutch 380/220-kV network. The result of the simulation, with and without voltage support, is shown in Figure 3.10. It can be observed that the recovery with voltage support activated is a few milliseconds faster than without voltage support, but the voltage support causes a small overshoot. The overshoot, however, is still within the 1.05 pu (per unit) upper limit for voltage deviation. This example shows that voltage control by electrolysers

can have a positive effect on the recovery time of the local voltage after disturbances. It must be noted that this particular response can be improved by further tuning of the control system parameters, for example to reduce the overshoot.

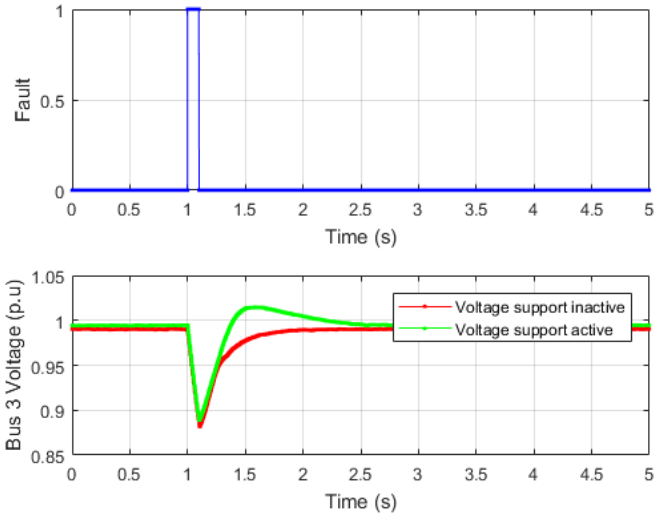

Figure 3.10: Response of the electrolyser model to a single-line-to-ground fault at bus 1.

Test 5: Double-line-to-ground Fault

In this simulation, a double-line-to-ground fault is created near bus 1 and is cleared after 100 ms. From Figure 3.11, it can be observed that the response is quite comparable to that for the single-line-to-ground fault. Voltage control enables a faster recovery of the bus voltage back to the pre-disturbance level, but causes a small overshoot in the voltage.

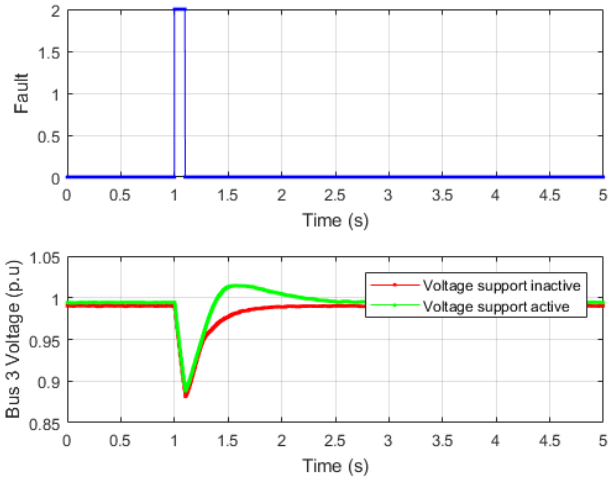

Figure 3.11: Response of the electrolyser model to a double-line-to-ground fault at bus 1.

Test 6: Symmetrical Three-phase-ground Fault

The response of the electrolyser model to a symmetrical three-phase-ground fault created at bus 1 for 100 ms is shown in Figure 3.12. This type of fault, though not very frequent, is more severe in terms of potential damage to power system components. As with the other types of faults, an improvement in recovery time, albeit with some overshoot, is observed.

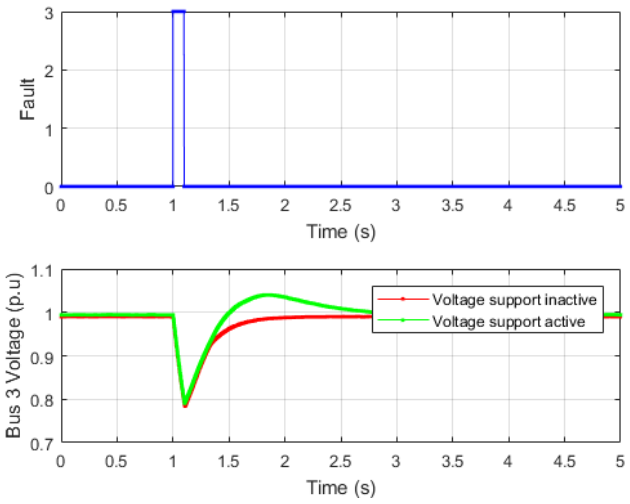

Figure 3.12: Response of the electrolyser model to a three-phase-ground fault at bus 1.

These three simulations of the voltage response after a fault show that electrolysers can have a positive effect on the recovery time of the local grid voltage. The response can be improved by further tuning the parameters of the control system, for example to reduce the overshoot of the voltage. The impact on the local voltage is however dependent on the capacity of the electrolyser and the local grid situation. A smaller electrolyser or an electrolyser located in a relatively strong part of the grid will have a smaller impact on the voltage. Furthermore, voltage control requires a certain capacity of the electrolyser converter that must be reserved for reactive power support. Participation in voltage control therefore requires electrolyser operation at a capacity smaller than rated or an overdimensioned electrolyser converter.

3.4 Validation against Field Measurements

The developed electrolyser model has been validated against field measurements of the 1-MW pilot electrolyser installed in the northern part of the Netherlands in Veendam-Zuidwending [34]. The parameters of the electrolyser model have been adjusted to the field measurements, such that the model is able to accurately replicate the behaviour of a real electrolyser. This section discusses the network configuration and measurement setup, the measurement procedure, the measurement results and the adjustment of the developed electrolyser model to the measurements.

3.4.1 Network Configuration and Measurement Setup

An illustration of the measurement setup is given in Figure 3.13. Measurements have been performed at all three windings of the three-winding transformer, i.e. points 3, 4 and 5 in the figure. The measurements at 33 kV were performed within the substation. The current was measured in the secondary circuit of the 33-kV installation with a current clamp of 1A/1V. The secondary current comes from a (200/1A, 5p20, 10VA) current transformer. The voltage was measured at the secondary side with a (33kV/√3/100V/√3) voltage transformer. The 33-kV measurements were performed using a Dewetron measurement system, equipped with a DAQP-VB measurement card for the current measurements and a DAQP-HV measurement card for the voltage measurements. The current measurements were performed using Universal Technic M1.UB 1A/1V and Chauvin Arnoux 20-200A/2V MN 38 current clamps.

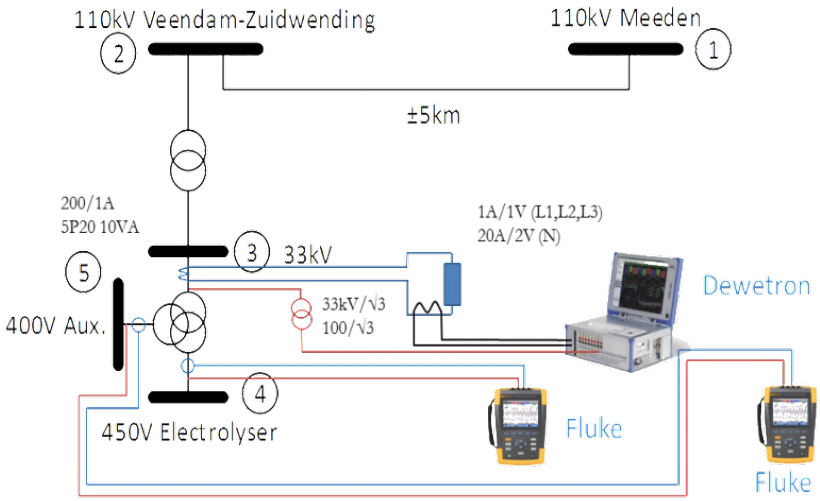

Figure 3.13: Setup of the electrolyser measurements at Veendam-Zuidwending.

The measurements at 450 V and 400 V were performed directly at the secondary and tertiary windings of the transformer, respectively. For these measurements, Fluke 435 series 2 power quality and energy analysers were used. For the current measurements, I430-FLEXI-TF-II Ragowski coils were used, while the voltages were measured directly.

3.4.2 Description of the Measurement Procedure

During the test, the operation of the electrolyser was tested in two cycles, as illustrated in Figure 3.14. These cycles consisted of starting up the unit, varying its operation setpoint between various levels (i.e. 10/50/70/100%), and shutting down the unit. As the electrolyser needs to build up pressure and perform some safety checks first, the operation level is limited to 50% directly after starting up the unit. After a certain time, the operation level goes to the desired setpoint. This is indicated in the graph by the dashed lines. During the test, measurements were recorded at the three mentioned voltage levels, where the main quantities of interest were: the voltage and current magnitudes, the total active power and the total harmonic distortion of the voltage and current.

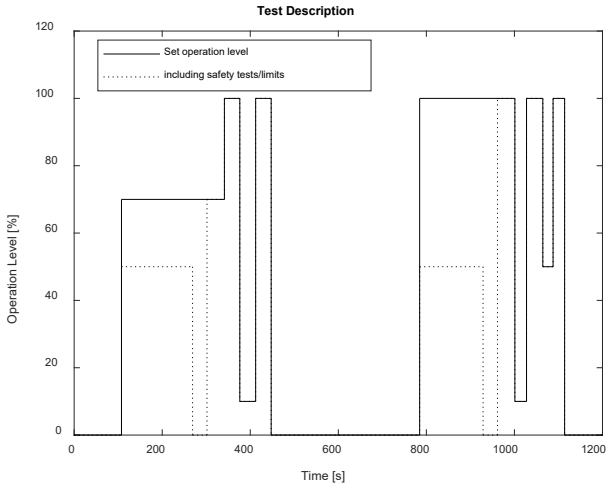

Figure 3.14: Operation cycles followed during the electrolyser test.

3.4.3 Most Relevant Measurement Results

The active power consumed by the electrolyser, measured at the 450-V side of the transformer, is illustrated in Figure 3.15. It can be seen that the active power consumption clearly follows the test cycles shown in Figure 3.14, apart from the inrush currents when starting up the unit. The active power consumed deviates however somewhat from the operation level setpoints, in the sense that the setpoints of 50/70/100% lead to a power consumption of about 0.4/0.6/0.9 MW.

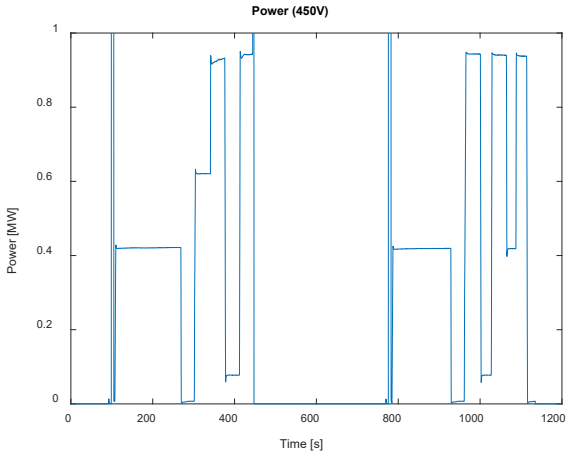

Figure 3.15: Active power of the electrolyser measured at the 450-V bus.

The graphs shown in Figure 3.16 zoom in on the active power ramps during the setpoint changes, which are aligned at t = 0. For this graph, the measurements at 33 kV were used, as the Dewetron device has a higher resolution than the Flukes. The graphs show that the active power ramps are linear and quite similar during normal operation (i.e. between 10 and 100%). This is caused by the control system implemented in the pilot electrolyser. The active power ramps after starting up the unit are typically slower. From these graphs, the average ramp rate of the electrolyser can be estimated. It can be seen that the average ramp up rate is about 0.5 MW/s (0.5 pu/s) during normal operation, while it is about 0.2 MW/s (0.2 pu/s) during startup of the electrolyser. The average ramp down rate is about 0.4 MW/s (0.4 pu/s).

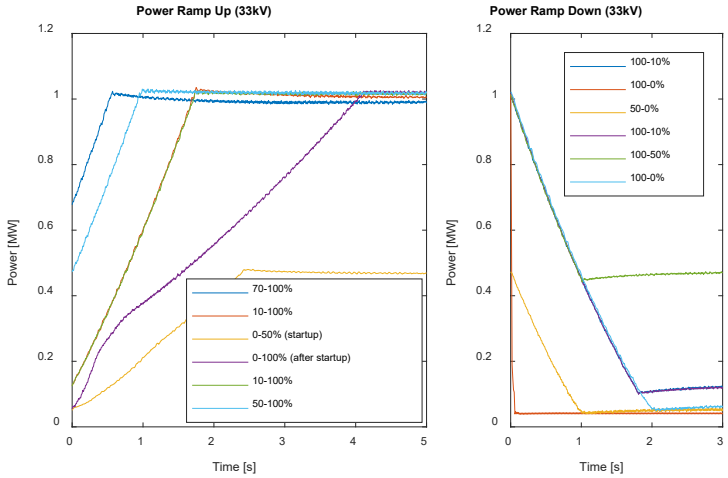

Figure 3.16: Response of the electrolyser to operation level setpoint changes.

3.4.4 Adjustment of the Electrolyser Model

Based on the field measurements, it is possible to estimate the ramp rate of a larger electrolyser unit. It was found that the 1-MW pilot electrolyser shows a linear response to setpoint changes, and has a ramp rate of about 0.5 MW/s (0.5 pu/s). Large electrolyser facilities consist of many small electrolysers in parallel. This means that a 300-MW electrolyser plant consisting of 300 units of 1 MW can reach a ramp rate of 150 MW/s (0.5 pu/s). This result can, roughly, be compared with data available in literature. In [22], the response of a 40-kW PEM electrolyser was tested. It was found that this electrolyser shows a non-linear behaviour, where the response time changes only slightly for larger setpoint changes. Ramping up or down is generally completed within 0.2 s. A capacity change of 50% within 0.2 s gives a ramp rate of 20kW/0.2s = 0.1 MW/s (2.5 pu/s). Under the assumption that the response time does not increase significantly for electrolyser capacities in the range to a MW and the fact that a 300-MW electrolyser plant consists of many smaller units, this would lead to a ramp rate of 750 MW/s (2.5 pu/s) for a 300-MW electrolyser plant. Although this comparison is based on rough assumptions, it still gives an indication of the range of ramp rate to consider in further studies, i.e. 150–750 MW/s (0.5–2.5 pu/s).

The parameters of the developed electrolyser model have been adjusted, such that the electrolyser model is able to accurately follow the response of a real electrolyser. The electrolyser has been extended with a ramp rate limiter, which has been empirically tuned to follow the desired response. Figure 3.17 shows the response of the 1-MW electrolyser model. It can be seen that the developed model is able to replicate the response of a real electrolyser. The response of a second, simplified and scaled-up, version of the electrolyser model is shown in Figure 3.18. It can be seen that this scaled-up version is able to follow the measurements accurately as well. As the response of this simplified version was already inherently linear, this scaled-up model follows the measurements somewhat more accurately. The scaled-up version will be used in Chapter 4 to study the impact of a large electrolyser facility in Eemshaven.

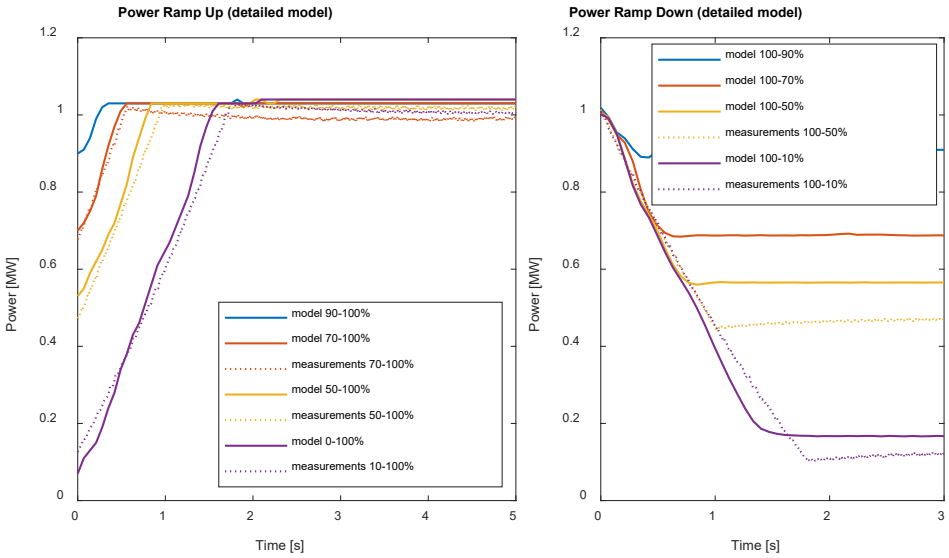

Figure 3.17: Response of the detailed electrolyser model.

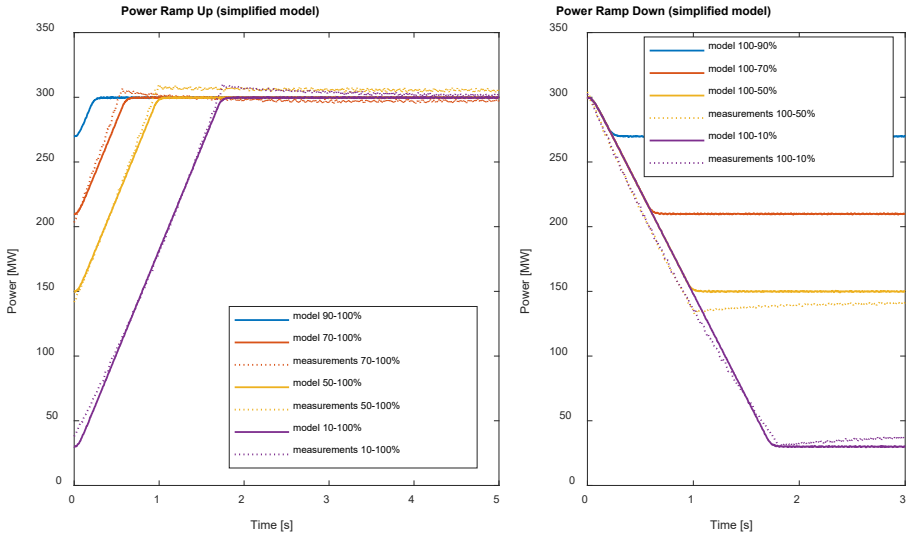

Figure 3.18: Response of the simplified, scaled-up electrolyser model.

3.5 Conclusions

This chapter discussed the case study of the pilot 1-MW electrolyser at Veendam-Zuidwending. A model of the electrolyser has been developed in RSCAD, to be simulated in real time on the RTDS. The performance of the electrolyser was analysed for several disturbances which are likely to occur in reality. The results were compared with the response of electrolysers in literature and with field measurements of the 1-MW electrolyser at Veendam-Zuidwending. The capability of the electrolyser to participate in frequency and voltage support was discussed as well.

The simulations of the electrolyser model's response to selected disturbances and the comparison with literature data demonstrates that the developed model is able to replicate an accurate response similar to the response of real electrolysers. The response of the electrolyser model can be adjusted to field measurements of a real electrolyser. The simulations in this chapter are a first indication of the potential of electrolysers to participate in grid support. For this purpose, an electrolyser needs to be equipped with appropriate controllers. The added value electrolysers can bring is mainly linked to their fast response time in comparison to conventional generators. Simulations in this chapter showed that the electrolyser model is able to adjust its active power consumption based on power system frequency variations (i.e. frequency support) and to adjust its reactive power based on voltage variations (i.e. voltage support). Although a 1-MW electrolyser will not influence the system frequency, it could possibly be used for local voltage support. For this purpose, there must be a certain amount of converter capacity available, which means over-dimensioning of the electrolyser converter or electrolyser operation at a capacity lower level than rated.

4 Electrolyser Model Scale-up and the Eemshaven Case Study

For the future, the installation of a large-scale electrolyser plant is foreseen in the northern Netherlands. This part of the network includes a large-scale generation centre, the connection of large-scale offshore wind and submarine interconnections with Norway (NorNed) and Denmark (COBRAcable) at Eemshaven and Eemshaven Oudeschip substations. Eemshaven Oudeschip is also a suitable location for a future 300-MW electrolyser plant, as abundant renewable energy generated by the offshore wind farm can be converted into hydrogen gas. The electrolyser plant can also support the power system stability by participating in ancillary services. In this chapter, various simulations are performed to study the behaviour of a large-scale electrolyser in such an interconnected power system and to study the potential impact of ancillary services provision by large-scale electrolysers. For real-time simulations, the transmission network of the northern part of the Netherlands has been modelled as a test system in RSCAD (RTDS), based on a model in PSS/E provided by TenneT TSO. For qualitative validation and comparison purposes, a simplified version of the network has also been implemented in PowerFactory.

This chapter starts with a description of the network configuration, operational scenarios and considered disturbances in Section 4.1. Then, the adjustment and scaling up of the developed electrolyser model are discussed in Section 4.2. Section 4.3 discusses the implementation of frequency control in COBRAcable. The main simulation results are presented and discussed in Section 4.4. General conclusions from these studies are then summarised in Section 4.5.

4.1 Network Topology, Operational Scenarios and Contingencies

In this case study, the impact of a large-scale electrolyser on the stability of an interconnected power system is analysed. As a 300-MW electrolyser would not have a significant impact on the frequency of a large power system like the European, the impact on a smaller test system is studied instead. This provides general insight into the impact of electrolysers on larger power systems if the number of electrolysers increases in the future. For this case study, the test model of Northern Netherlands Network (N3) has been selected as test system. The size of the test system is limited by the capacity (i.e. memory space) of the Real-Time Digital Simulator (RTDS), which is used for the simulations of this study.

Two different topologies of the test system of Northern Netherlands Network are considered, as illustrated in Figure 4.1. First, in the intermediate situation, only two circuits between the buses EOS-VVL are in service, while the 380-kV connection between the buses VVL-ENS has not been installed yet and only one 430-MW generator linked to the bus EOS is operative. For the final situation, the four 380-kV circuits between EOS-VVL and the 380-kV connection between the buses VVL-ENS are in service, while all the generating capacity is operative. For the year 2030, both network topologies are considered, while for the year 2040, the final network topology is selected.

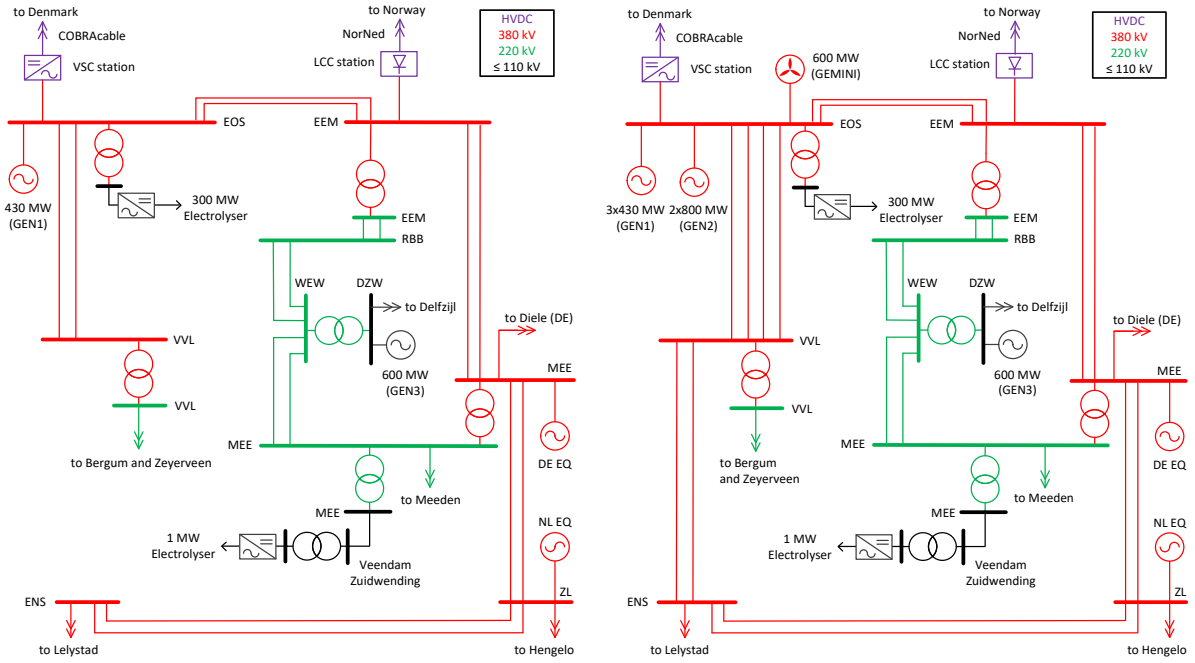

intermediate topology *final topology*

Figure 4.1: Considered network topologies: intermediate (left) and final (right).

Table 4.1 gives an overview of the operational scenarios that are considered in this study. As shown in the table, three generation scenarios are considered for 2030, while one scenario is considered for 2040. Scenario 1 is based on the intermediate network topology shown in Figure 4.1, in which generation and demand are reduced due to some of the circuits not being available. Scenarios 2 and 3 apply to the final network topology. For the 2040 case study, the generating capacity from Scenario 2 in the 2030 model is modified. The 800-MW coal-fired power plants (GEN2) are assumed to be refurbished to biomass, respecting the same power rating, but dispatched at 500 MW. Also, a second offshore wind farm of 600 MW is installed at EOS substation, in a similar way as GEMINI.

Table 4.1: Operational scenarios in the N3 area for the years 2030 and 2040 (in MW).

Generator / HVDC link	Year 2030 Scenario 1	Year 2030 Scenario 2	Year 2030 Scenario 3	Year 2040 Scenario 2
GEMINI wind farm (EOS)	0	600	450	2 × 600
GEN1 (EOS)	430	3 × 430	3 × 430	3 × 430
GEN2 (EOS)	0	2 × 800	2 × 800	2 × 500
GEN3 (DZW)	400	233	233	233
NorNed import (EEM)	700	700	700	700
COBRAcable import (EOS)	300	700	-700	700
Total	**1830**	**4890**	**3490**	**4890**

The network shown in Figure 4.1 contains two synchronous generators that represent the remainder of the Dutch network (NL EQ) and a section of the German network (DE EQ), respectively. These were added to make the frequency response in the simulations more realistic. The inertia values of these equivalent generators were estimated from the PSS/E grid model. The control structure and parameters of the generators within the N3 network are based on these of comparable generators in a larger-size system model.

The system load in this region is about 2 GW and is projected from 2018 to the years 2030 and 2040, considering the estimated growth proportion obtained from the Quality & Capacity Plan 2017 (KCD 2017) published by TenneT [35]. Table 4.2 and Table 4.3 show the distribution of the load over the three provinces in this region, together with the aggregation of the load to the higher voltage levels.

Table 4.2: Projected regional electricity demand for the years 2030 and 2040.

Region	Load 2018 [MW]	Load 2030 [MW]	Load 2040 [MW]
Groningen-Drenthe	824	875	893
Overijssel	760	803	820
Friesland	372	397	406
Total	**1956**	**2075**	**2119**
Projected growth w.r.t. 2018	–	+6.1%	+8.3%

For 2030, the demand in each region grows a 6.2%, 5.6% and 6.8% respectively. For 2040, the growth for every region has been estimated as a 2.1% with respect the 2030 values.

Table 4.3: Aggregated system load in the N3 area for the years 2030 and 2040 (in MW).

Voltage	Bus	Year 2030 Scenario 1	Year 2030 Scenario 2	Year 2030 Scenario 3	Year 2040 Scenario 2
≤ 110 kV	DZW	144	229	225	240
220 kV	VVL	579	988	830	989
	MEE	256	255	247	257
380 kV	ENS	27	1194	899	1192
	ZWL	354	869	489	854
	MEE	64	1065	412	1015
Total		**1424**	**4601**	**3101**	**4547**

For scenario 2, although the regional demand is higher in 2040 than in 2030, the influence of the PSS/E grid model for 2040 makes the total power exchange to be lower than in 2030.

A selection of possible contingencies was defined to study the impact of electrolysers on power system stability. Table 4.4 gives an overview of these severe contingencies. Because of the network configurations and the generator dispatches, not all contingencies are simulated for all scenarios. In particular, the disconnection of 2 generators at EOS is not included for the year 2030, since this disturbance would be too severe in comparison with the total frequency support reserve assigned in the studied part of the Dutch transmission network, and therefore, the electrolyser influence cannot be determined accurately for such contingency.

Table 4.4: List of the contingencies considered for each scenario.

Contingency	Year 2030 Scenario 1	Year 2030 Scenario 2	Year 2030 Scenario 3	Year 2040 Scenario 2
Disconnecting COBRA	✓	✓	✓	✓
Disconnecting NorNed	✓	✓	✓	✓
Disconnecting GEMINI	–	✓	✓	✓
Disconnecting 1 generator at EOS	✓	✓	✓	✓
Disconnecting 2 generators at EOS	–	–	–	✓
Tripping 2 circuits between EOS-VVL	–	✓	✓	✓
3-phase short circuit at VVL	✓	✓	✓	✓

4.2 The 300-MW Electrolyser Model

In order to study the impact of a large-scale electrolyser in the Northern Netherlands Network, the 1-MW electrolyser model presented in Section 3.2 has been scaled up to a model of a 300-MW electrolyser plant. An aggregated electrolyser model was created by scaling up the electrolyser stack, thereby assuming a series connection of individual electrolyser cells. The electrolyser is connected to the grid by a AC/DC converter, as illustrated in Figure 4.2. Similar to the 1-MW electrolyser model, this 300-MW electrolyser model has been equipped with a control system to provide frequency and voltage control. A detailed description of this control system can be found in Appendix B.

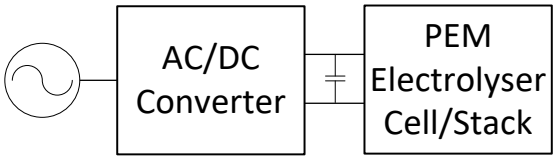

Figure 4.2: Component of the power conversion system of the 300-MW electrolyser.

Although the electrolyser model shown in Figure 4.2 does not represent the real implementation of an electrolyser plant, this simplified model is sufficiently accurate for grid studies. Research is currently being continued to develop a model that accurately corresponds to the actual configuration of an electrolyser farm, which is a parallel connection of many smaller electrolyser stacks, each with a capacity of several MWs. As shown in Appendix B, the electrical response of such a detailed model is effectively the same as the response of the simplified model shown in Figure 4.2. However, the detailed electrolyser model can provide more insight into the dynamics within an electrolyser plant. The main challenge of implementing this model in real-time simulations is however the limited capacity of the Real-Time Digital Simulator (RTDS).

4.3 Implementation of COBRAcable Frequency Control

HVDC connections like COBRAcable could contribute to frequency support in power systems as well. To study the potential of frequency control by HVDC connections, the impact of frequency support in the Northern Netherlands Network by COBRAcable has been studied. Although frequency support of

the European power system by COBRAcable would not have an impact as COBRAcable is embedded within the European system (unless in the case of a system split), this study provides general insight into the possibilities of frequency support by HVDC connections. For this purpose, frequency control has been implemented in the COBRAcable model, as illustrated in Figure 4.3. Frequency control requires variation of the power transferred through the cable, based on frequency deviations in one of the national power systems. This is relatively easy if the frequency deviation occurs at the side of the HVDC connection where the power is controlled, but becomes more complicated if the power is controlled at the other side of the connection. In this case, the converter station in the Netherlands sets the DC voltage, while the converter station in Denmark controls the power. If a frequency deviation occurs in the Netherlands, this must be communicated to the Danish side of the system. In this case, this is done by superimposing a signal onto the DC voltage, which is detected and decoded in the converter station in Denmark. The converter station in Denmark then changes its power setpoint based on the frequency deviation in the Netherlands. Further controls can be implemented to enable frequency control under various operational scenarios and in cases of frequency deviations at both sides.

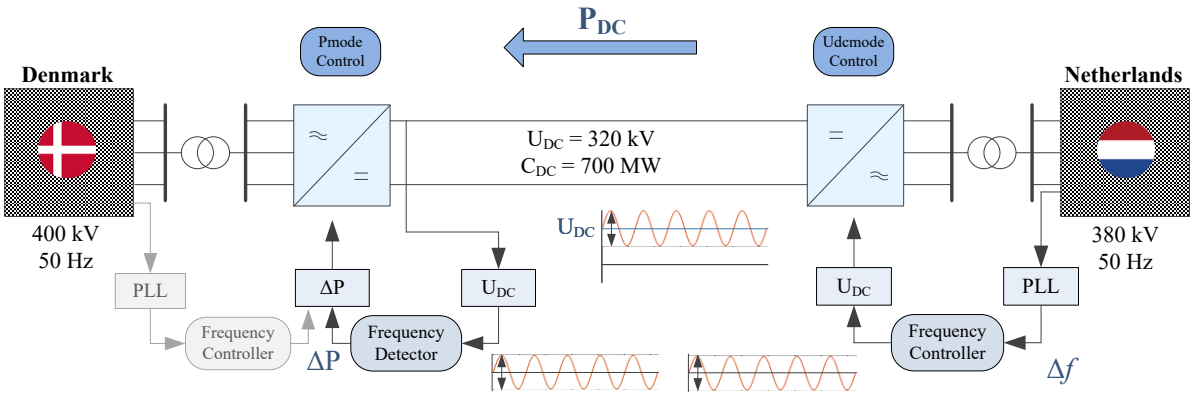

Figure 4.3: Implementation of frequency control by COBRAcable.

4.4 Simulations of Disturbances and Contingencies

The contingencies previously listed in Table 4.4 have been simulated to study the potential participation of electrolysers in ancillary services. The following sections discuss the impact of electrolysers on frequency stability, voltage stability and congestion management, respectively.

4.4.1 Contribution of Electrolysers to Frequency Stability

For the frequency simulations, several assumptions regarding FCR provision were made. In line with [10] and [12], a capacity of ±300 MW was assigned in the N3 network. In scenarios 2 and 3 (cf. Table 4.1), the three power plants within the N3 network and the equivalent generator that represents the rest of the Netherlands have an approximate reserve of ±25 MW each, while the equivalent generator that represents part of the German grid has a reserve of ±200 MW. In scenario 1, the values of the Dutch generators were increased to ±35 MW to keep the total FCR support constant. The electrolyser operates at rated capacity in all three scenarios (i.e. 300 MW). For such reason, FCR reserve is not symmetric, as the electrolyser can only reduce its consumption in response to frequency drops. The reserve is set to -25 MW in scenarios 2 and 3, and to 35 MW in scenario 1. The

FCR reserves of the Dutch generators and the electrolyser are the same, such that the simulations can effectively compare the cases in which the frequency support comes exclusively from synchronous generators with the case in which the frequency support of one of the generators in the Netherlands is substituted by the electrolyser. Thus, the share of FCR reserve provided by electrolyser is 8.5% in the proposed case study (i.e. 25 out of 300 MW).

Simulations of the Frequency Response

Figure 4.4 shows an example frequency response for the disconnection of COBRAcable in scenario 2 of 2030. As COBRAcable is importing power, the frequency drops as the synchronous generators in the system slow down. The frequency response is influenced by the inertia of the system, the control parameters of the generators (and other frequency reserve suppliers) and the severity of the disturbance. As the graph shows, electrolysers contribute to limit the maximum frequency deviation (i.e. frequency nadir) by reducing their power consumption. The effects are more noticeable for larger installed electrolyser capacities. The oscillations in the first seconds of the frequency response are caused by electromechanical oscillations of the generators in the system. The relatively large frequency deviation is a direct result of the limited size of the selected test network (i.e. the Northern Netherlands Network). Moreover, disconnection of COBRAcable would not affect the frequency of the European power system in reality, as it is embedded within the European system. The frequency deviation within the European system would be significantly smaller for a loss of import (or generation) of this size. Nevertheless, the studies described in this section provide general insight into the theoretical possibilities of frequency support by electrolysers and HVDC connections.

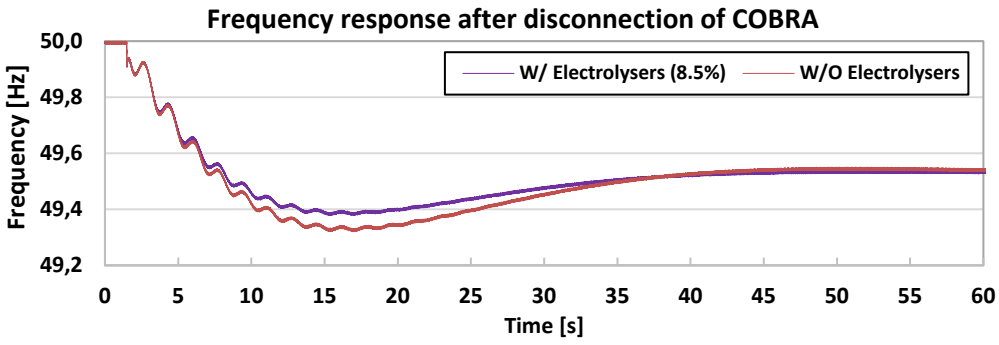

Figure 4.4: Frequency response after disconnection of COBRA, for 300 MW FCR reserve (2030 scenario 2).

Similar simulations have been performed for all contingencies listed in Table 4.4. A summary of the results is shown in Table 4.5. Table 4.6 to Table 4.9 show the numerical results of these simulations. The results show that the participation of electrolysers improves every situation in which generation or power import is lost. Since the electrolyser is operating at rated power in the considered scenarios, support cannot be provided in the case of a loss of energy export (or demand), which is the case when COBRAcable is disconnected in scenario 3 of 2030. Because in this simulation, some FCR support by conventional generators is replaced by the electrolyser, which cannot ramp up its consumption further, the total FCR support in the system is reduced, which leads to a worse situation. As shown later in the sensitivity analyses in this section, this changes to an improvement if the electrolyser is operating at a smaller capacity. A combination with fuel cells could be another solution (see also Appendix A). Table 4.5 also shows that the frequency performance for the short-

circuit and line-tripping contingencies is not influenced significantly by the electrolyser. This is because in these cases, there is no significant change in the power balance.

Table 4.5: Improvement of the frequency nadir when electrolysers are installed in the system.

Contingency	Year 2030 Scenario 1	Year 2030 Scenario 2	Year 2030 Scenario 3	Year 2040 Scenario 2
Disconnecting COBRAcable	6%	6%	< 0%	6%
Disconnecting NorNed	12%	6%	6%	6%
Disconnecting GEMINI	–	6%	4%	5%
Disconnecting 1 generator at EOS	7%	5%	6%	4%
Disconnecting 2 generators at EOS	–	–	–	3%
Tripping 2 circuits between EOS-VVL	–	0%	0%	0%
3-phase short circuit at VVL	0%	0%	0%	0%

The improvement in % is calculated by: $\left(f_{with.electrolyser} - f_{without.electrolyser}\right) / \left(50 - f_{without.electrolyser}\right)$.

Table 4.6: Summary of the results obtained for the 2030 scenario 1.

Contingency	Frequency Nadir [Hz]		Improvement	
	w/o electrolysers	with Electrolysers	[mHz]	[%]
Disconnecting COBRAcable (300 MW)	49.700	49.718	18	6%
Disconnecting NORNED (700 MW)	49.168	49.267	99	12%
Disconnecting 1 gen. EOS (430 MW)	49.504	49.537	33	7%
3-phase short circuit at VVL	Equal performance in both cases		-	0%

Table 4.7: Summary of the results obtained for the 2030 scenario 2.

Contingency	Frequency Nadir [Hz]		Improvement	
	w/o electrolysers	with electrolysers	[mHz]	[%]
Disconnecting COBRAcable (700 MW)	49.211	49.255	44	6%
Disconnecting NORNED (700 MW)	49.210	49.255	45	6%
Disconnecting GEMINI (600 MW)	49.318	49.357	39	6%
Disconnecting 1 gen. EOS (800 MW)	49.033	49.086	53	5%
Tripping 2 circuits at EOS-VVL	Equal performance in both cases		-	0%
3-phase short circuit at VVL	Equal performance in both cases		-	0%

Table 4.8: Summary of the results obtained for the 2030 scenario 3.

Contingency	Frequency Nadir [Hz]		Improvement	
	w/o electrolysers	with electrolysers	[mHz]	[%]
Disconnecting COBRAcable (-300 MW)	50.882	51.102	-220	-25%*
Disconnecting NORNED (700 MW)	49.224	49.269	45	6%
Disconnecting GEMINI (450 MW)	49.553	49.569	16	4%
Disconnecting 1 gen. EOS (800 MW)	49.035	49.090	55	6%
Tripping 2 circuits at EOS-VVL	Equal performance in both cases		-	0%
3-phase short circuit at VVL	Equal performance in both cases		-	0%

*As in the simulation, the electrolysers are operating at rated capacity and cannot ramp up their consumption further, while FCR support of some conventional generators is replaced by electrolysers, the total FCR support in the system reduces and the frequency nadir becomes worse in this specific case.

Table 4.9: Summary of the results obtained for the 2040 scenario 2.

Contingency	Frequency Nadir [Hz]		Improvement	
	w/o electrolysers	with electrolysers	[mHz]	[%]
Disconnecting COBRAcable (700 MW)	49.204	49.249	45	6%
Disconnecting NORNED (700 MW)	49.203	49.249	46	6%
Disconnecting GEMINI (600 MW)	49.382	49.414	32	5%
Disconnecting 1 gen. EOS (500 MW)	49.487	49.506	19	4%
Disconnecting 2 gen. EOS (1000 MW)	48.192	48.240	48	3%
Tripping 2 circuits at EOS-VVL	Equal performance in both cases		-	0%
3-phase short circuit at VVL	Equal performance in both cases		-	0%

Sensitivity Analysis: Loss of Generation Capacity

To study the potential contribution of electrolysers to frequency stability further and to compare it to the performance of COBRAcable, two sensitivity analyses have been performed. In the first, a loss of generation capacity is considered. This case study is based on scenario 3 of 2030 (Table 4.1). For this purpose, the generation at EOS substation is reduced by 200 MW by decreasing the power generated by GEMINI wind farm. In this study, there is a total of 300 MW FCR support in the system, divided over the generators (i.e. DE-EQ 190 MW, NL-EQ 30 MW, GEN1 2×15 + 1×20 MW, GEN2 0 MW, GEN3 30 MW). The participation of the electrolyser or COBRAcable in FCR is varied from 0 to 100% by replacing FCR support of some generators with FCR support by the electrolyser or COBRAcable.

The results of these simulations are shown in Figure 4.5. It can be seen that the replacement of FCR support by the electrolyser or COBRAcable has a positive effect on the frequency stability of the system, as the electrolyser and COBRAcable have the ability to respond faster to deviations of the frequency than conventional generators. The performance of the electrolyser is slightly better than the performance of COBRAcable, which is caused by the delay in the communication system implemented in COBRAcable. The oscillation of the frequency completely disappears when the electrolyser takes over the full FCR support, as electro-mechanic oscillations of the generators do not occur then. Simulations with different electrolyser ramp rates (i.e. 150 and 750 MW/s; 0.5 and 2.5 pu/s) have been performed, but this did not result in significantly different results as the Rate-of-Change-of-Frequency (RoCoF) is small in comparison to the ramp rate of the electrolyser.

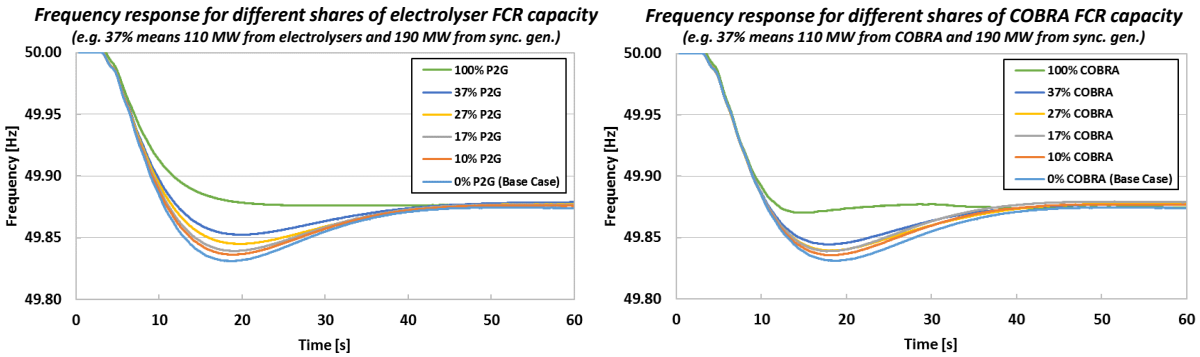

Figure 4.5: Frequency response of the system with different shares of electrolyser FCR capacity (left) or COBRAcable FCR capacity (right) for a loss of 200 MW generation capacity.

Sensitivity Analysis: Loss of Load

In the second case study, a loss of load is considered. For this purpose, operational scenario 3 of 2030 (Table 4.1) has been modified. GEN2 at EOS substation has been reduced to 2× 650 MW; COBRAcable import has been reduced to -510 MW; the electrolyser operational setpoint has been reduced to 190 MW. This enables upwards regulation of the electrolyser consumption in the case of a loss of load. Electrolyser FCR support and COBRAcable FCR support up to 37% of the total FCR support is considered. In this sensitivity analysis, the loss of load is simulated by reducing the load at MEE380 substation by 200 MW. The results of these simulations are shown in Figure 4.6. Similar to the loss of generation capacity, it can be concluded that the electrolyser and COBRAcable have a positive effect on the frequency stability as the electrolyser and COBRAcable are able to respond faster than conventional generators to deviations of the frequency. Also in these simulations, the electrolyser performs somewhat better than COBRAcable.

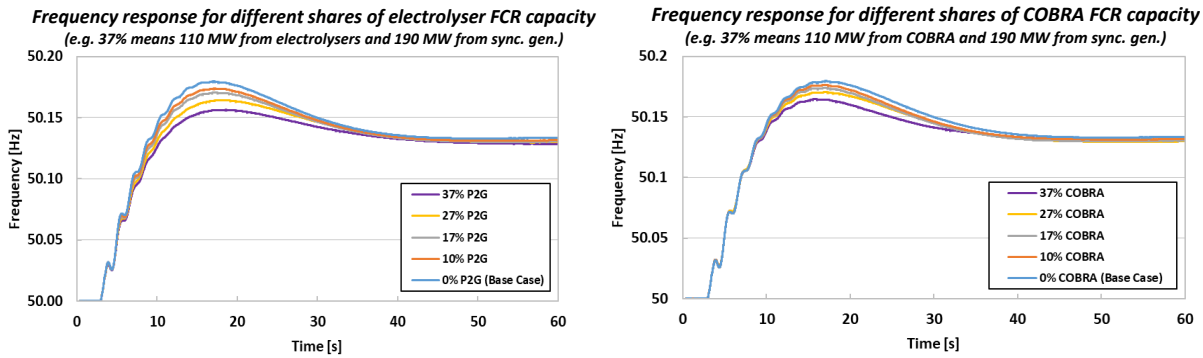

Figure 4.6: Frequency response of the system with different shares of electrolyser FCR capacity (left) or COBRAcable FCR capacity (right) for a loss of 200 MW demand.

4.4.2 Contribution of Electrolysers to Voltage Stability

Simulation of the Voltage Response

The simulations of the voltage response concentrates on the disturbance case of Table 4.4 in which a grid fault occurs, i.e. the 3-phase short circuit at VVL. Voltage control by the electrolyser has been implemented by a droop characteristic that injects the maximum possible reactive power during the short-circuit, while respecting the converter rating.

Figure 4.7 shows an example voltage response for a 3-phase short-circuit fault with a duration of 100 ms for scenario 2 of year 2030. In this case, the electrolyser operates at rated power and, thus, no extra converter capacity is available for voltage control. If operating below rated power, it is possible to influence the voltage response, either directly by reactive power control or indirectly by active power control. Nevertheless, the measured voltage response complies with the grid code requirements in every scenario (i.e. the fault is cleared within 250 ms and the voltage is 0.70 pu 50 ms, and 0.85 pu 1.25 seconds after clearing the fault).

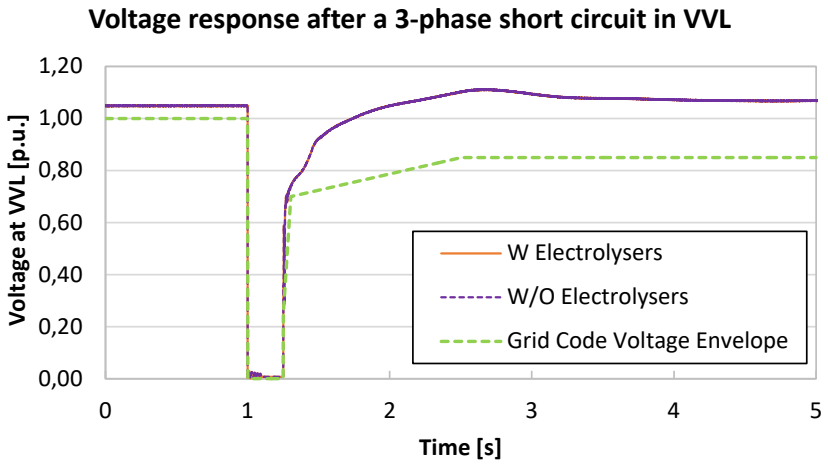

Figure 4.7: Voltage response after a 3-phase short circuit in VVL (2030 scenario 2).

Sensitivity Analysis: 3-Phase Short Circuit at VVL

To study the potential contribution of electrolysers and COBRAcable to voltage support further, a sensitivity analysis has been performed. This sensitivity analysis is based on 2030 scenario 3, in which the electrolyser is operating at 300 MW. For this sensitivity analysis, the grid is weakened by disabling some of the generator AVRs (Automatic Voltage Regulators). Electrolyser operation at 190 MW is considered as well by making the same modifications as in the second sensitivity analysis of the frequency response (i.e. the loss-of-load case).

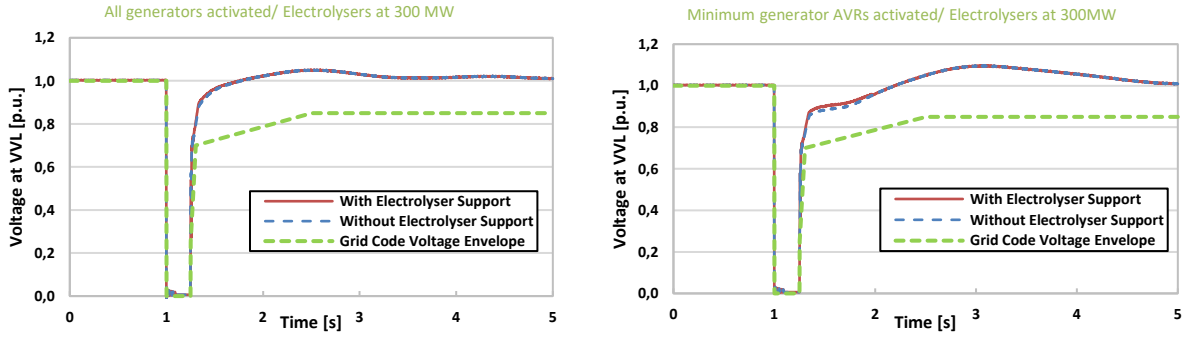

Figure 4.8: Voltage response after a 3-phase short circuit in VVL with the electrolyser operating at 300 MW.

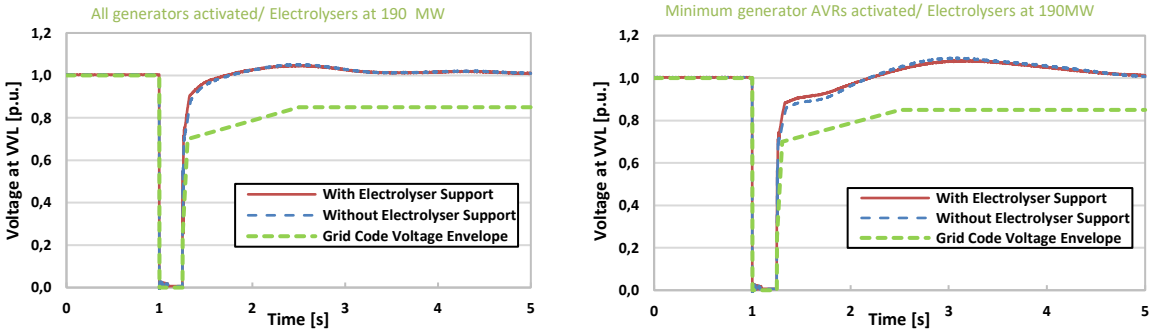

Figure 4.9: Voltage response after a 3-phase short circuit in VVL with the electrolyser operating at 190 MW.

Figure 4.8 and Figure 4.9 show the results of these simulations. The simulations show that the contribution of the electrolyser to voltage support is only marginal, but somewhat larger when it is operating at 190 MW or when some of the generator AVRs are disabled. This limited contribution is because there are already several other facilities (e.g. generators, HVDC, offshore wind farms) that contribute to voltage stability in this area. Furthermore, as the electrolyser's voltage support is limited by its converter capacity, the electrolyser can only manage reactive power when operating below 300 MW and the amount of available reactive power depends on the active power consumption. Because of the current requirements for voltage support, participation in voltage support would mean operation at a capacity smaller than rated or an over-dimensioned converter.

4.4.3 Contribution of Electrolysers to Congestion Management

Load Flow and Contingency Analysis

Electrolysers can potentially contribute to congestion management by reducing the loading of transmission lines when these tend to become overloaded during contingencies or during period with an abundance of generation from renewable sources. To study the potential contribution of electrolysers to congestion management, load flow and contingency analyses of the test model of Northern Netherlands Network have been performed for all operational scenarios of Table 4.1. First, the load flow during normal operation (i.e. without contingencies) was performed. The results of this can be seen in Figure 4.10 and Figure 4.11. Due to its similar net consumption per substation, the load flow of 2040 scenario 2 is essentially the same to the load flow of 2030 scenario 2. From the figures, it can be seen that the maximum loading percentage of any transmission line in all of the scenarios does not surpass the 45%. This shows that the transmission network in this area is rather robust, under the assumed operational scenarios.

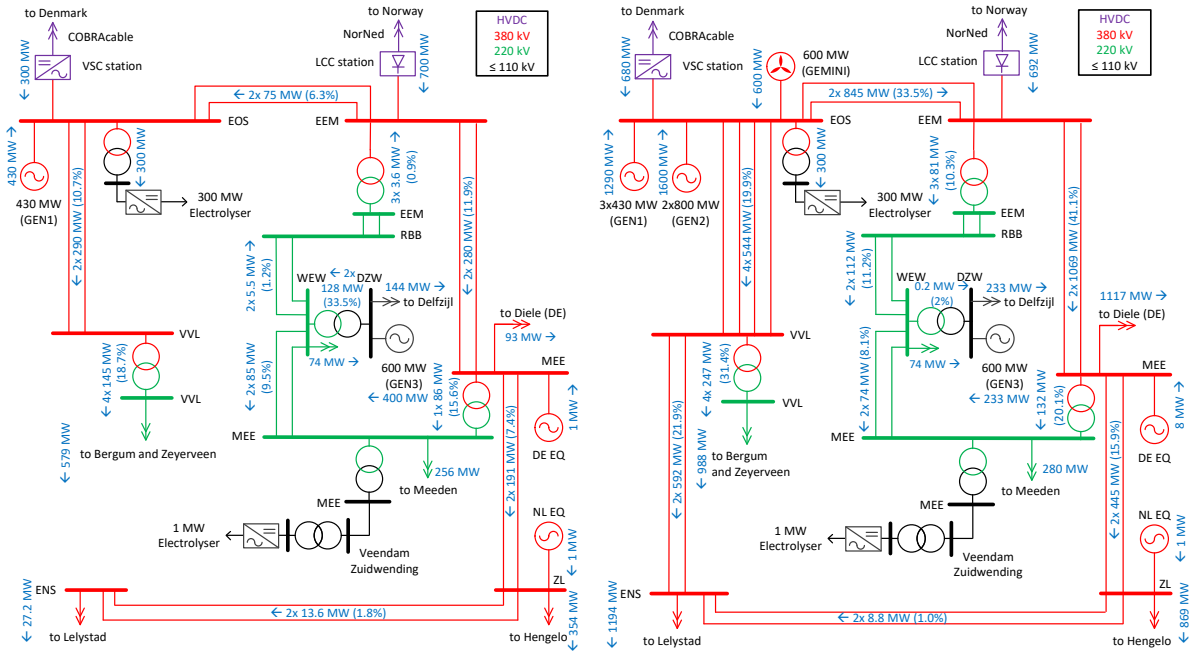

Figure 4.10: Power flow result for year 2030 scenario 1 (left) and 2030 scenario 2 (right).

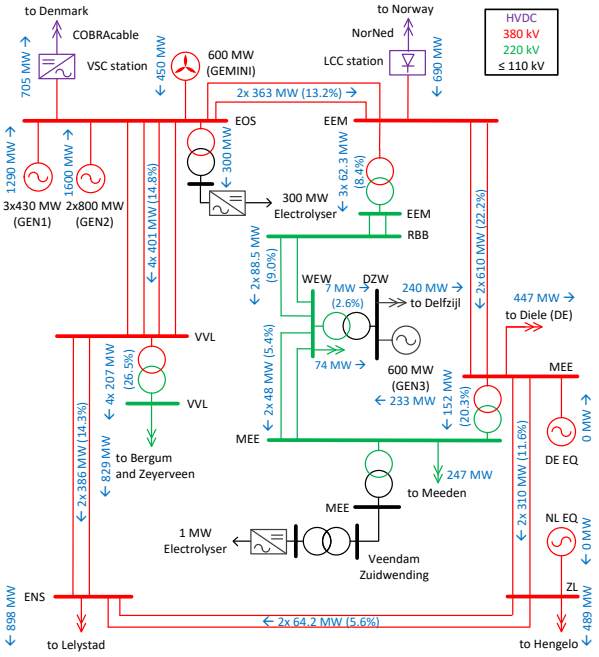

Figure 4.11: Power flow for year 2030 scenario 3.

For all operational scenarios, contingency analyses have been performed to find the component loadings during single and double contingencies. Table 4.10 gives an overview of the most severe contingencies. It can be seen that the highest component loading is about 70%. Consequently, the grid infrastructure in this area is robust and critical congestion issues are not foreseen for the considered operational scenarios. Network congestion could however be an issue for operational scenario with more production in this area. Then, electrolysers could contribute to congestion management by varying their power consumption.

Table 4.10: Most severe contingencies.

Scenario	Component	Loading	Contingency	Level
2	L_EEM_MEE(1/2)	70.7%	L_EEM_MEE(1/2)	1
1	TR_MEE	67.7%	L_EEM_MEE(1&2)	2
1	TR_WEW(1/2)	67.2%	TR_WEW(1/2)	1
2	L_EOS_EEM(1/2)	66.7%	L_EOS_EEM(1/2)	1
2	TR_VVL(2x)	63.1%	TR_VVL(2x)	2
2	TR_MEE	61.7%	L_EEM_MEE(1&2)	2
2	L_VVL_ENS(1&2)	54.4%	L_EOS_EEM(1&2)	2
3	TR_VVL(2x)	53.1%	TR_VVL(2x)	2
2	L_ENS_ZL(1&2)	51.3%	L_EOS_EEM(1&2)	2

Mitigating the Variability of Renewable Energy Sources

Besides the provision of the traditional electrical ancillary services, electrolysers could offer other functionalities for the short-term balancing of renewable energy sources. Specifically, the stochastic variability of these sources could be controlled by adapting the consumption of nearby electrolysers to the variations of wind speed and solar irradiance [22].

A theoretical example of the coordinated operation between a wind park and a large power-to-gas plant is shown in Figure 4.12. Assuming that both facilities are connected to the same bus in the grid, the ramping speed of electrolysers could facilitate the absorption of power fluctuations, allowing to forecast a constant active power injection to the remainder of the grid, in similar fashion to classic dispatchable generators. The electrolysers could still be scheduled to achieve the planned hydrogen production without compromising production at the highest capacity during periods of inexpensive electricity. When the electricity price is not competitive (e.g. peak hours), the system can completely shut down or it can operate at partial loading level. If shut down, the control system of the renewable energy power plant and/or other technologies should take care of the mitigation of its instantaneous variability. However, the electrolysers could be ordered to increase their consumption or to come back online at any moment to avoid the curtailment of surplus renewable power.

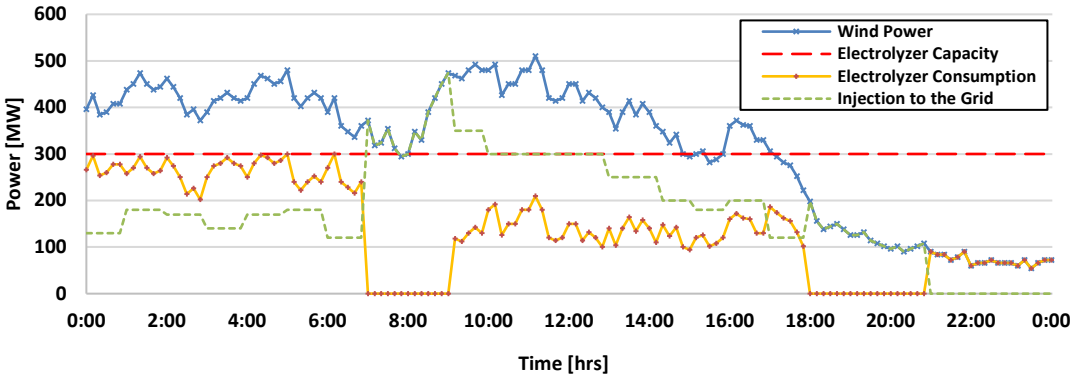

Figure 4.12: Coordinated operation between a wind park and a large-scale power-to-gas facility.

4.5 Conclusions

This chapter discussed the possible contribution of large-scale electrolysers to frequency and voltage stability and congestion management of interconnected power systems like the Northern Netherlands Network. The 1-MW electrolyser model of the previous chapter was scaled up to a model of a 300-MW electrolyser. Furthermore, frequency control was implemented in the model of COBRAcable. The network model was implemented in RSCAD and several operational scenarios and disturbances were defined. The behaviour of the electrolyser and COBRAcable was simulated in various simulations.

The simulations discussed in this chapter generally show that a large electrolyser can have a positive effect on the frequency stability of the power system when participating in FCR, as electrolysers are able to ramp up/down their power consumption must faster than conventional generators. Frequency control by HVDC connections like COBRAcable also has a positive impact, but the effect of the electrolyser is more pronounced. The electrolyser and COBRAcable can also help stabilise the frequency after a more severe event like a split of the European power system, as described in Appendix C. An electrolyser can provide frequency support after loss of a generator by decreasing its consumption and in the case of a loss of load, the electrolyser can increase its consumption. In order to make this possible, the electrolyser should operate between a certain minimum (i.e. larger than 0) and maximum (i.e. smaller than rated) level. Participation in this particular ancillary service is therefore a trade-off between a higher hydrogen production or participation in frequency support. Future asymmetric frequency support could be a solution in this case.

The simulations of the voltage stability showed that the impact of the electrolyser is small in this particular network. In this network, there already is a large capacity of facilities that contribute to voltage stability (e.g. conventional generators, HVDC interconnections, offshore wind farms). The added value of a large electrolyser in this area is therefore marginal. Nevertheless, electrolysers could help improve local voltage stability in more remote areas with less voltage support by other facilities (e.g. in the studied test system in Appendix D). In order to provide voltage support, the electrolyser must be able to vary its reactive power consumption independently from its active power consumption, as large changes in active power consumption can influence the frequency of the power system. For this purpose, a certain capacity of the converter must be reserved. This means either operation at a capacity smaller than rated or an over-dimensioned electrolyser converter.

The possibilities for contribution to congestion management have been analysed by performing load flow and contingency analysis of the network for the defined scenarios. The load flow analyses showed that all lines in the network are loaded below 45% during normal operation. The contingency analyses showed that the most severe loading under a contingency is 70%. From these studies, it can be concluded that the network in this area is rather robust and congestion issues are not foreseen for the considered operational scenarios. Nevertheless, electrolysers can theoretically contribute to congestion management by varying their consumption (e.g. in the studied test system in Appendix D), thereby influencing the load flow in the network. Electrolysers can also help to mitigate the variability of large-scale renewable generation like offshore wind. Electrolysers located near to renewable generation could absorb short-term variations of this renewable generation, thereby making the injection of power into the grid more predictable or, to some extent, dispatchable.

5 Implementation of Electrical Services Provision by Electrolysers

In order to facilitate participation of electrolysers in ancillary services, electrolysers must be equipped with appropriate controllers. The electrolyser models presented in the previous chapters include controllers to enable frequency and voltage support. The practical implementation of these controllers needs to be considered as well and is therefore discussed in this chapter. Hardware-in-the-Loop (HIL) simulation is useful when studying the possibilities of new control approaches. In HIL, part of the studied system (e.g. the Northern Netherlands Network) is simulated on the Real-Time Digital Simulator (RTDS), while a real device (e.g. a controller) is connected to the RTDS. This provides more information about how the device under study performs in reality. Section 5.1 presents the HIL setup as used for the studies described in this chapter. A next step towards participation in ancillary services provision is the fulfilment of prequalification requirements. These are defined by TSOs and all providers of ancillary services must comply with these requirements. For frequency support, it is studied whether electrolysers can comply with the FCR (Frequency Containment Reserve) requirements in Section 5.2. Various control strategies can be developed for FCR support by electrolysers. These control strategies are discussed and compared in Section 5.3. In this section, the frequency support by electrolysers is also compared to frequency support by other (renewable) technologies like solar plants with Battery Energy Storage Systems (BESS). The general conclusions of these studies are summarised in Section 5.4.

5.1 Hardware-in-the-Loop Testing

In Hardware-in-the-Loop (HIL) simulations, a real device is connected to power system simulator like the RTDS, in order to study its performance in reality. HIL simulations offer a cost-effective and safe method to test physical devices under real-time operating conditions. Real-time HIL simulation is the standard for developing and testing the most complex control, protection and monitoring systems. Real-time HIL is classified as Control Hardware-in-the-Loop (CHIL) and Power Hardware-in-the-Loop (PHIL). Testing of control systems has traditionally been carried out directly on physical equipment in the field, on the full system or on a power testbed in a lab. While offering testing fidelity, this practice can be expensive, inefficient and potentially unsafe, such that HIL is preferred.

For the grid studies of the TSO2020 project, an HIL test setup has been developed to design new electrolyser controllers and demonstrate their compliance to the prequalification tests of ancillary services. Figure 5.1 shown an overview of the HIL setup as implemented in the RTDS lab of the Intelligent Electric Power Grid (IEPG) group at TU Delft, while a photo of the actual setup is shown in Figure 5.2. In this case, the Northern Netherlands Network has been modelled in RSCAD and is simulated on the RTDS NovaCor. The NovaCor communicates with the Device Under Test (DUT), which is a AC/DC converter, via the Real Time Target (RTT) computer. This RTT also contains the model of the considered control strategy. An emulator of the electrical network, connected to the 3-phase 400-V grid, constitutes the electrical (power) connection of the DUT. This emulator consists of a combined front-end and voltage source converter. The following paragraphs describe the developed test setup in more detail.

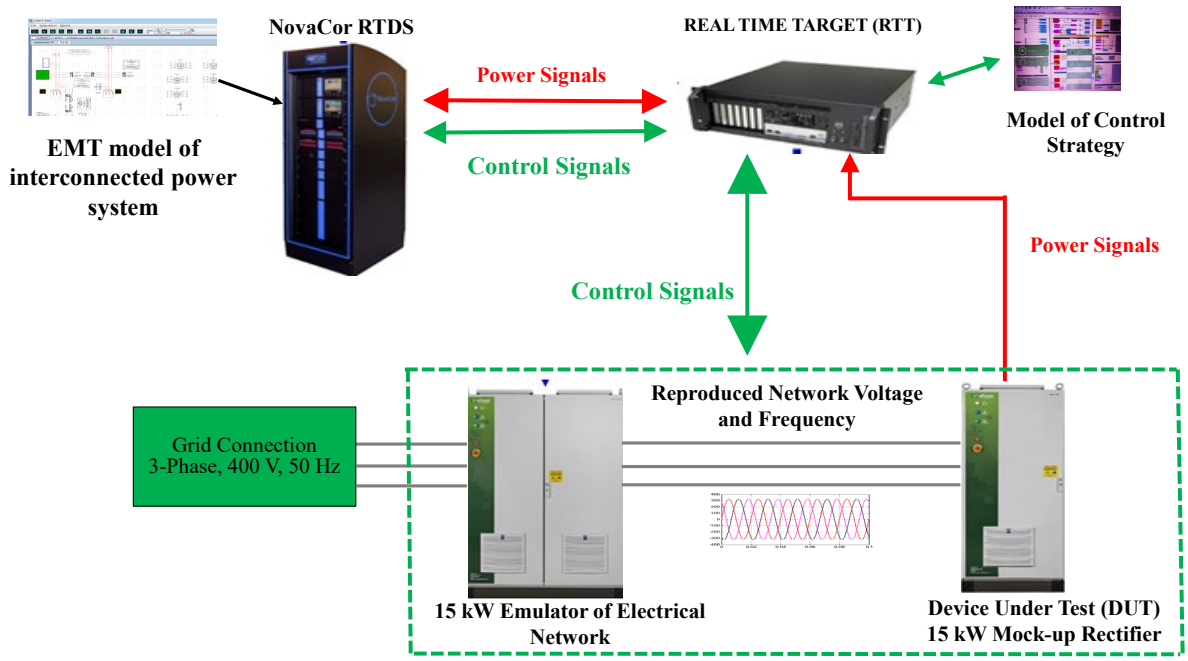

Figure 5.1: Overview of the Hardware-in-the-Loop (HIL) setup.

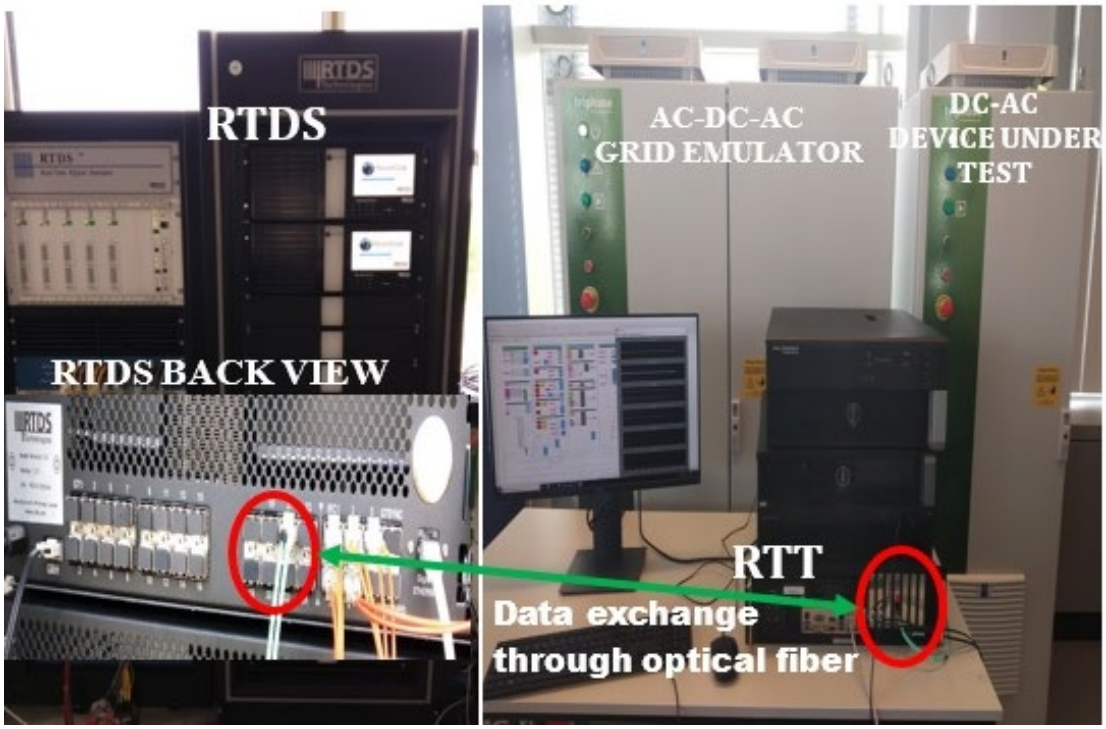

Figure 5.2: HIL test setup in the RTDS lab.

NovaCor Real-Time Digital Simulator

NovaCor is a new generation of simulation hardware for the RTDS. It is the world's fastest and most capable real-time power system simulator and is based on a powerful multicore processor. Hundreds of network nodes can be solved on a single core, such that NovaCor allows an entire power system simulation to be run on a single core. The RTDS allows external devices to be interfaced to the power system being simulated. By interfacing the physical devices to the simulation, the user is able to characterise the device's behaviour and impact on the system. Various contingency scenarios can be run in a controlled environment to evaluate the performance of the Device Under Test (DUT) before it is connected to the actual physical system. Simulation cases can be run to check that the device settings are appropriate and the device's behaviour under extreme or unusual operating conditions can be verified.

Real-Time Target

The Triphase Real-Time Target (RTT) is a powerful, multicore PC-based unit equipped with a real-time Linux/Xenomai-based operating system. The real-time inter-PC interface enables the RTT to connect in real time to other real-time simulators, such as the RTDS and OPAL-RT (OP5600), and external control units. This enables the creation of HIL setups as well as the supervisory control of clusters of Power Modules (PM) systems.

Grid Emulator Power Module

The grid emulator power module consists of a Back-to-Back (B2B) voltage source converter, i.e. a grid-connected active front-end converter and a voltage source converter. The front-end converter's main function is to keep the DC link voltage constant, while the voltage source converter produces the desired voltage and frequency at its terminals. The software model of the grid emulator power module was developed in Matlab/Simulink.

The functionalities of the grid emulator power module are divided into four subsystems:

1. A **hardware subsystem** offering a logical interface to the PM hardware measurements and actuators. This block is part of the firmware delivered with the PM system. It should never be changed by end-users.
2. An **interlocks subsystem** that checks whether it is safe or not to enable a particular control or software feature.
3. **Application components** that take care of voltage control, current control, motor drive control, and power flow management.
4. A **command centre subsystem** that provides a cockpit to operate the application from within the Simulink environment. The command centre subsystem is the part of the Simulink application managing user set-points. The command centre serves two major functions: (i) providing users with a local cockpit to manipulate application settings from the Simulink environment; (ii) setpoint selection and routing. Setpoints can originate from multiple sources. There is the possibility to have them set from within the Simulink environment. However, it is also possible for setpoints to be specified from the remote real-time simulator. The command centre implements the necessary logic to select the desired source of setpoints and to route setpoint values accordingly. When parameter values are changed in the Simulink environment, these changes propagate to the Triphase RTT and apply to the application as it runs in real time.

Similarly, real-time measurement data is continuously channelled from the RTT to the scopes in the Simulink model on the engineering PC. This allows to dynamically interact with a running application. In this setup, setpoints are taken from the RTDS on which the power system model is running.

Mock-Up Converter

The mock-up converter is an AC to DC converter. It has an active and reactive power current reference as setpoint. It injects active and reactive power into the grid depending on the control strategy and grid operating parameters (i.e. voltage and frequency). The reference current can be set locally or from other real-time processors.

The Communication Protocol between RTDS and RTT

The setpoints or reference values for the grid emulator or mock-up converter are fed either locally or from another RTDS on which the power system model is running. The data exchange protocol between RTT and RTDS is illustrated in Figure 5.3. Aurora is a communication protocol which helps in exchanging information between RTDS simulations and external devices (i.e. RTTs), while the RTT uses a Circular Inter-Process Communication (CIPC) buffer. It is a shared memory strategy based on ring-buffers to allow Matlab/Simulink models to communicate with each other and other processors. Each buffer has one writer block that writes data into the buffer, from which multiple readers can read out the data. A standard Simulink model using buffers as communication infrastructure has a write functionality and/or a read functionality. To interpret the data in the buffers correctly, the read and write blocks in Simulink make use of bus definitions. The bus definitions contain the names and sizes of the signals in the buffer. The sizes of the signals entered in the write block need to cohere to these bus definitions and the signals extracted from the read block will have the names and sizes defined in the bus definitions.

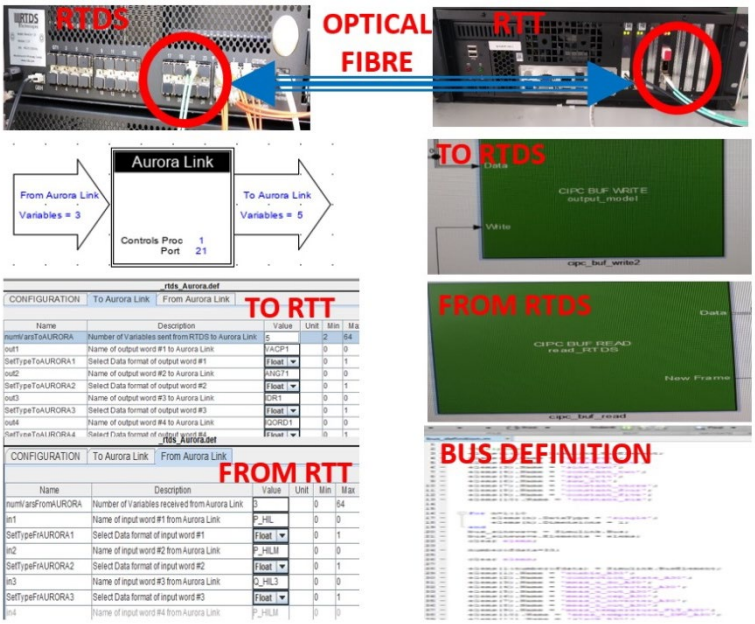

Figure 5.3: Data exchange protocol between the RTT and the RTDS.

5.2 Frequency Containment Reserve Prequalification

In order to participate in frequency support, providers of this service must comply to the requirements set by the TSOs. For example, the prequalification requirements for FCR (Frequency Containment Reserve) are described by TenneT TSO in [36], while the prequalification requirements for Enhanced Frequency Response (EFR) are specified by NationalGrid in [13]. An overview of the FCR prequalification requirements by TenneT is shown in Figure 5.4. The prequalification tests consist of step changes and linear sweeps, which must be completed within a specified time. A duration test is performed to study whether the device is able to follow a system frequency for a longer duration.

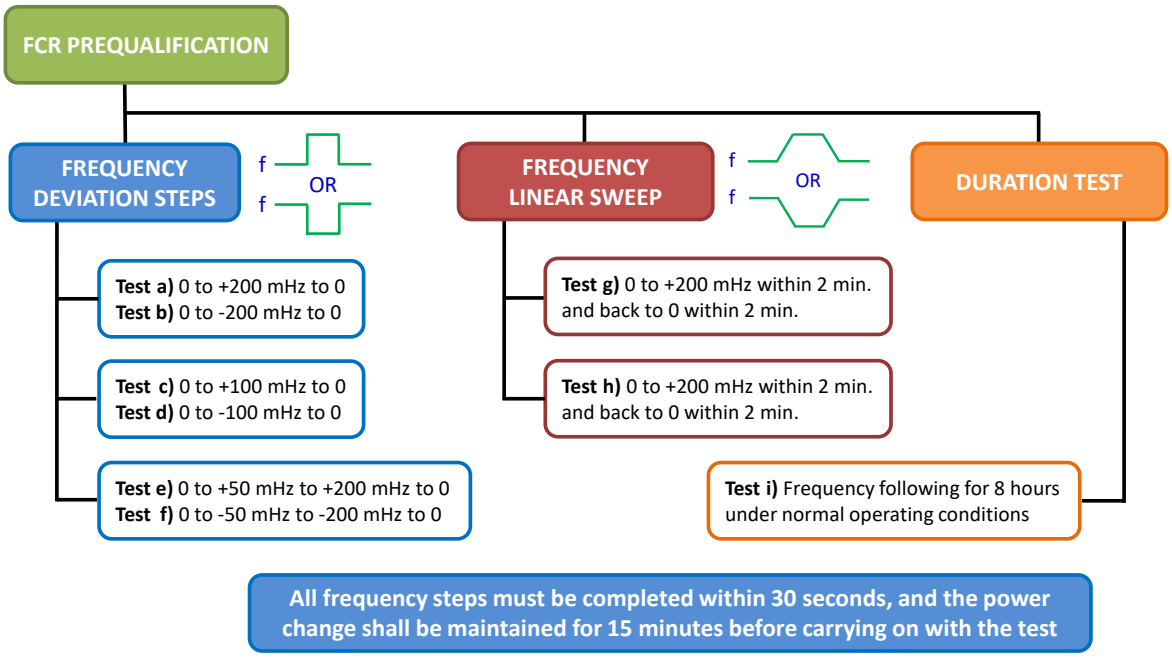

Figure 5.4: Overview of the FCR prequalification requirements as specified by TenneT TSO.

With the developed electrolyser model, it is possible to study whether an electrolyser is theoretically able to comply with the FCR prequalification requirements. For this purpose, the frequency control of the electrolyser has been changed to respond to an external signal rather than responding to the measured system frequency. This external signal can then be a step change, a ramp or a time series. Figure 5.5 shows the result of the simulations for the frequency step changes and the frequency sweeps. As the ramp rate of the electrolyser is much faster than the required 30 seconds, the electrolyser easily complies with the step change requirements. In addition, the electrolyser is able to accurately follow the specified frequency sweeps.

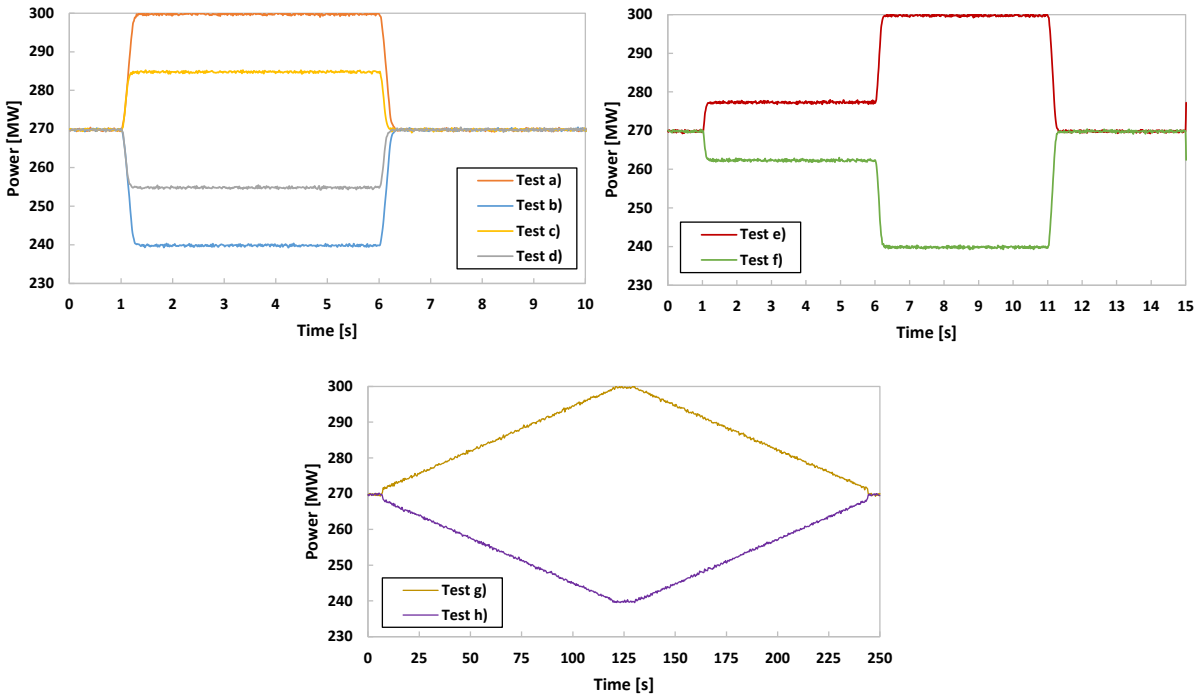

Figure 5.5: Simulation of the electrolyser response in the FCR prequalification tests.

Figure 5.6 shows the simulation result of the frequency following test. Here, a time series of measured frequencies from the UK power system was used as an external signal for the electrolyser model. The response of the electrolyser shows that it follows the frequency deviations by varying its active power consumption. The active power variation of the electrolyser is limited by the capacity reserved for this purpose.

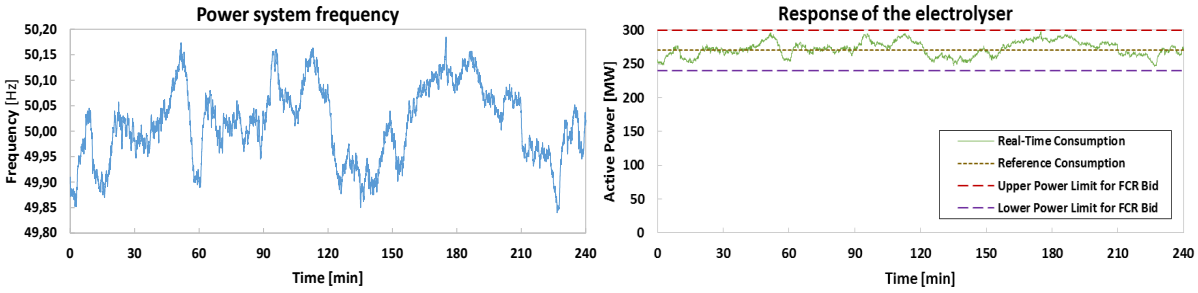

Figure 5.6: Simulation of frequency following by the electrolyser (data from [37]).

In the UK, the requirements for fast frequency support are defined in the EFR prequalification requirements [13]. In general, these contain various tests similar to the Dutch FCR prequalification requirements, but stricter in the sense of a shorter response time. Also, as the desired power ramps depend on the frequency deviation in EFR, the frequency step test consists of a series of increasing frequency deviations. The maximum required ramp rate is 200%/s. The simulations of the frequency step tests for FCR, illustrated in Figure 5.5, show that the ramp rate of an electrolyser is much faster. Therefore, it is expected that an electrolyser can also comply with the frequency step tests of EFR.

The EFR prequalification tests also contains a frequency sweep test. This test was simulated and the result is shown in Figure 5.7. As can be seen, the electrolyser varies its active power consumption depending on the power system frequency. The response of the electrolyser starts somewhat later and stops somewhat earlier because of the deadband as specified by the EFR requirements. The EFR prequalification also consists of a duration test and a frequency following test. Regarding the first one, no issues are foreseen in the electrolyser operating at a constant setpoint for a certain time. Regarding the second one, the frequency following test is similar to the one in the FCR prequalification tests, as illustrated in Figure 5.6. Electrolysers therefore have the potential to participate in fast frequency support services like EFR.

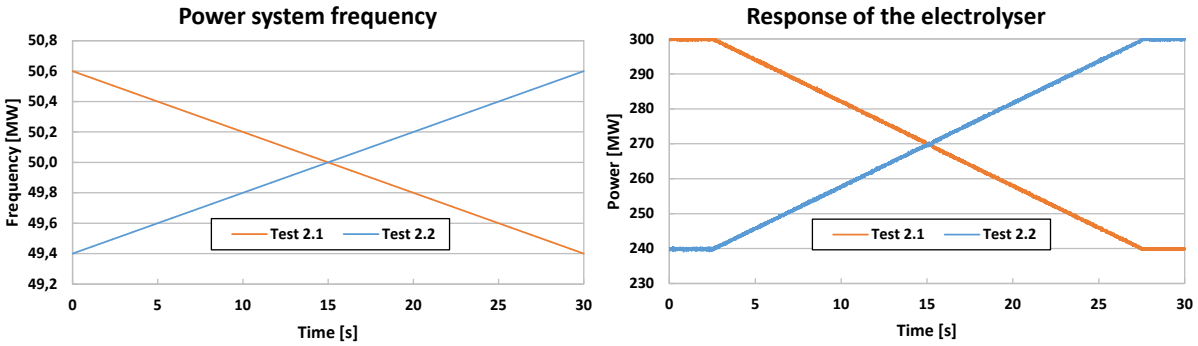

Figure 5.7: Simulation of the electrolyser response in the EFR frequency sweep tests.

The compliance of the electrolyser model to FCR prequalification tests has been verified in HIL simulations as well. Figure 5.8 shows the response of the electrolyser model to step changes in the active power setpoint. As the graphs show, the electrolyser model is able to complete these step changes within a short time. Further HIL simulations have been performed as well. These simulations showed that the electrolyser model is able to comply with the FCR prequalification tests.

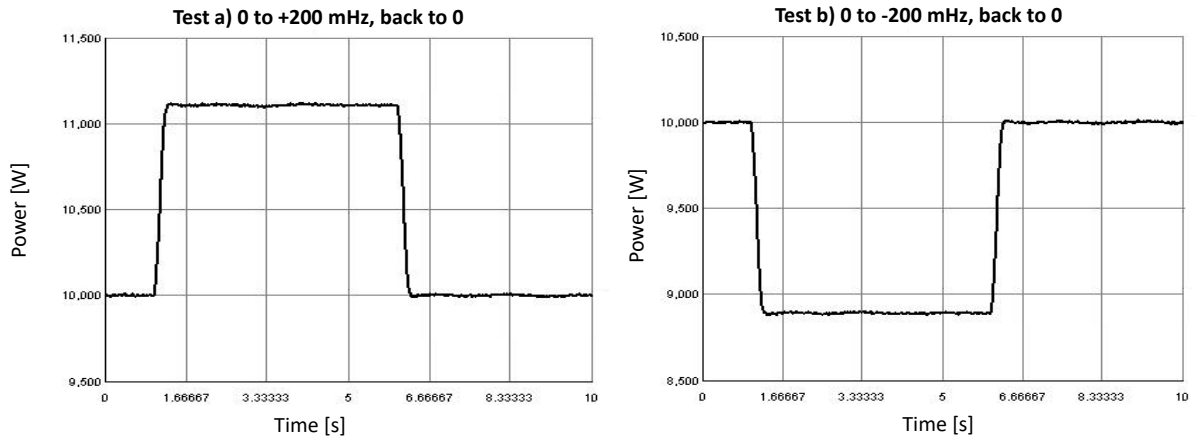

Figure 5.8: Results of the HIL simulation of tests a and b of the FCR prequalification.

5.3 Controllers for Frequency Support by Electrolysers

As the studies discussed in the previous chapters showed that the main contribution of electrolysers to power system stability is the provision of frequency support, FCR in particular, various control strategies for this purpose have been analysed [38]. These controllers have been implemented in the electrolyser model in the test model of Northern Netherlands Network (N3) and simulations have been performed on the RTDS with HIL.

5.3.1 Implementation of the Electrolyser Controllers

In order to provide frequency support, a control strategy based on Fast Active Power-frequency Regulation (FAPR) has been implemented in the electrolyser model N3 network [38]. FAPR allows Power Electronics (PE)-connected technologies such as wind, solar photovoltaics (PV), batteries and responsive demand to vary their active power consumption/production to correct a power imbalance and, thereby, stabilise the power system frequency. FAPR essentially is a mechanism to quickly regulate the active power injection/absorption to mitigate frequency variations in low-inertia systems. Since it may overlap with the time window of the inertial response of conventional generators (i.e. 0.5 seconds from the occurrence of an active power imbalance), it is sometimes also called 'Inertia Emulation' (IE). The actual source of energy for emulating inertia is stored in systems behind the PE interfaces, such as batteries and rotating masses in wind turbines. A supplementary control loop for inertia emulation enables the wind turbine or storage element to release stored kinetic energy up to 10 seconds to arrest frequency deviations.

In the studies described in this chapter, three different kinds of FAPR control have been considered for the implementation of frequency control by electrolysers:

- **Droop control**: Similar to conventional generators, the electrolyser varies its active power consumption based on the deviation of the frequency from its nominal value.
- **Combined droop-derivative control**: In addition to droop control, the electrolyser also varies its active power consumption based on the Rate-of-Change-of-Frequency (RoCoF) after a disturbance. This derivative control strategy enables the electrolyser to respond faster than with only droop control as it anticipates large frequency deviations based on the RoCoF.
- **Virtual Synchronous Power (VSP)-based control**: This control strategy does not depend on the system frequency as a signal, but instead compares a measurement of the power required with the reference power available at a bus to determine how much the electrolyser should vary its active power consumption.

The following paragraphs describe the implementation of these control approaches in more detail.

Droop-based FAPR Controller

Frequency droop control is a control strategy where active power is injected/extracted based on the deviation of the frequency from nominal (i.e. 50 Hz or 60 Hz) under the condition of dynamically changing loads/generations. In droop-based approaches, as well as in derivative-based approaches, the input signal is the frequency deviation, and confident measurement of the frequency in these approaches is very important. If the grid is large, the system frequency will be slightly different in different areas and hence inter-area oscillations exist. Therefore, frequency at the most critical bus has to be considered. The most critical bus is the bus where the highest load frequency variation can

be observed. As illustrated in Figure 5.9, the measured frequency is compared to the nominal value (i.e. 50 Hz or 60 Hz) and the error is passed through a deadband filter. The resulting signal is multiplied with a proportional (or droop) gain, tuned as to have a linear dependency between the total power output from the PE-interfaced device and the system frequency. This is now added as an additional signal to the electrical power reference signal determining the active power setpoint of the PE-interfaced device.

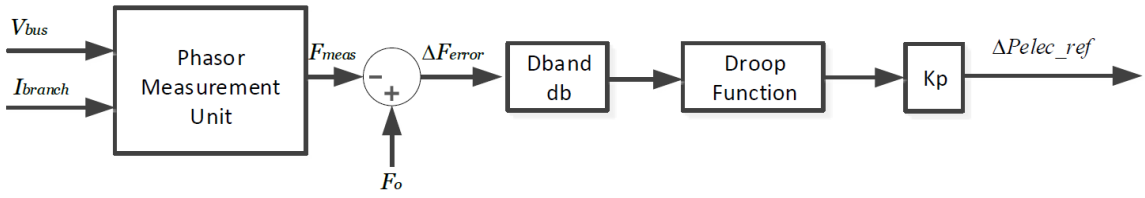

Figure 5.9: Control scheme of droop-based FAPR control.

Combined Droop-derivative-based FAPR Controller

Frequency-based derivative approach is a control strategy where active power is injected/extracted based on the derivative of frequency from nominal under the condition of dynamically changing loads/generations. In this method, there are two controllers, namely the droop controller and the derivative controller. The droop controller remains the same as discussed before, as illustrated in Figure 5.10. The derivative-based controller is added to provide a faster response during the initial few seconds right after the fault, when the RoCoF is the highest. The application of derivative control alone provides a satisfactory response up to the point of nadir, but once the frequency reaches a settling point, the derivative approaches zero, such that the addition of droop-based control can be considered to produce an additional change in the active power reference in proportion to the system frequency deviation for better recovery and enhancement of nadir. The derivative controller takes the frequency error as input, which is first passed through a deadband and a low-pass filter. The signal is then derived to find its slope and then multiplied by a gain to defines the response sensitivity of the derivative controller. The derivative control alone cannot mitigate the frequency discrepancy, as the derivative control will only be active during a large dynamic frequency deviation and be zero during slow frequency deviations or stable frequencies. Therefore, derivative control is applied complimentary to droop control for improvement of both the RoCoF and the frequency nadir.

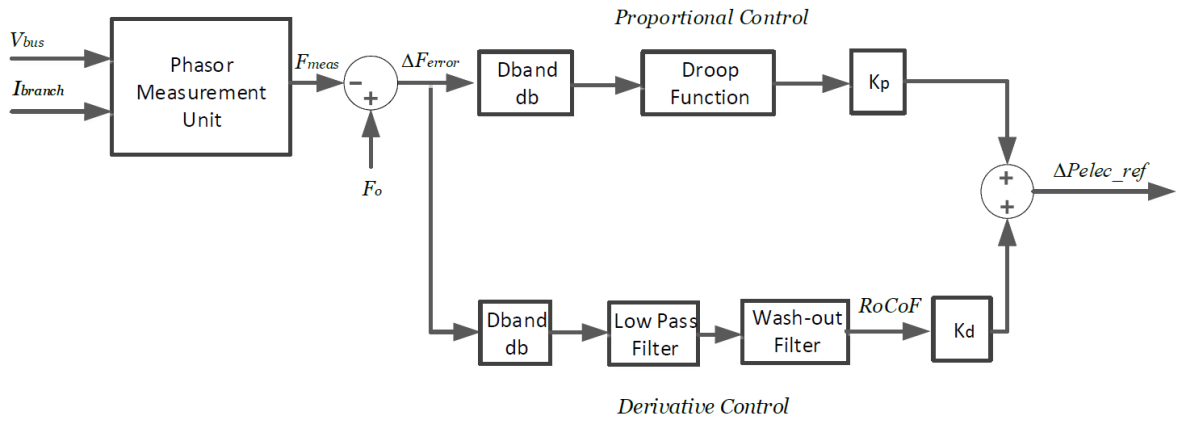

Figure 5.10: Control scheme of combined droop-derivate-based FAPR control.

Virtual Synchronous Power (VSP)-based FAPR Controller

In contrast to droop- and combined derivative-droop-based control, VSP-based FAPR control operates using the measurement of the power required at the bus with respect to the reference power available at this bus. Usually, both these values are equal during steady state conditions, but during a load-frequency variation event, the measured power on the grid side deviates while the reference power that the Renewable Energy Source (RES) delivers will remain the same. As illustrated in Figure 5.11, the resulting error is used to vary the power withdrawn from or injected into the grid by the RES [38]. With VSP-based control, frequency measurement ambiguities can be eliminated completely. When implemented in renewable generation, like a wind or solar PV farm, the overall VSP setup consists of two parts, namely a Battery Power Management System (BPMS) and a VSP controller, which is a signal generator. The BPMS controls a Battery Energy Storage System (BESS), which can instantly supply power to the grid in case of a frequency disturbance.

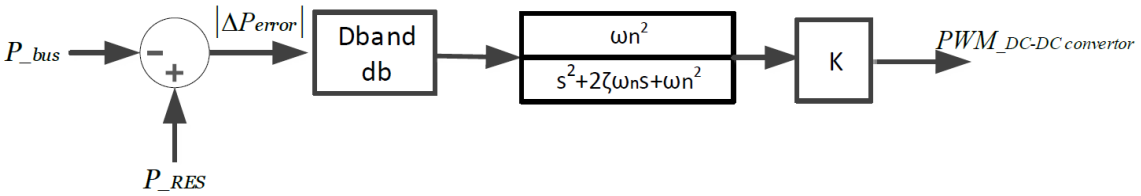

Figure 5.11: Control scheme of VSP-based FAPR control.

Implementation of the Controllers in the Electrolyser Model

The electrolyser model present in the N3 network has been modified to include droop, combined droop-derivative and VSP-based FAPR control. So during a frequency disturbance, the FAPR controllers vary the active power absorption, which will improve the system frequency. In the implementation of these control strategies in the electrolyser model, the output of the specific controller are the input of the active power reference of the electrolyser model. The VSP-based control is not implemented with a BPMS and BESS, since an electrolyser is a load and power regulation is performed by varying its active power demand. Droop control is always active in combination with derivative and VSP-based control. However, the time duration and active power reduction applied by derivative and VSP-based control are different. Various simulations have been performed to study the frequency response if frequency support is provided by one of the three control strategies as described previously. These simulations are based on Scenario 3 of 2030 (see Table 4.1) and consider a 200-MW sudden loss of Gemini wind generation capacity, leading to under-frequency in the power system.

5.3.2 Simulation of the Frequency Response

The response of the active power variation of the electrolyser after a 200-MW loss of generation of Gemini wind farm is shown in Figure 5.12 for each of the three proposed control strategies. Figure 5.13 depicts the resulting frequency response in these cases. As the black lines in the graphs show, the electrolyser on its own does not regulate its power demand in the case of a frequency disturbance event. However, with operational droop-based FAPR control, the power demand of electrolyser is reduced based on the frequency deviation, resulting in improvement in the frequency nadir. With the combined droop-derivative controller in action, faster active power reduction can be

achieved. This improves the RoCoF significantly, while also improving the frequency nadir as a by-product. The last controller implemented is the VSP-based FAPR controller. As can be seen in the graphs, this results in the best improvement of the frequency response.

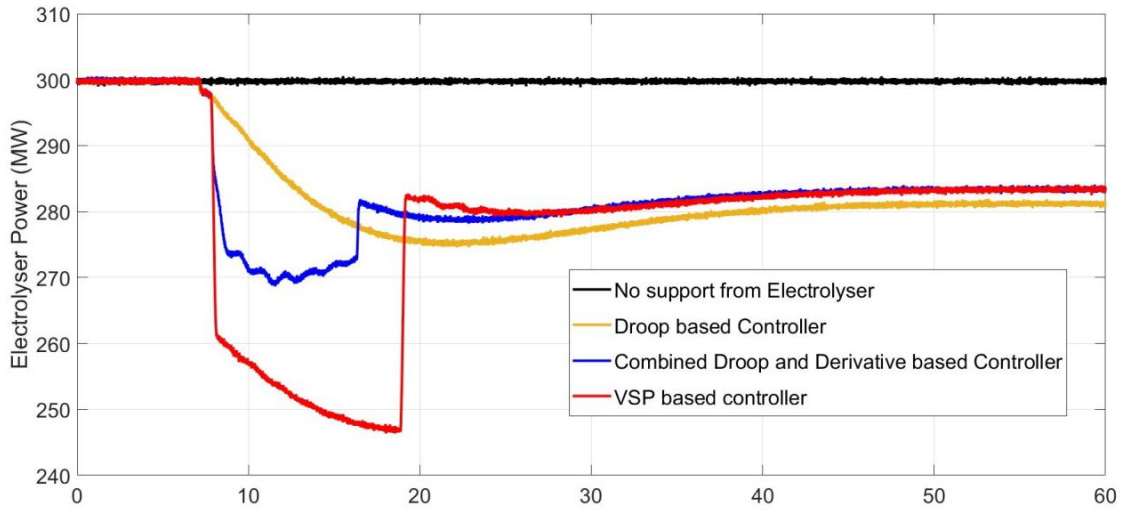

Figure 5.12: Power response of the electrolyser with FAPR controllers.

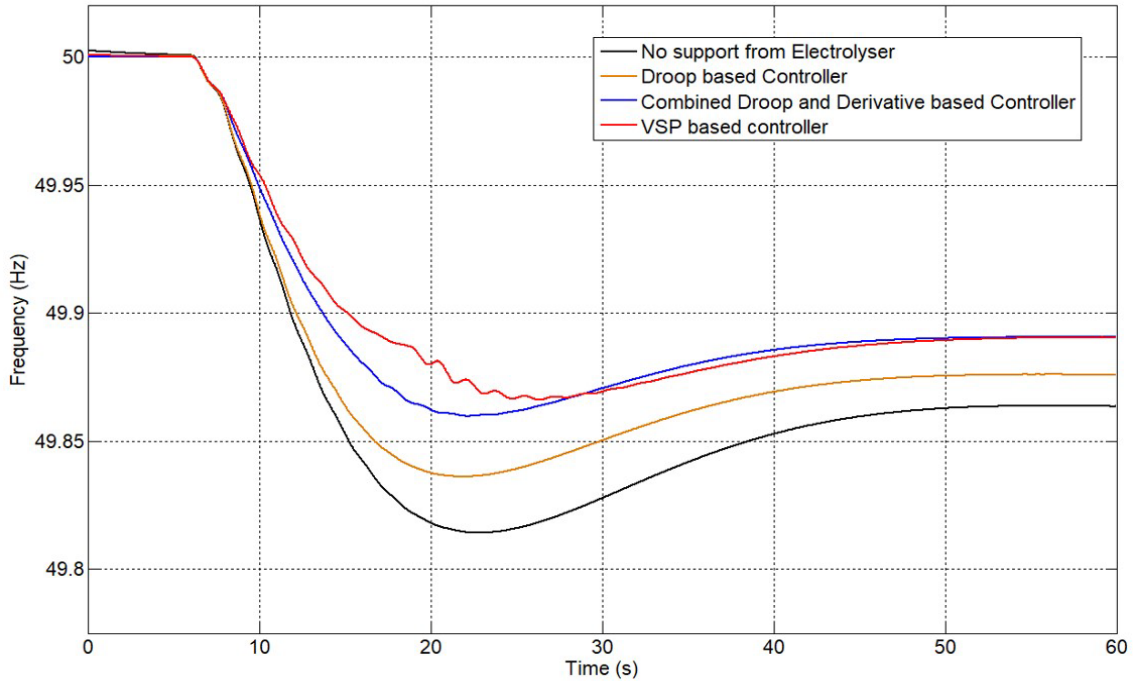

Figure 5.13: Frequency response of the electrolyser with FAPR controllers.

5.3.3 Frequency Support by a Multi-Energy Hub

In order to compare the frequency support by an electrolyser with frequency support by other technologies like wind farms, solar farms and Battery Energy Storage Systems (BESS), the Northern Netherlands Network (N3) as presented in Section 4.1 has been extended to include a multi-energy hub [38], as shown in Figure 5.14. For this purpose, three main modifications were performed. First, a FAPR control strategy was implemented in the electrolyser as described in Section 5.3.1. Secondly,

an 85-MW full-scale Type-4 wind turbine was implemented with integrated FAPR controllers. Thirdly, a solar farm of 300 MW was implemented with a VSP-based FAPR controller including a Battery Energy Storage System (BESS) with Battery Power Management System (BPMS). The loads in the system were adjusted accordingly. Here, the congestion in the grid was increased mainly for two reasons: (i) to observe the effects due to the reduction in the total inertia of the system; (ii) to observe if there are any other effects of congestion that could lead to system instability.

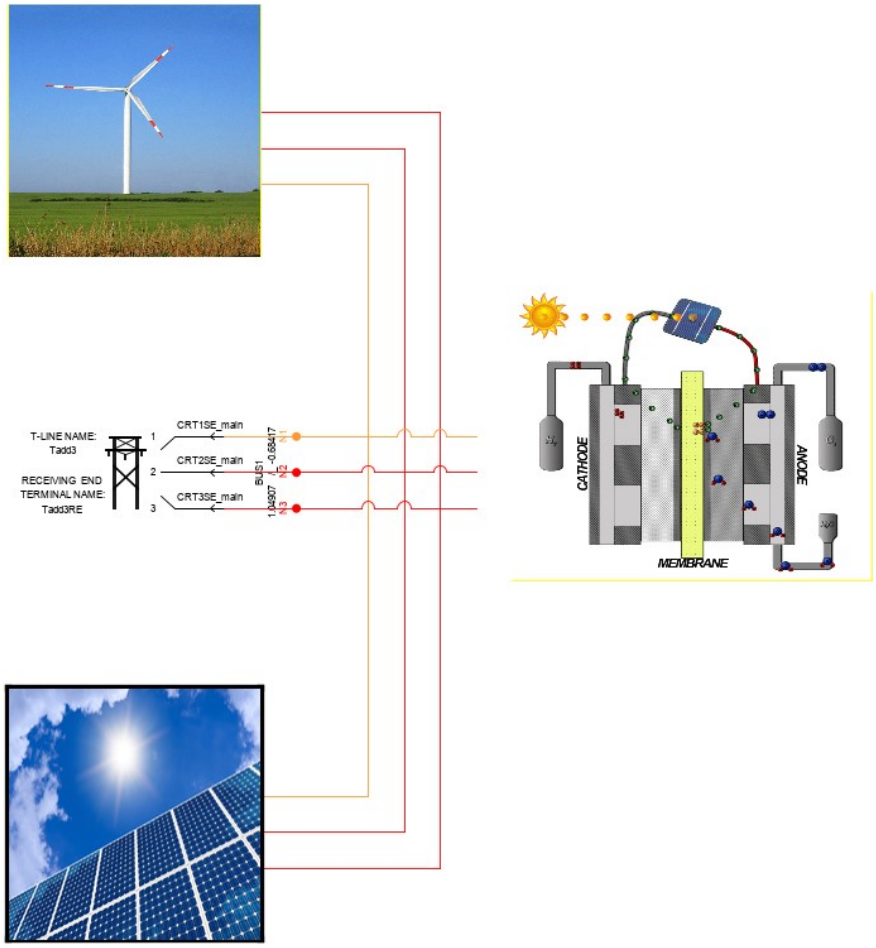

Figure 5.14: Configuration of the multi-energy hub.

Again, the simulations consider a 200-MW sudden loss of Gemini wind generation capacity. The solar farm reacts to this event by increasing its active power injection. Naturally, the time of operation is limited by the size of the BESS in the solar farm and grid-side converter capabilities. Figure 5.15 depicts the improvement in the frequency response caused by this implementation, also in comparison to frequency support by the electrolyser. It can be seen that the electrolyser has a more positive impact on the RoCoF, frequency nadir and steady-state frequency than the BESS. The best improvement of the RoCoF and frequency nadir is obtained when frequency support is provided by both the electrolyser and the BESS. It should be noted here that the higher the support in active power during the frequency containment period, the higher will be the frequency improvement. This is regardless of any inverter-interfaced renewable energy source.

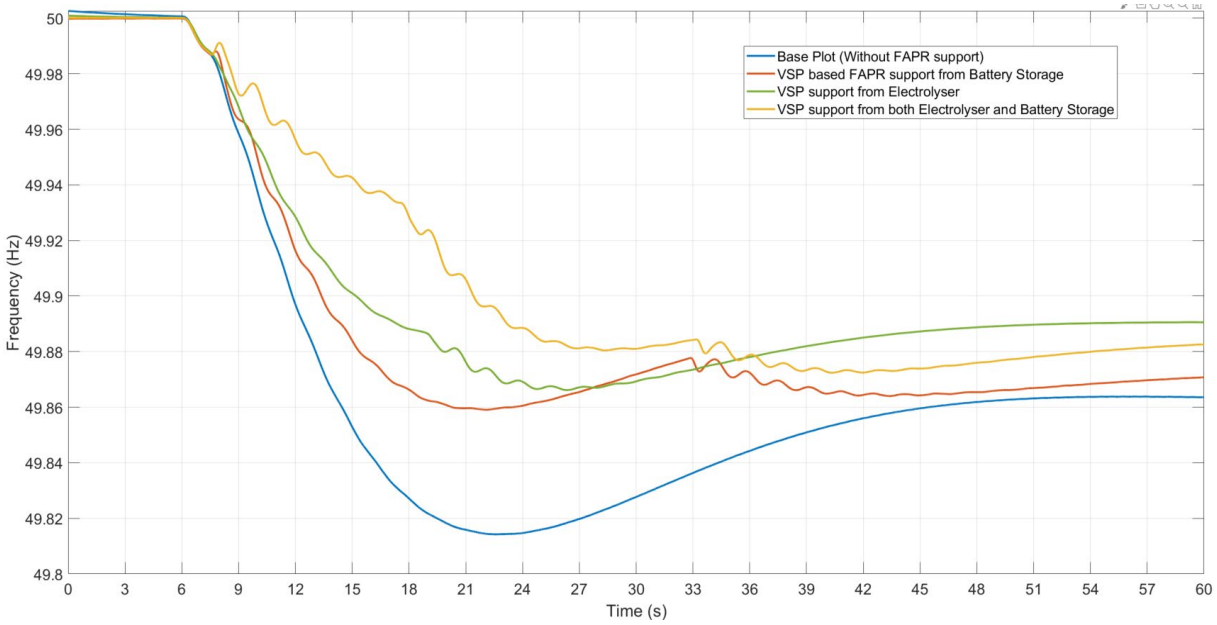

Figure 5.15: Frequency support from a VSP-based electrolyser and solar farm.

When studying Figure 5.15 in more detail, it is evident that if more RES are able to respond by quickly altering their active power, the system frequency dynamics measured by the RoCoF and nadir will improve. However, also the downside of sudden injection of active power in a low-inertia system should be considered. For example, the VSP controller in the solar farm is suddenly activated when sensing the frequency disturbance, thereby instantly injecting 30 MW into the system. By comparing the graphs in Figure 5.15, it can be seen that the more RES suddenly regulate their active power, the more crooked the frequency response becomes. This is because in low-inertia systems, rotor swings of synchronous generators become predominant. Previously, the total system inertia was high since all demand was supplied by synchronous generators, but with the inclusion of RES, the overall inertia in the system reduces. This makes the synchronous generators more responsive, especially if the disturbance event is close to them. This effect becomes more pronounces for increasing use of RES in systems with low inertia and may disturb the desired frequency response. This is, therefore, a thing worth to consider in the design of frequency controllers for newer technologies.

5.4 Conclusions

This chapter considered the practical implementation of control approaches in electrolysers in order to provide ancillary services support. As the most promising potential of large-scale electrolysers is the provision of frequency support, this chapter concentrated on frequency support by electrolysers, thereby concentrating on FCR support. As the simulations have been performed on the RTDS using HIL, the HIL setup of the RTDS at Delft University was discussed first. After this, the compliance of electrolysers to FCR prequalification tests was studied. Based on simulations of the electrolyser model, it can be expected that electrolysers can easily comply with the FCR prequalification tests because of their fast ramping capabilities. Electrolysers could even participate in faster frequency support ancillary services, like EFR in the UK.

In this chapter, also various control strategies for Fast Active Power-frequency Regulation (FAPR) by electrolysers were developed and simulated. The studies considered three control strategies: (i) droop-based control; (ii) combined derivative-droop-based control; (iii) Virtual Synchronous Power (VSP)-based control. In droop-based control, the electrolyser varies its active power consumption based on the deviation of the power system frequency from the nominal value (e.g. 50 Hz). A faster response can be obtained with combined derivative-droop-based control, as this control also responds to the RoCoF, thereby anticipating large frequency deviations. The third control approach considered, VSP-based control, does not use the power system frequency as a signal, but compares a measurement of the power required with the reference power available at a bus to determine how much the electrolyser should vary its active power consumption. In this way, frequency measurement ambiguities can be eliminated completely. The simulations performed show that VSP-based control results in the best frequency response of these three control strategies. Generally, the simulations discussed in this chapter show that electrolysers can have a positive effect on the frequency response after a disturbances because of their fast ramping capabilities.

6 Conclusions and Recommendations

In this report, electrical ancillary services provision by electrolysers was investigated. The study started with a review of the current regulations for ancillary services. Then, a model of a 1-MW electrolyser was developed and used to study the impact on local grid stability in the Veendam-Zuidwending case study. This model was then scaled up to represent a 300-MW electrolyser. The northern part of the Dutch transmission network was modelled and various simulations were performed to study the impact of ancillary services provision by large-scale electrolysers. The study was completed by the development of control approaches that enable electrolysers to participate in the provision of electrical ancillary services.

A review of the current regulations for electrical ancillary services shows that there are mainly three ancillary services to which electrolysers can contribute: frequency balancing, voltage control and congestion management. Due to their fast dynamics, electrolysers are a promising flexibility solution for frequency balancing in future power systems. Electrolysers can prioritise in short-term frequency support like Frequency Containment Reserve (FCR), possibly followed by participation in mid-term frequency support like Automatic Frequency Restoration Reserve (aFRR). If an electrolyser is installed in an area of the network in need of voltage control or congestion management, it could also be deployed for such purposes. The modifications of the framework of balancing markets expected in the coming years will allow broader operating flexibility for electrolysers.

As models of larger (≥1 MW) electrolysers were not existent in literature, a model of a 1-MW electrolyser has been developed specifically for this project. The performance of this model has been studied for various possible grid disturbances and comparison of the simulations with literature examples and field measurements of the 1-MW electrolyser in Veendam-Zuidwending showed that the model is able to accurately replicate the behaviour of a real electrolyser. The model has been equipped with controllers that enable it to respond to disturbances in the power system. Simulations show that the electrolyser model is able to adjust its active power consumption based on power system frequency variations (i.e. frequency support) and to adjust its reactive power based on voltage variations (i.e. voltage support). Although a 1-MW electrolyser will not influence the system frequency, it could potentially be used for local voltage support. For this purpose, there must be a certain amount of converter capacity available, which means over-dimensioning of the electrolyser converter or electrolyser operation at a capacity lower level than rated.

After scaling the electrolyser model, the possible contribution of a 300-MW electrolyser to frequency and voltage stability and congestion management was investigated. For this purpose, the reduced size model of northern part of the Dutch transmission network, including an offshore wind farm and COBRAcable, was considered as a test system. The impact of the electrolyser and HVDC connections like COBRAcable on power system stability was studied in various simulations. These simulations show that a large electrolyser has a positive effect on the frequency stability when participating in FCR, as electrolysers are able to ramp up/down their power consumption must faster than conventional generators. Frequency control by HVDC connections like the hypothetical case of COBRAcable also has a positive impact, but the effect of the electrolyser is more pronounced. An electrolyser can provide frequency support after loss of a generator by decreasing its consumption

and in the case of a loss of load, the electrolyser can increase its consumption. To make this possible, the electrolyser should operate between a certain minimum (i.e. larger than 0) and maximum (i.e. smaller than rated) level. Participation in this particular ancillary service is a trade-off between a higher hydrogen production or participation in frequency support. Future asymmetric frequency support could be a solution.

Simulations of the voltage showed that the impact of the electrolyser is small in this network, as there already are enough facilities that contribute to voltage stability (e.g. conventional generators, HVDC interconnections, offshore wind farms). Nevertheless, electrolysers can improve local voltage stability in more remote areas with less voltage support (see also Appendix D). In that case, the electrolyser must be able to vary its reactive power consumption independently from its active power consumption, as large changes in active power consumption can influence the system frequency. A certain capacity of the converter must then be reserved, which means either operation at a capacity smaller than rated or an over-dimensioned converter. The possible contribution to congestion management has been analysed as well. It can be concluded that the considered network is rather robust and congestion issues are not foreseen for the considered operational scenarios. Nevertheless, electrolysers can theoretically contribute to congestion management by varying their consumption. Electrolysers can also help mitigate the variability of large-scale renewable generation like offshore wind. Electrolysers located near to renewable generation can absorb short-term variations, thereby making the injection of power into the grid more predictable.

The last part of the study considered the practical implementation of control approaches. As the most promising potential of large-scale electrolysers is in the provision of short-term frequency support, the analysis concentrated on FCR support. First, the compliance to FCR prequalification tests was studied. Based on simulations of the electrolyser model, it is expected that electrolysers can easily comply with the FCR prequalification tests because of their fast ramping capabilities. Electrolysers could even participate in faster frequency support ancillary services, like EFR in the UK. Three control approaches of Fast Active Power-frequency Regulation (FAPR) by electrolysers were considered: droop-based control, combined derivative-droop-based control and Virtual Synchronous Power (VSP)-based control. In droop-based control, the electrolyser varies its active power consumption based on the deviation of the system frequency from its nominal value. A faster response is obtained with combined derivative-droop-based control, as this control also responds to the Rate-of-Change-of-Frequency (RoCoF), thereby anticipating large frequency deviations. VSP-based control does not use the power system frequency as a signal, but compares a measurement of the power required with the reference power available at a bus to determine how much the electrolyser should vary its active power consumption. In this way, frequency measurement ambiguities can be eliminated completely. The simulations performed show that VSP-based control results in the best frequency response.

The studies described in this report generally show that electrolysers hold promising potential for the contribution to ancillary services in the future power system. This is mainly because of their fast (up and down) power ramping capabilities in comparison to conventional generators. Although electrolysers could contribute to local voltage stability and congestion management, as shown in Chapters 4 and 5, their main potential is in the provision of frequency support, especially in the short

term (e.g. FCR or EFR). When equipped with the appropriate controllers, electrolysers are able to respond relatively quickly to disturbances of the power system frequency, thereby positively contributing to frequency stability.

A Impact of Fuel Cells on Frequency Performance

A.1 Introduction

The generation of electricity with fuel cells, which uses hydrogen as feedstock, has proved its feasibility for diverse sectors, such as stationary power applications (e.g. telecommunication services, backup power generators), transportation services (e.g. buses, cars, material handling vehicles) and portable power applications [39]. PEM (Proton Exchange Membrane) technology in particular, raises the most interest for electric vehicles, since it can provide fast time response and high power density [40]. The combination of fuel cells with electrolysers is also very promising, as it opens the possibility to create a cheap hydrogen supply that can be stored and later used by fuel cells to support the demand of the power system.

So far, the maximum size for a PEM fuel cell plant is 2 MW [41]. In similar fashion to electrolysers, multiple units can be operated in parallel to achieve larger capacities. For instance, one of the largest facilities in the world is based on individual 2.8-MW molten carbonate fuel cells, amounting for a total of 59 MW [42]. The reported PEM fuel cell efficiency is in the range of 40–60% according to most sources [40], [43], [44], with an estimated annual capacity factor of 95% [45], and a lifetime reaching the 40,000 hours [45]. The capital cost of PEM fuel cells lies between 1.5 M€/MW to 3 M€/MW [43], with an associated payback period of around 8 years [45]. The high capital cost is caused by the expensive price of platinum catalysts [46], which on the other hand can be salvaged after the decommission of the cells. The annual operational cost is less than 1% of the initial investment [43].

In general, fuel cell technology has demonstrated the ability to provide stable and independent electricity to individual consumers [47], to the power grid and even to microgrids [48]. However, very little research has been performed to specifically address their potential to participate in electrical ancillary services. For future frequency balancing markets, PEM fuel cells share comparable ramping technical capabilities to electrolysers, as it is also possible to complete active and reactive power setpoint changes within 1 second [49]. For aFRR (Automatic Frequency Restoration Reserve), fuel cells can take advantage of the cheap hydrogen supplied by electrolysers to place voluntary bids for upward regulation during periods with high settlement prices. For voltage support, PEM fuel cells can be more effective than electrolysers, as the presence of a DC/AC inverter allows complete control over the output power factor. Furthermore, fuel cells can provide additional benefits in the case of distributed generation, where multiple units can participate in local voltage support at different locations of the low voltage network or within a microgrid [48]. Lastly, large fuel cell plants can contribute to the relief of transmission line congestions via bidirectional power redispatch.

PEM fuel cells are characterised by high current density and fast power injection, which makes them ideal for frequency containment. This appendix presents a study on the performance of fuel cells in a reduced-size dynamic model of the northern Netherlands. For this study, a generic model for PEM fuel cells has been developed in PowerFactory [50], [51].

A.2 Simulation of Frequency Support

A.2.1 Description of the Test Network

The fuel cell is tested for its availability to support the frequency by using a reduced representation of the 380-kV Northern Netherlands grid as shown in Figure A.1. This region is considered to be a promising location for the installation of large-scale power-to-gas capacity in the future. The modelled system covers the 380-kV and several key connections of the 220-kV EHV network of the year 2030. The topology of the system, the power flow conditions and the electricity demand were derived from the guidelines of the ten-year development plan of the Dutch TSO TenneT B.V. [52]. The system features a generation capacity composed by two 2250-MVA thermal power plants equipped with two generation units each, 600 MW of offshore wind energy (Gemini wind park) and 3058 MW onshore wind energy distributed around the area and further aggregated into the corresponding 380-kV substations. Additional renewable energy is imported via the HVDC interconnectors with Norway (NorNed) and Denmark (COBRAcable), both of them operated at the rated power transfer capacity of 700 MW.

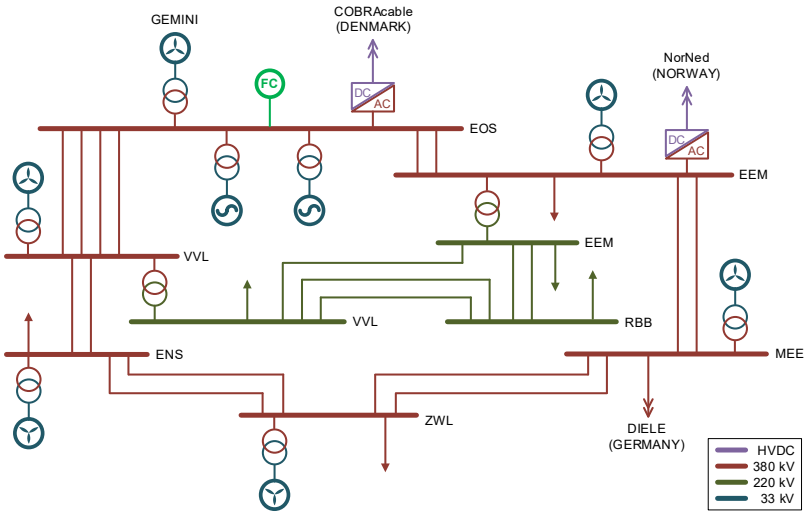

Figure A.1: Northern Netherlands test network.

The network was modelled in DIgSILENT PowerFactory, version 2018 SP1. The wind turbines and the synchronous generators were represented by generic models of each technology, which are available in the software. Generic steam turbine governors with droop control, exciter and power stabiliser were also implemented with the synchronous generators to enable dynamic control and the provision of ancillary services. For this particular study, it was assumed that the wind parks and the HVDC interconnectors did not participate in the regulation of the system. For such reason, the model of the HVDC links was simplified as a constant negative load. The connections to other parts of the network and the local demands were also modelled as constant loads.

A.2.2 Frequency Support by Fuel Cells

In the simulation of frequency support by fuel cells, the simulated disturbance is a decrease in wind generation of 30 MW at t=5 s at the bus EEM, which creates an imbalance between generation and load causing significant frequency deviation and dramatic value of Rate-of-Change-of-Frequency (RoCoF). In this system, the inertia is only provided by the synchronous generators and it is calculated by summing the inertia constants of the synchronous generators. The FCR support is provided only through the synchronous generators, the fuel cells, or both. The disturbance is simulated for several scenarios with different FCR contributions from the synchronous generators and the fuel cells, for a decreasing level of inertia. The system inertia is reduced by reducing the inertia constant of the synchronous generators. A list of these scenarios and a summary of the frequency response are provided in Table A.1, while the frequency response is shown in Figure A.2.

Table A.1: Summary of simulation scenarios.

№	Scenario	System inertia*	FCR bids	Nadir [Hz]	RoCoF [mHz/s]
1	Base case	100%	50 MW by SG	49.845	28.575
2	Full inertia with FC	100%	50 MW by FC	49.900	28.399
3	Lowered inertia with FC	50%	50 MW by FC	49.899	60.138
4	Min inertia with SG	25%	50 MW by FC	49.794	122.964
5	Min inertia with FC	25%	50 MW by FC	49.894	118.682

* The value of the system inertia for the base case is 10 seconds.

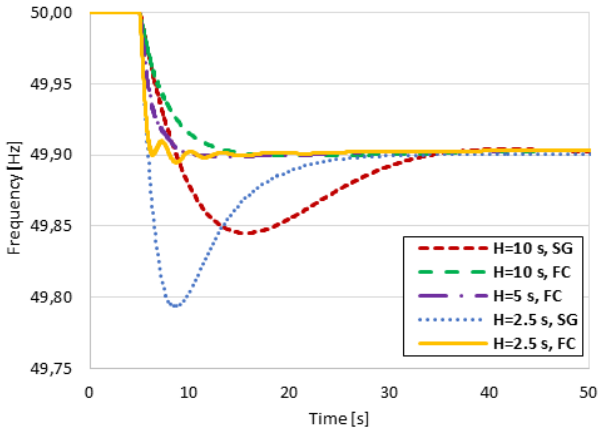

Figure A.2: Frequency response of the Northern Netherlands test network.

The results of the simulation in Figure A.2 show that for the same FCR bid value and system inertia, the PEM fuel cells result in better frequency nadir, smaller oscillations and faster convergence to the steady state value. The improvement in performance becomes more prominent as the system inertia decreases, such as in scenario 4 and 5, in which the faster power injection by the PEM fuel cell is able to contain the frequency deviation quickly resulting in significantly smaller nadir. The oscillations observed in scenario 5 are due to the reduced inertia of the synchronous generators.

A.2.3 Frequency Support by Fuels Cells and Electrolysers

In a second study, it was studied how the combined operation of large-scale PEM electrolysers and fuel cells influences the frequency performance in different future scenarios. The installed capacity of each technology in the test system amounts to a total of 300 MW and 50 MW, respectively, and it is achieved by aggregation of smaller units. Both facilities operate at a reference power setpoint that allows participation in the future FCR market via symmetrical bidding. The FCR capacity available in the test network is set to 50 MW (45% of the total in the Netherlands [10]), while the synchronous generators provide a cumulative rotational inertia of 12 seconds. Both values constitute about 1.5% of the total with respect to the entire synchronous area of Continental Europe and therefore, the proposed model can be considered as a reasonably accurate small-scale grid representation.

The network is subjected to a sudden decrease in generation, originated by the disconnection of several wind turbines or the loss of imported power from the HVDC links. The most representative scenarios studied are summarised in Table A.2. For each of the four scenarios, several simulations were performed, varying the location of the disturbance and the distribution of the electrolysers and fuel cells within the network. Nonetheless, the initial conditions before the event and the amount of generation lost are constant in every case to ensure a fair comparison between the results. The frequency indicators shown in Table A.2 and the frequency responses plotted in Figure A.3. belong to a disturbance occurring at the EEM bus and a location of the hydrogen technologies at the EOS bus.

Table A.2: List of scenarios, FCR bid sizes per technology and obtained values of the frequency indicators.

Nº	Scenario	System inertia*	Synchronous generators	PEM electrolyser	PEM fuel cell	Nadir [Hz]	RoCoF [mHz/s]
1	Base case (2018)	100%	2x25 MW FCR bid	Not installed	Not installed	49.851	26.972
2	Base case with H_2 (2018)	100%	No FCR support	40 MW FCR bid	10 MW FCR bid	49.902	26.376
3	Energy transition (2030)	50%	1x25 MW FCR bid	20 MW FCR bid	5 MW FCR bid	49.876	53.882
4	Low inertia with H_2 (2050)	25%	No FCR support	40 MW FCR bid	10 MW FCR bid	49.902	99.600

* The value of the system inertia for the base case is 12 seconds.

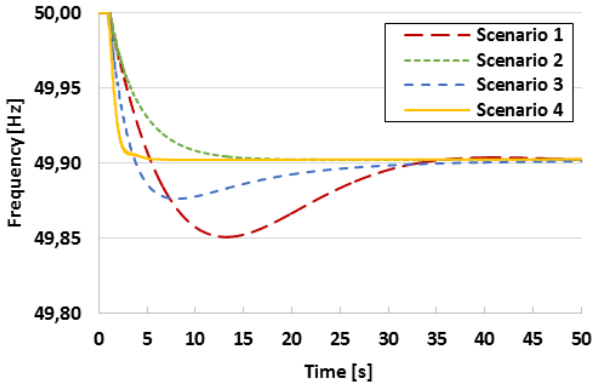

Figure A.3: Frequency response for the described scenarios.

The first scenario is set as the base case, derived from the current grid conditions. Rotational inertia is very high, there is no presence of PEM electrolysers or fuel cells and FCR support comes exclusively from the synchronous generators. The second scenario is a hypothetical variation of the base case in which the hydrogen technologies were already installed and providing FCR. By comparing these situations in Figure A.3, it is apparent how the fast dynamics of the PEM hydrogen technologies improve the frequency response. During the first seconds after the disturbance, the frequency drop in both simulations is almost equal, as the inertia of the system is identical. On the other hand, the action of PEM electrolysers and fuel cells translates into a more linear response and improves the maximum frequency deviation considerably (i.e. frequency nadir). This is attributed to their ability to quickly change the operating setpoint, in contrast to the inherent oscillating behaviour of synchronous generators.

The third scenario depicts the energy transition in the power system. Rotational inertia is decreased by half to represent the decrease in synchronous generation over time, the PEM hydrogen technologies are in place and these procure FCR in combination with the synchronous generators. From the results, it can be observed that the reduction of inertia translates into a steeper slope in the frequency response, technically known as Rate-of-Change-of-Frequency (RoCoF). Nevertheless, the inclusion of PEM electrolysers and fuel cells still improves the value of the frequency nadir with respect to the base case. In the final scenario, it is assumed that most of the thermal generation has been phased out, thus reducing the inertia to a low level. The PEM hydrogen technologies are the only suppliers of FCR. In this case, the frequency drop right after the disturbance is even steeper (around 4 times faster than the base case) because of the lack of dominant inertial behaviour. Yet once again, the fast recovery by the PEM electrolysers and fuel cells is able to limit the frequency nadir to a better value than in the base case.

Furthermore, while keeping the FCR bid size constant, the fast dynamics of PEM electrolysers and fuel cells could be exploited to enhance the frequency response by increasing the delivered regulation capacity for the same frequency deviations. This can be achieved by modifying the maximum frequency deviation below the default value of ±0.20 Hz in the control system, which effectively increases the slope of the droop characteristic. The frequency responses for increasingly droop slope values in the low inertia scenario are shown in Figure A.4. As expected, a better steady state value and frequency nadir are accomplished with steeper slopes. Also, the time it takes to reach the nadir is lowered, which indirectly improves the RoCoF, albeit not significantly. However, small oscillations are induced in the system.

During the course of the simulations, different disturbance locations were tested, but the aforesaid findings (cf. Table A.2 and Figure A.3) did not deviate significantly. Several distributed setups for the PEM hydrogen technologies were examined as well, but it was found that concentrated capacity performs slightly better for frequency regulation. It is worth noting that the used test network is a very strong grid. For weaker grids and more severe disturbances the impact of the distribution and location of the frequency reserve capacity gains importance. Locations of PEM electrolysers and fuel cells close to critical buses in the network tend to produce an improved dynamic performance [53].

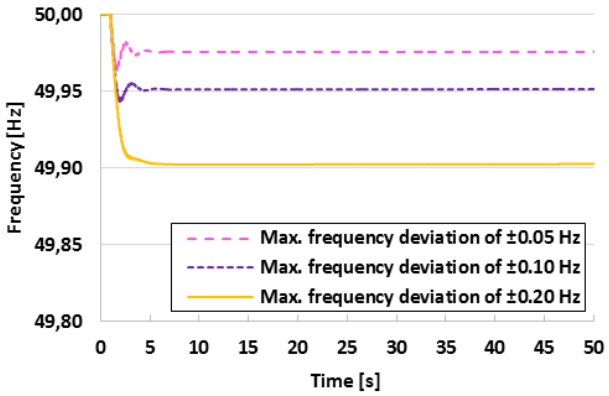

Figure A.4: Frequency response for different droop slopes in the low inertia with H2 scenario.

To conclude, the presented case study exemplifies why the participation of PEM hydrogen technologies in the FCR market benefits the frequency stability of the future power system. The decommissioning of traditional power plants will decrease the level of rotational inertia in the grid, which has a negative impact on the robustness of the system against disturbances. Regardless, the introduction of large amounts of flexible and fast technologies (e.g. PEM electrolysers, PEM fuel cells, battery storage) should be able to strengthen the frequency stability of the system, mainly by limiting the frequency deviations.

A.3 Conclusions

In this study, a representative dynamic model was developed to represent PEM fuel cells in dynamic simulations concerning frequency performance during the containment period. The simulations of the model show that it resembles the expected performance shown in literature. When tested in a reduced representation of the Northern Netherlands system, the fuel cells proved effective in containing the frequency change. A comparison between the PEM fuel cell and the synchronous generators performance in frequency containment showed that the fuel cell's fast current injection results in better nadir value and smaller oscillations, however the RoCoF value remains unaffected.

In a second study, fuels cells were combined with electrolysers to provide frequency support. From the point of view of the electrical power system, the capability of PEM electrolysers to rapidly change the power consumption and the fast power injection of PEM fuel cells emerges as a very attractive feature for frequency stability. The examined case study, based on realistic projections of the northern Netherlands grid for the year 2030, further highlights the value of PEM hydrogen technologies in the ongoing energy transition. It was observed that the reduction of rotational inertia inevitably causes a detrimental effect in the frequency response during the first seconds after a sudden mismatch between generation and demand. However, when PEM electrolysers and fuel cells provide FCR support (whether in a centralised or distributed manner), the frequency deviations can be limited. As a result, better frequency nadir values are obtained than when using synchronous generators, even in the case of minimum system inertia. Further, the ramping requirements of the frequency-power characteristic could be intensified to optimally exploit the capabilities of PEM hydrogen technologies for FCR.

B Electrolyser Model and Control System

B.1 Control System of the 1-MW Electrolyser

The electrolyser model as presented in Chapter 3 (Section 3.2) of this report has been equipped with a control system in order to provide frequency and voltage support. A high-level overview of this Front End Controller is shown in Figure B.1, while the detailed implementation is shown in Figure B.2, Figure B.3 and Figure B.4.

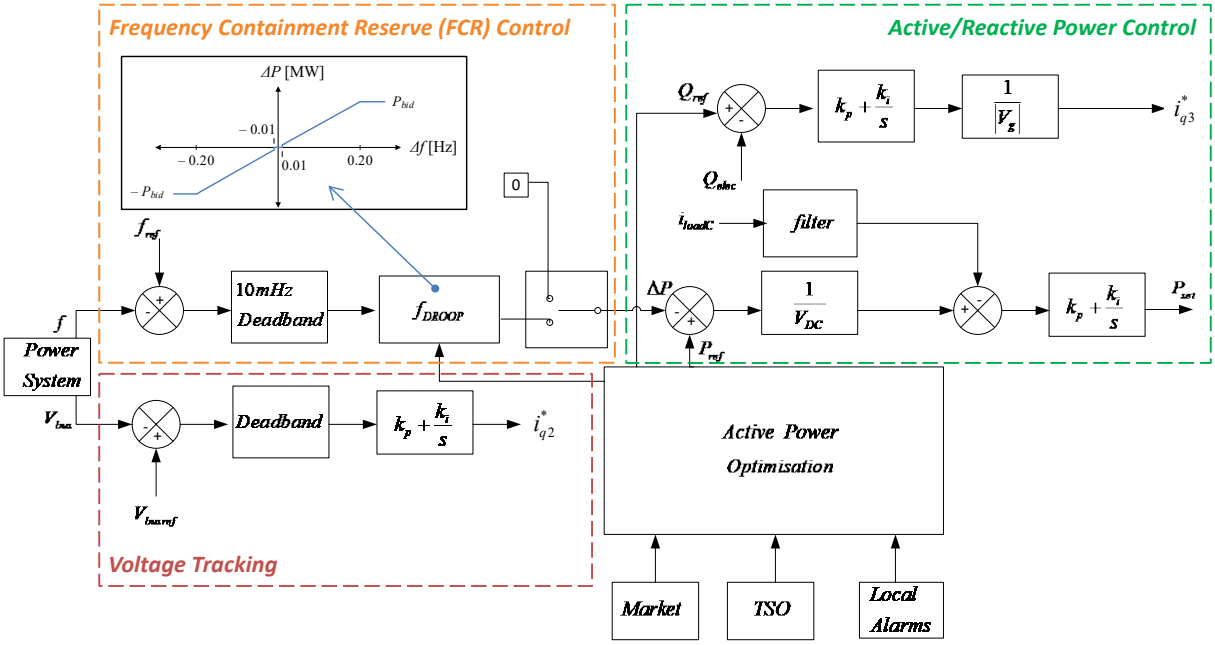

Figure B.1: Overview of the electrolyser Front End Controller.

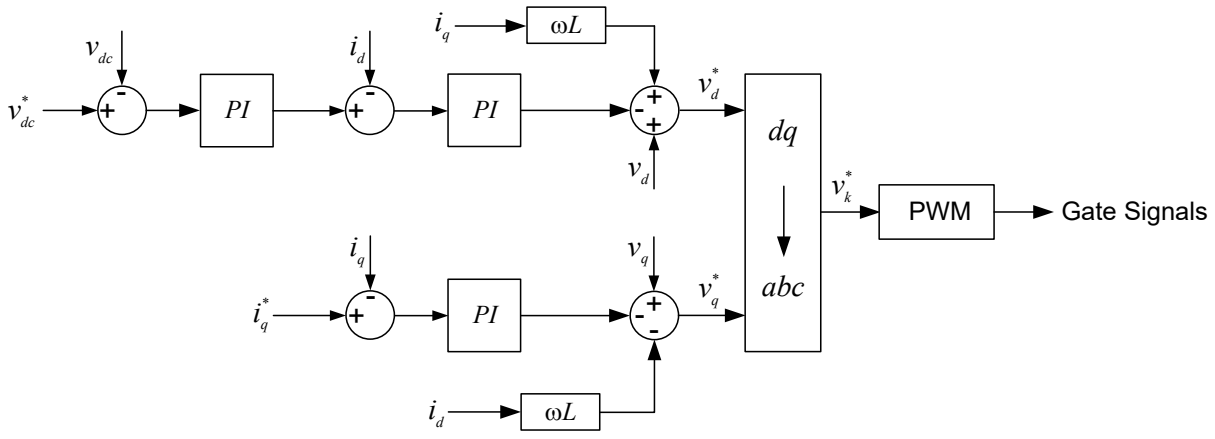

Figure B.2: Implementation of the AC/DC converter controller.

$i_q^* = i_{q1}^*$ or i_{q2}^* or i_{q3}^*, in order to implement a power factor 1 (i.e. $i_{q1}^* = 0$), voltage control (i_{q2}^*) or reactive power control (i_{q3}^*), as illustrated in Figure B.1 and Figure B.3.

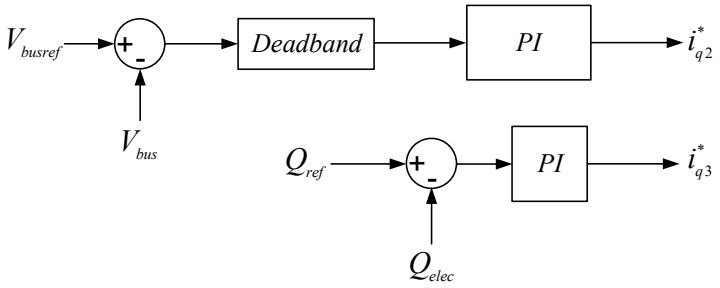

Figure B.3: Definition of i_{q2}^* and i_{q3}^* for the AC/DC converter controller.

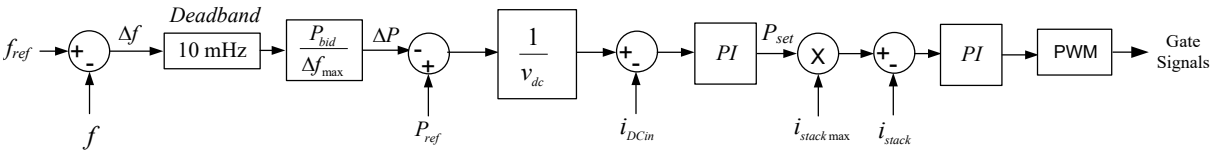

Figure B.4: Implementation of the DC/DC converter controller.

B.2 Control System of the 300-MW Electrolyser

The implementation of the control system in the model of the 300-MW electrolyser is shown in Figure B.5 and Figure B.6.

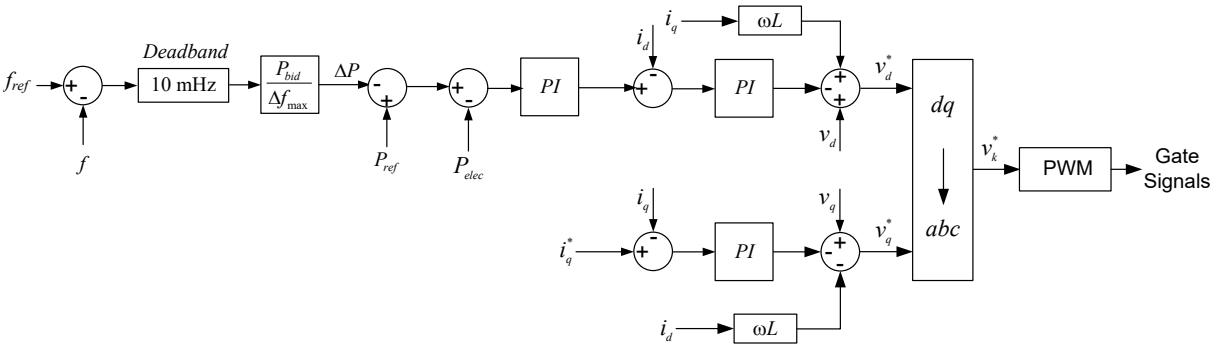

Figure B.5: Implementation of the AC/DC converter controller.

$i_q^* = i_{q1}^*$ or i_{q2}^* or i_{q3}^*, in order to implement a power factor 1 (i.e. $i_{q1}^* = 0$), voltage control (i_{q2}^*) or reactive power control (i_{q3}^*), as illustrated in Figure B.6.

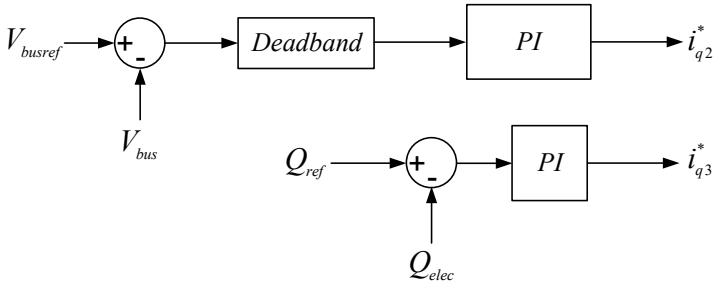

Figure B.6: Definition of i_{q2}^* and i_{q3}^* for the AC/DC converter controller.

B.3 Modular Converter Topology for large Electrolyser Plants

In Chapter 3 (Section 3.2) of this report, a model of a 1-MW electrolyser was presented. This model was scaled up in Chapter 4 (Section 4.2) to represent a 300-MW electrolyser plant. Although the scaled model is sufficiently accurate for the grid studies performed in this report, this model does not reflect the actual configuration of a real electrolyser plant of this size. This appendix considers the development of a model that reflects the actual configuration of an electrolyser plant and compares it to the electrolyser models used for the grid studies as presented in this report.

Currently, the scale of pilot Power-to-Gas projects built to date ranges from 100 kW to 10 MW. The maximum rated capacity of an electrolyser module already available on the market is about 2 MW to 3 MW. In the future, the capacity required for commercial projects will likely be large scale, with capacities in the range of tens to hundreds of MW. Therefore, a modular topology is proposed in order to fulfil the needs of future power system industry. In addition, understanding of the interactions of large-scale electrolysers within power systems can be facilitated with practical models. The challenge is to model the proper topology for accurate modelling of large-scale electrolyser systems. To achieve this purpose, one electrolyser module with the maximum rated power has been implemented in PowerFactory, after which modular topology of electrolyser modules have been formed to represent the real layout of large-scale electrolyser. Figure B.7 shows a possible modular topology design for a 300-MW electrolyser.

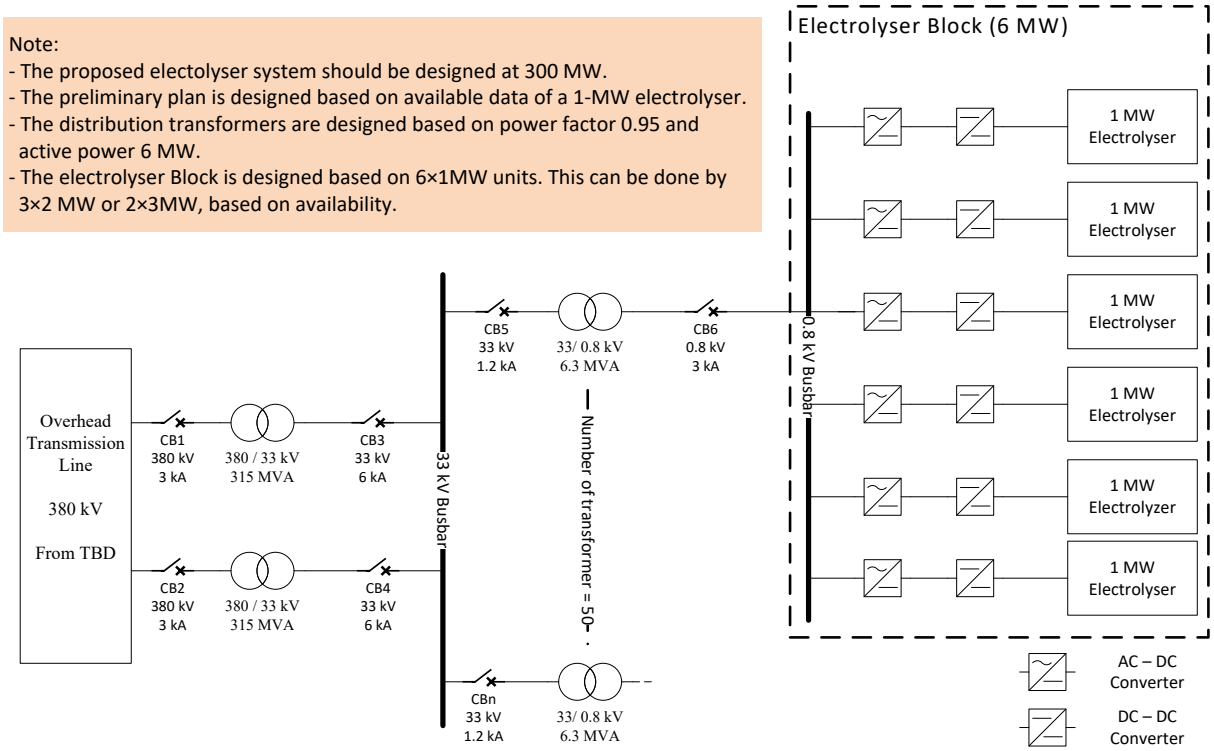

Figure B.7: Modular topology design of a 300-MW electrolyser plant.

To compare the model of the modular-topology electrolyser with the electrolyser model as used in the grid studies in this report, the frequency response after a disturbance is studies with both models. The results are shown in Figure B.8. It can be seen that the frequency response is identical for both models. Figure B.9 shows the response of the electrolyser power consumption after a disturbance. Also here, the response of both models are nearly identical. Similar simulations have been performed for other percentages of electrolyser frequency stability support. Based on these simulations, it can be concluded that the electrolyser model used in the grid studies of this report is sufficiently accurate.

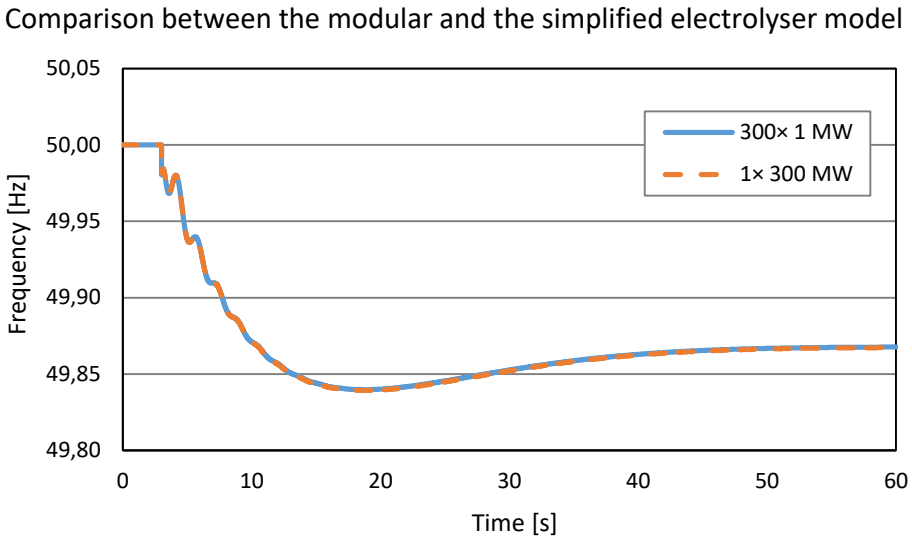

Figure B.8: Comparison of the frequency response of the modular and the simplified electrolyser model.

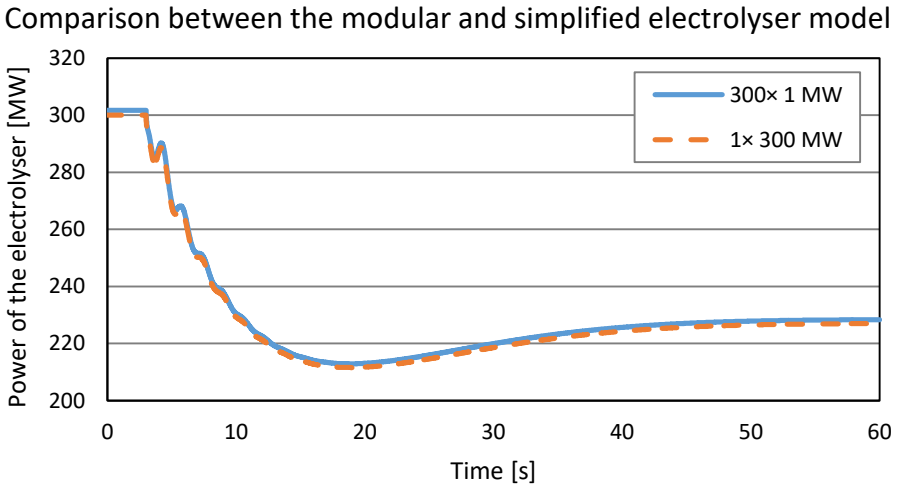

Figure B.9: Comparison of the power consumption of the modular and the simplified electrolyser model.

C Frequency Support by Electrolysers and COBRA in case of Network Splitting

In Chapter 4 (Section 4.4.1) of this report, it was discussed how an electrolyser and COBRAcable can contribute to the frequency stability of the Dutch power system after a disturbance. COBRAcable and the 300-MW electrolyser could potentially contribute as well to frequency stability after more severe disturbances like splitting of the European power system. This situation is studied in this appendix.

In Figure C.1, the transmission network as considered in this study is shown. This network consists of the Northern Netherlands Network (as presented in Section 4.1), the northern part of the German transmission network and the southern part of the Danish transmission network. In the studied case, the electrolyser (located at EOS substation) is operating at 190 MW, while COBRAcable is importing 300 MW into the Netherlands. In the simulations, the network will be split in Germany at the location as indicated in the network diagram. Because splitting of the systems results in an imbalance between generation and demand in the two remaining parts, the system frequency in these remaining parts will start to increase and decrease, respectively. This process is stopped by frequency control of the conventional generators. The 300-MW electrolyser and COBRAcable are equipped with controllers as well, such that these can also provide frequency support in this case.

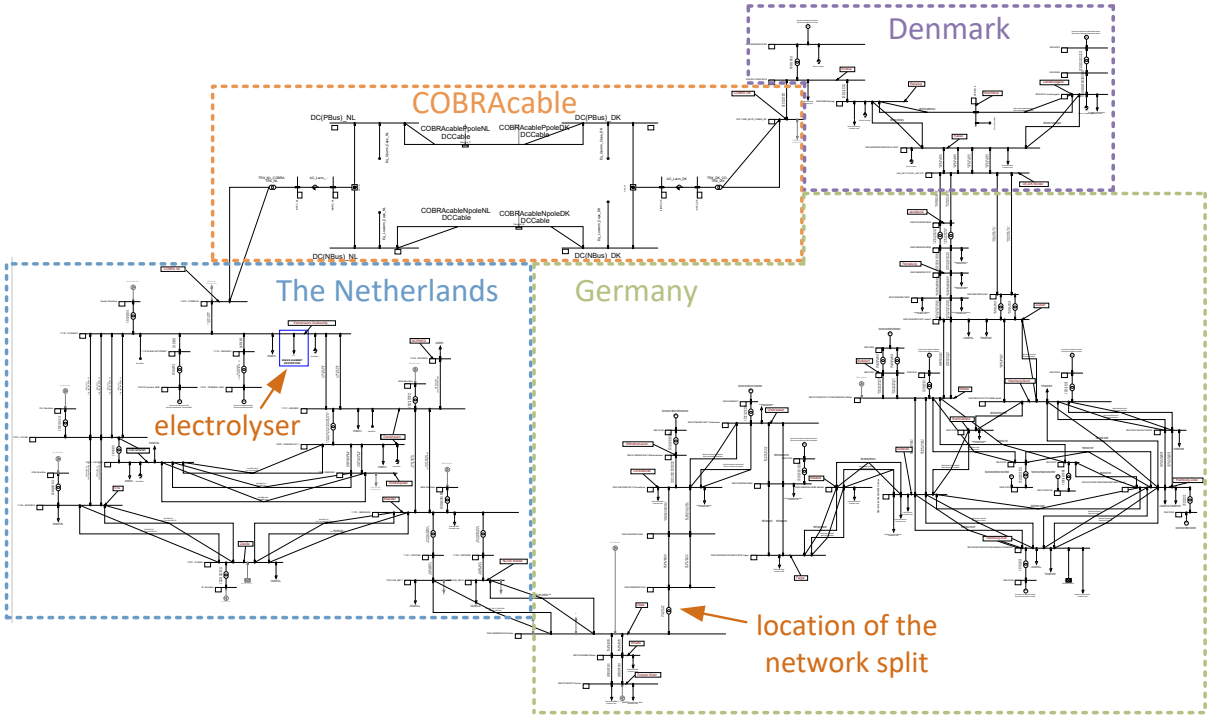

Figure C.1: Network configuration considered in the studies of network splitting.

The results of the simulations are shown in Figure C.2. Initially, the system frequency is exactly 50 Hz. After 10 seconds, the network is split by opening the specific connection in Germany. As there is relatively much generation capacity located in Germany, the frequency of the German/Danish part of the system starts to increase. The graph shows small oscillations in the system frequency in Denmark, which are caused by electromechanical oscillations of the generators.

As the total generation capacity in the Netherlands is much smaller than in Germany in this study, the frequency of the Dutch power system decreases much faster compared to the rate of change in Germany and Denmark. This can be clearly seen in Figure C.2 as well.

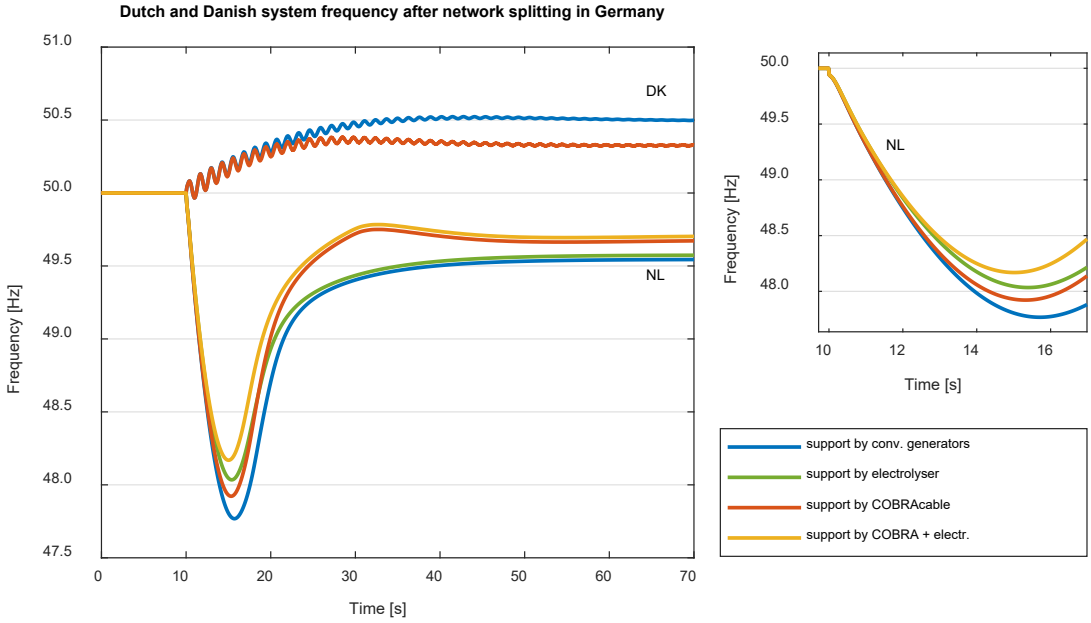

Figure C.2: Frequency response of the Dutch and Danish power systems after splitting of the networks.

In Denmark, COBRAcable can help stabilise the frequency by varying its operational level. As the frequency increases in Denmark, it can increase the power export to the Netherlands to increase the demand in the German/Danish system. Figure C.2 shows that the frequency increases somewhat more slowly in this case, while the steady-state frequency is smaller with support from COBRAcable.

In the Netherlands, COBRAcable and the 300-MW electrolyser can support the frequency stability. Figure C.2 shows the simulations of the four possible scenarios. When studying the graphs, it can be seen that both COBRAcable and the electrolyser have a positive impact on the frequency stability, as the RoCoF (Rate-of-Change-of-Frequency), the frequency nadir (lowest frequency point after a disturbance) and the steady-state frequency improve. While the electrolyser seems to have the highest impact on the RoCoF and frequency nadir, COBRAcable has a higher impact on the steady-state frequency. This difference in steady-state frequency is because COBRAcable can increase its operational level by 300 MW (to 600 MW) in this case, while the electrolyser can only decrease its consumption by 190 MW. The difference in RoCoF and frequency nadir is caused by the fact that the electrolyser has a higher active power ramp rate than COBRAcable in this study. The ramp rate of the electrolyser is 150 MW/s (based on the field measurement as described in Section 3.4), whereas COBRAcable has a ramp rate of 16.66 MW/s (based on the work published in [54]). In the future, the ramp rates of both technologies might increase, such that the impact on frequency stability becomes stronger as well. Obviously, when both COBRAcable and the electrolyser are used for frequency support, this has the highest impact, as Figure C.2 shows.

An overview of the steady-state frequencies of the Dutch power system is given in Table C.1, while the RoCoF and frequency nadirs are shown in Table C.2. Here, the differences between the four possible scenarios are somewhat clearer. Because of its capacity, COBRAcable has the highest impact on the steady-state frequency, while the electrolyser has a higher impact on the RoCoF and frequency nadir because of its fast ramping capability. As mentioned before, this might improve in the future when controllers of both technologies are developed further.

Table C.1: Steady-state frequency in the Dutch power system after splitting of the networks.

Scenario	Steady-state frequency [Hz]	Improvement [mHz]	Improvement [%]
Without support	49.5450	0	0%
Support by electrolyser	49.5746	30	7%
Support by COBRAcable	49.6765	131	29%
Support by COBRA and electrolyser	49.7069	162	36%

Table C.2: Frequency nadir and RoCoF in the Dutch power system after splitting of the networks.

Scenario	Nadir [Hz]	Improvement [mHz]	Improvement [%]	RoCoF [Hz/s]	Improvement [mHz/s]	Improvement [%]
Without support	47.7679	0	0%	0.6987	0	0%
Support by electrolyser	48.0344	267	12%	0.6706	28	4%
Support by COBRAcable	47.9218	154	7%	0.6949	4	1%
Support by COBRA and electrolyser	48.1687	401	18%	0.6670	32	5%

D Power System Stability Support in Sustainable Multi-Energy Systems[1]

This appendix describes a study on the provision of ancillary services by electrolysers in the context of multi-energy systems. The emphasis is put on the participation in active power-frequency control, reactive power-voltage control and the reduction of network congestion. To illustrate the value of demand side response as part of multi-energy sector coupling, a fundamental case study is built upon a three-area test system, which includes conventional and renewable power plants as well as Power-to-Gas (P2G) conversion by electrolysers. Computer-based simulations are performed using PowerFactory to investigate the impact of the response of the electrolysers on power system operation. The results show that positive impact on steady state and dynamic performance can be achieved by contributing to reduce the system stress. The extent of the contribution depends on the location, activation time, rating, and size of demand side response by the electrolyser.

D.1 Description of the Test System

Based on the simple two-area system described in [55], the three-area system displayed in Figure D.1 serves as test network for the proposed study. The modifications include additional generation and demand (in Area 3) connected to the midpoint of the network (i.e. bus 8). The total installed generation capacity in the network is 4600 MVA, divided over four synchronous generators of 900 MVA and two wind parks of 500 MW each. The peak total active load is 3300 MW, from which 300 MW (9%) corresponds to P2G conversion through electrolysers, 900 MW to load L7, 700 MW to L8, and 1400 MW to L9. A peak load scenario (i.e. worst case) is considered, since the impact of disturbances (e.g. generator outages causing power imbalance) on the network can seriously jeopardise the performance of the system. The study cases are intended to show the impact of the size and location of electrolysers on the power flow profile, as well as frequency, voltage and oscillatory stability.

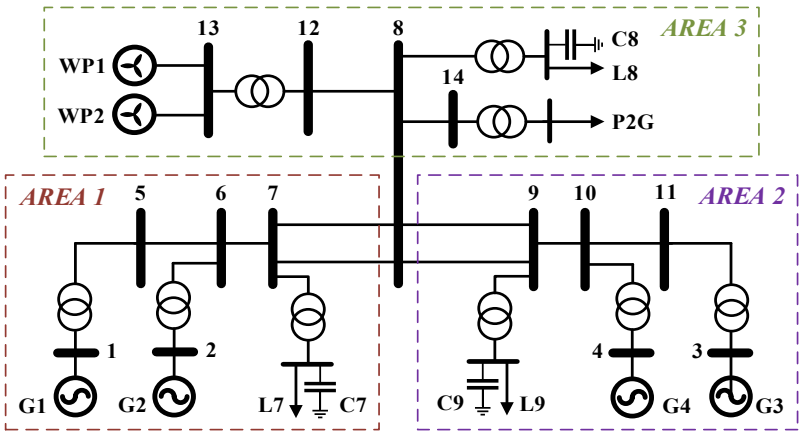

Figure D.1: Three-area six-generator test system.

[1] This appendix is based on the work as published in [53].

The models of the system components were obtained from the (built-in) library models available in DIgSILENT PowerFactory v.15.2.5. In order to concentrate on the impact of P2G, wind generators (Type 4 model) were not considered to participate in the provision of reserves nor in damping control. The electrical representation of the P2G is a controllable load, capable of ramping down (to emulate demand reduction) from a current operating point to a new setpoint within 200 ms, based on [22].

To allow comparison of the results, several dynamic performance indices were calculated. A detailed description of the calculation procedure of each index can be found in [56]. The Power Flow Index (PFI) symbolises the effect on network congestion; the Maximum Frequency Deviation Index (MFDI) describes the deviation of the frequency nadir with respect to the rated frequency (e.g. 50/60 Hz); the Dynamic Voltage Index (DVI) analyses the maximum voltage deviation during transients; the Quasi-Stationary Voltage Index (QSVI) compares the steady state voltage value after a disturbance to the admissible range; and the Angle Index (AI) measures maximum generator rotor angle deviations to give an indication of the ability of the system to remain synchronised after a disturbance. The indexes are normalised between 1 (i.e. system instability/collapse) and 0 (i.e. negligible effects). The admissible (limit) performance values (e.g. frequency deviation) needed to normalise the indices depend on national grid codes (taken from [56] for this study).

D.2 Results of the Analysis

D.2.1 Effects on Power Flow profiles

For a sudden loss of 400 MW of wind power generation, Figure D.2 exhibits the performance of the system for different demand reductions, occurring at equal activation time (i.e. 220 ms after the disturbance). As can be seen, the reduction of power demand during highly loaded (peak) hours results in favourable effects for steady state operation. Overall voltage profiles improve (especially local voltages), and congestion through transmission branches and power losses are reduced. The PFI indicator, computed for lines above 60% loading level, shows a close-to-linear decrease as the amount of load is reduced. Nevertheless, it is worth clarifying that depending on the location of the electrolyser, the effect of the system performance can be different, as discussed in the next sections.

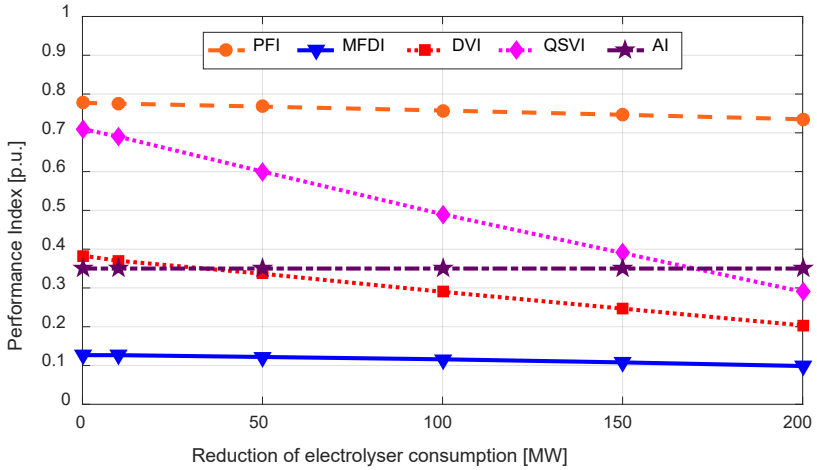

Figure D.2: Performance of the test system for a loss of generation of 400 MW.

D.2.2 Effects on Frequency Stability

As indicated in [22], participation of electrolysers in FCR provision can be faster than the reaction and activation times of governors in conventional generators. Activating the load reduction shortly after the disturbance helps to reduce the frequency nadir, as perceived in Figure D.3. Both the size and the location of the electrolyser hold capital importance in the results. Decreasing consumption by larger amounts accentuates the improvement. Regarding the location, buses closer to the source of the disturbance that induce limited stress in the surrounding power lines (i.e. reduced inter-area power transfers) lead to better results. Notice that when the electrolyser is located in buses 7 or 8, a small amount of curtailment (<10 MW) shows insignificant effects, whereas if it is located in other buses, like 9 or 10, a significant load reduction (>100 MW or 150 MW) is needed to prevent system collapse. The latter is because those locations cause more stress in the system. Note also that location at bus 10 entails better frequency nadir w.r.t. location at bus 9, which is due to the closer location to generators in Area 2.

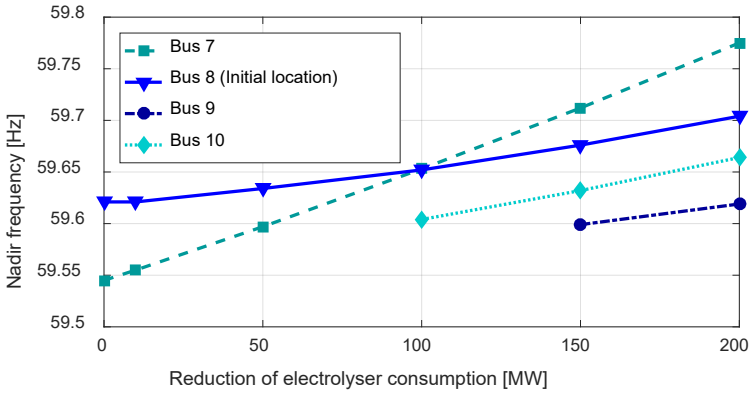

Figure D.3: Frequency nadir for different electrolyser locations.

D.2.3 Effects on Voltage Stability

As shown in Figure D.2, the slope of the QSVI and DVI indicators provide useful insight into the dynamic voltage performance of the system. Note that a larger electrolyser consumption reduction translates into greater contribution to improving the post-disturbance voltage. During the transient stage, there is also a positive effect (i.e. smaller DVI), but this impact is less pronounced than in steady state. This effect is associated to the fact that the reduction of the power consumption of the electrolysers helps to reduce the active and reactive power transfer through the long transmission lines of the system, which improves the voltage. This observation deserves further investigation to consider possible addition of reactive power control features to the rectifier of the electrolyser.

D.2.4 Effects on Oscillatory Stability

The angle index (AI) was found to be sensitive to the electrolyser location, similar to the previously discussed indices. From Figure D.4, it can be seen that lower overall demand at the bus to which the electrolyser is connected improves the AI. Location at bus 7 entails better performance w.r.t. bus 8, because the reduction of electrolyser demand induces less stress on the system. The interplay between electrolyser activation time and the FCR controls of the synchronous generators is shown in Figure D.5. As observed, the AI improves with faster activation times and thus, a fast activation

combined with a larger proportion of demand reduction (in comparison to the size of the generation lost) lessens the risk of losing synchronism. For a fixed location, AI's sensitivity to delay in activating the electrolyser was only significant for up to 2 seconds. Longer delays did not show any significant improvement. This observation deserves further investigation to consider possible addition of damping control features to the rectifier of the electrolyser.

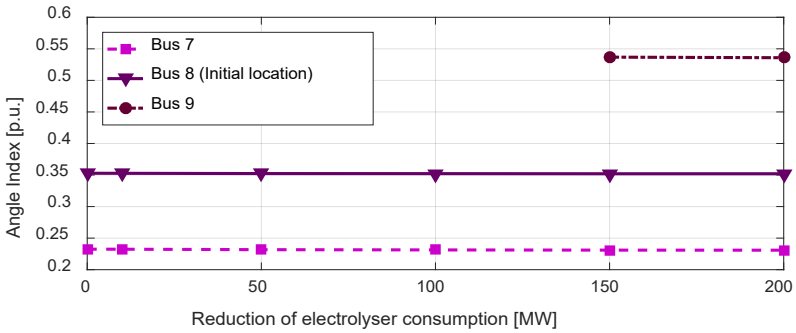

Figure D.4: Angle Index (AI) for different electrolyser locations.

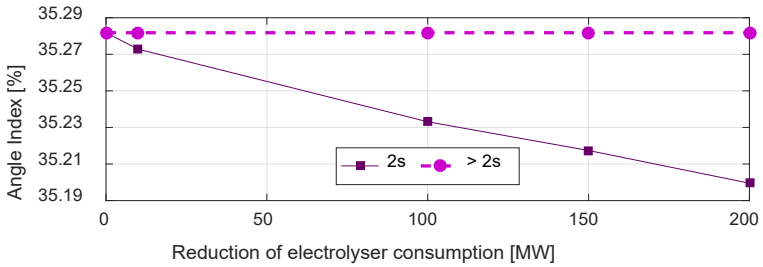

Figure D.5: Angle Index (AI) for different activation times at initial location.

D.3 Conclusions

The fundamental study, based on a three-area system, showed that the reduction of power system stress through electrolyser demand response can enhance the steady state and dynamic performance (e.g. frequency nadir, voltage profiles, rotor angle stability) of a power system. The extent of the contribution depends on the rating, location and activation time of the electrolysers. For installed capacity in the order of hundreds of MWs, locations in the grid that produce the most relief on system congestion and fast activation times, the best results were obtained.

The main limitation of the test system as presented in this appendix lies in the lack of a detailed model of the electrolyser's rectifier and associated controllers. Although the presented trends are valid, the extent of the results is expected to vary with the inclusion of a complex controller able to change electrolyser variables (e.g. amount of load reduction, ramping times, activation times) based on inputs such as system frequency (or other signals from the network).

References

[1] TSO2020 Consortium, “TSO2020 Grant Agreement,” TSO2020 Consortium, July 2014.

[2] V. Garcia Suarez, J. Rueda Torres, B.W. Tuinema, A. Perilla Guerra, and M. van der Meijden, "Integration of Power-to-Gas Conversion into Dutch Electrical Ancillary Services Markets," presented at *ENERDAY 2018*, Dresden, Germany, 2018.

[3] V. García Suárez, “Exploitation of Power-to-Gas for Ancillary Services Provision,” MSc. dissertation, Delft University of Technology, Delft, the Netherlands, August 2018. Available online at: repository.tudelft.nl

[4] ENTSO-E, “Survey on Ancillary Services Procurement, Balancing Market Design 2016,” Mar. 2017. [Online]. Available: https://www.entsoe.eu/Documents/Publications/Market%20Committee%20publications/WGAS_Survey_final_10.03.2017.pdf

[5] P. Kundur et al., “Definition and classification of power system stability IEEE/CIGRE joint task force on stability terms and definitions,” in *IEEE Transactions on Power Systems*, vol. 19, no. 3, pp. 1387-1401, Aug. 2004.

[6] J. Beerten et al., “Modeling and control of HVDC grids: a key challenge for the future power system,” in *proc. of Power System Computation Conference (PSCC’14)*, Wroclaw, Poland, 2014.

[7] ENTSO-E, “Consultation on the design of the platform for automatic Frequency Restoration Reserve (aFRR) of PICASSO region,” Nov. 2017.

[8] TenneT TSO B.V., “Market Review 2016 – Electricity Market Insights,” Arnhem, the Netherlands, Mar. 2017. [Online]. Available: https://www.tennet.eu/fileadmin/user_upload/Company/ Publications/Technical_Publications/Dutch/2016_Market_Review_TenneT.pdf

[9] ENTSO-E, “Proposal for the Establishment of Common and Harmonised Rules and Processes for the Exchange and Procurement of Frequency Containment Reserve,” Jan 2018. [Online]. Available: https://consultations.entsoe.eu/markets/draft-proposal-for-fcr-cooperation-market-design/supporting_documents/FCR%20Draft%20Proposal.pdf

[10] Regelleistung.net, “Internetplattform zur Vergabe von Relleistung,” 2019. [Online]. Available: https://www.regelleistung.net

[11] TenneT TSO B.V., “Productspecificatie FCR,” November 2015. [Online]. Available: https://www.tennet.eu/fileadmin/user_upload/Bijlage_B_-_Productspecifications_FCR_ENG.pdf

[12] ENTSO-E, “Consultation Report: FCR Cooperation,” May 2017. [Online]. Available: https://www.entsoe.eu/Documents/Consultations/20170601_FCR_Consultation_Report.pdf

[13] K. Smethurst, S. Williams, and V. Walsh, “Testing Guidance for Providers of Enhanced Frequency Response Balancing Service,” National Grid, March 2017. [Online]. Available: https://www.nationalgrid.com/sites/default/files/documents/EFR%20Testing%20Guidance%20VD3%20%28Final%29.pdf

[14] EirGrid, “Consultation on DS3 System Services Volume Capped Competitive Procurement,” March 2018. [Online]. Available: http://www.eirgridgroup.com/site-files/library/EirGrid/Consultation-on-DS3-System-Services-Volume-Capped-Competitive-Procurement.pdf

[15] TenneT TSO B.V., “Regel- en Noodvermogen per 1 januari 2018,” October 2017. [Online]. Available: https://www.tennet.eu/fileadmin/user_upload/Company/News/Dutch/2017/Notitie_FRR_2018_V1.0.pdf

[16] TenneT TSO B.V., “Productinformation aFRR (Regulating power),” January 2018. [Online]. Available: https://www.tennet.eu/fileadmin/user_upload/Company/Publications/ Technical_ Publications/Dutch/Product_information_aFRR_-regulating_power-_16-01-2018.pdf

[17] EXPLORE (TenneT, ELIA, 50hertz, APG, Amprion, Transnet BW), “Target Model for Exchange of Frequency Restoration Reserves,” October 2016. [Online]. Available: https://www.tennet.eu/ fileadmin/user_upload/Company/Publications/Technical_Publications/Dutch/20161021_EXPL ORE_FRR_TARGET_MODEL.PDF

[18] ENTSO-E, “Imbalance Netting,” 2018. [Online]. Available: https://www.entsoe.eu/major-projects/network-code-implementation/electricity-balancing/igcc/Pages/default.aspx

[19] 50Hertz Transmission GmbH, Amprion GmbH, Elia System Operator NV, TenneT TSO B.V., TenneT TSO GmbH, TransnetBW GmbH, “Potential Cross-Border Balancing Cooperation between the Belgian, Dutch and German Electricity Transmission System Operators,” Technical Report, October 2014. [Online]. Available: http://www.elia.be/~/media/files/Elia/users-group/ 141008_Final_report.pdf

[20] A. Kakorin, L. Laurisch and G. Papaefthymiou, “FLOW Dynamic Power Management, WP2.2: Market Interaction,” Report WIENL14568, ECOFIS Netherlands B.V., Utrecht, the Netherlands, December 2014.

[21] TenneT TSO B.V., “Market Review 2017 – Electricity Market Insights,” TenneT TSO B.V., Arnhem, the Netherlands, March 2018. [Online]. Available: https://www.tennet.eu/fileadmin/ user_upload/Company/Publications/Technical_Publications/Dutch/2017_TenneT_Market_Rev iew.pdf

[22] J. Eichmann, K. Harrison and M. Peters, “Novel Electrolyser Applications: Providing More Than Just Hydrogen,” Technical Report NREL/TP-5400-61758, National Renewable Energy Laboratory, Denver CO, USA , September 2014.

[23] V. Ruuskanen, J. Koponen, K. Huoman, A. Kosonen, M. Niemelä, and Ahola, “PEM water electrolyzer model for a power-hardware-in-loop simulator,” *International Journal of Hydrogen Energy*, vol. 42, no.16, pp.10775-10784, 2017.

[24] P.K.S. Ayivor, “Feasibility of Demand Side Response from Electrolysers to support Power System Stability,” MSc. dissertation, Delft University of Technology, Delft, the Netherlands, July 2018. Available online at: repository.tudelft.nl

[25] P. Ayivor, J. Torres, M.A.M.M. van der Meijden, R. van der Pluijm, and B. Stouwie, “Modelling of Large Size Electrolyzer for Electrical Grid Stability Studies in Real Time Digital Simulation,” in *Proc. of Energynautics 3rd International Hybrid Power Systems Workshop*, Tenerife, Spain, May 2018.

[26] P. Ayivor, J.L. Rueda Torres, and M.A.M.M. van der Meijden, “Modelling of Large Size Electrolyser for Electrical Grid Stability Studies - A Hierarchical Control,” in *Proc. 17th Wind Integration Workshop, Stockholm*, Sweden, 17-19 October 2018.

[27] R. Harvey, R. Abouatallah, and J. Cargnelli, “Large-scale water electrolysis for power-to-gas,” in *PEM Electrolysis for Hydrogen Production: Principles and Applications*, 2016, pp. 303-313.

[28] T. Smolinka, E.T. Ojong, and T. Lickert, “Fundamentals of PEM water electrolysis,” in *PEM Electrolysis for Hydrogen Production: Principles and Applications*, pp.11-33, 2016.

[29] F. da Costa Lopes, and E.H. Watanabe, “Experimental and theoretical development of a PEM electrolyzer model applied to energy storage systems,” in proc. of *Power Electronics Conference* 2009 (COBEP'09), pp. 775-782, 2009.

[30] O. Schmidt et al., “Future cost and performance of water electrolysis: An expert elicitation study,” in *International Journal of Hydrogen Energy*, vol. 42, no. 52, pp. 30470-30492, Nov. 2017.

[31] S. Karim, Teshmont Consultants, “Transformer Modeling Guide,” (revision), AESO: Alberta Electric System Operator, Canada, 2014.

[32] M. Mohanpurkar, Y. Luo, D. Terlip, F. Dias, K. Harrison, J. Eichman, R. Hovsapian, and J. Kurtz, “Electrolyzers enhancing flexibility in electric grids,” *MDPI - Energies*, vol. 10, no. 11, pp. 1836, November 2017.

[33] J.J. Grainger and W.D. Stevenson*, Power system analysis*. McGraw-Hill New York, 1994, vol. 621.

[34] B.W. Tuinema, M.E. Adabi, P.K.S. Ayivor, V. García Suárez, J.L. Rueda Torres, M.A.M.M. van der Meijden, and P. Palensky, “TSO2020 – Electrolyser Measurements Veendam-Zuidwending,” TSO2020 internal report, Delft University of Technology, Delft, the Netherlands, March 2019.

[35] TenneT TSO B.V., “Kwaliteits- en Capaciteitsdocument 2017 (KCD2017),” TenneT TSO B.V., Arnhem, the Netherlands, 2017. [Online]. Avalaible: https://www.tennet.eu/fileadmin/user_upload/Company/Publications/Technical_Publications/Dutch/TenneT_KCD2017_Deel_I_web.pdf

[36] TenneT TSO B.V., “FCR Manual for BSPs – Requirements and Procedures for Supply of FCR,” TenneT TSO B.V., Arnhem, the Netherlands, November 2018.

[37] NationalGird, “Historic frequency data for Great Britain at a second resolution,” NationalGrid, 2019. [Online]. Available: https://www.nationalgrideso.com/balancing-services/frequency-response services/historic-frequency-data

[38] N. Veera Kumar, “Real-time Simulation based Analysis of Fast Active Power Regulation Strategies to enhance Frequency Support from PE interfaced Multi-Energy Systems,” MSc. dissertation, Delft University of Technology, Delft, the Netherlands, August 2019. Available online at: repository.tudelft.nl

[39] S. Curtin and J. Gangi, “Fuel Cell Technologies Market Report 2016,” Fuel Cell and Hydrogen Energy Association, Washington, D.C., DOE/EE-1672, October 2017.

[40] A. Alaswad et al., “Fuel Cell Technologies, Applications, and State of the Art. A Reference Guide,” in *Reference Module in Materials Science and Materials Engineering, Elsevier*, 2016.

[41] S. Barrett. (2017). *Dutch partners deliver first 2 MW PEM fuel cell plant in China* [Online]. Available: http://www.renewableenergyfocus.com/view/45502/dutch-partners-deliver-first-2-mw-pem-fuel-cell-plant-in-china/

[42] POWER Magazine (2014). *59-MW Fuel Cell Park Opening Heralds Robust Global Technology Future* [Online]. Available: http://www.powermag.com/59-mw-fuel-cell-park-opening-heralds-robust-global-technology-future/

[43] S. Mekhilef, R. Saidur, and A. Safari, “Comparative study of different fuel cell technologies,” in *Renewable and Sustainable Energy Reviews*, vol. 16, no. 1, pp. 981-989, January 2012.

[44] S.J. Peighambardoust, S. Rowshanzamir, and M. Amjadi, “Review of the proton exchange membranes for fuel cell applications,” in *International Journal of Hydrogen Energy*, vol. 35, no. 17, pp. 9349-9384, Sep. 2010.

[45] V. Das et al., “Recent advances and challenges of fuel cell based power system architectures and control – A review,” in *Renewable and Sustainable Energy Reviews*, vol. 73, pp. 10-18, Jan. 2017.

[46] P.C. Ghosh, “High platinum cost: obstacle or blessing for commercialization of low-temperature fuel cell technologies,” in *Clean Technologies and Environmental Policy*, vol. 19, no. 2, pp. 595-601, March 2017.

[47] S. Curtin and J. Gangi, “State of the States: Fuel Cells in America 2016,” Fuel Cell Technologies Office, U.S. Department of Energy, November 2016.

[48] S. Morozumi, “Micro-grid Demonstration Projects in Japan,” *2007 Power Conversion Conference - Nagoya*, Nagoya, 2007, pp. 635-642.

[49] K. Nikiforow et al., “Power ramp rate capabilities of a 5 kW proton exchange membrane fuel cell system with discrete ejector control,” in *Journal of Power Sources*, vol. 381, pp. 30-37, March 2018.

[50] F.A. Alshehri, J.L. Rueda Torres, A. Perilla Guerra, and M.A.M.M. van der Meijden, “Generic Model of PEM Fuel Cells and Performance Analysis in Frequency Containment Period in Systems with Decreased Inertia,” in *Proc. of 28th IEEE International Symposium on Industrial Electronics*, Vancouver, Canada, 12-14 June 2019.

[51] F.A. Alshehri, “Ancillary Services from Hydrogen Based Technologies to Support Power System Frequency Stability,” MSc. dissertation, Delft University of Technology, Delft, the Netherlands, September 2018. Available online at: repository.tudelft.nl

[52] TenneT TSO B.V., “Samenvatting KCD 2017,” Arnhem, the Netherlands, 2017. [Online]. Available: https://www.tennet.eu/fileadmin/user_upload/Company/Publications/Technical_Publications/Dutch/TenneT_KCD2017_samenvatting.pdf

[53] V. Suárez, P. Ayivor, J. Torres, and M.A.M.M. van der Meijden, “Demand Side Response in Multi-Energy Sustainable Systems to Support Power System Stability,” presented at *16th Wind Integration Workshop*, Berlin, Germany, 2017.

[54] A. Perilla, J.L. Rueda Torres, M.A.M.M. van der Meijden, A. Alefragkis, and A.M. Lindefelt, “Analysis of a power factor regulation strategy for an embedded point-to-point MMC-HVDC system,” in *2018 IEEE International Energy Conference (ENERGYCON)*, Limassol, 2018, pp. 1-6.

[55] P. Kundur, *Power System Stability and Control*, McGraw-Hill, 1994.

[56] G. Schweickardt and J.M. Gimenez, “On-Line Security Assessment of a Micro-Grid Using Fuzzy Logic and Distributed Processing", 2013. [Online]. Available: http://revistas.unal.edu.co/index.php/dyna/article/view/31568/45907

Project-related Publications

journal	conference	presentation	thesis	report	
	X				V. García, P. Ayivor, J.L. Rueda, and M.A.M.M. van der Meijden, "Demand Side Response in Multi-Energy Sustainable Systems to Support Power System Stability," in *Proc. of 16th Wind Integration Workshop*, Berlin, Germany, October 2017.
	X				V. García, J.L. Rueda, B. Tuinema, A. Perilla, and M.A.M.M van der Meijden, "Integration of Power-to-Gas Conversion into Dutch Electrical Ancillary Services Markets," in *Proc. of ENERDAY 2018 – 12th Conference on Energy Economics and Technology*, Dresden, Germany, April 2018.
	X				P. Ayivor, J. Torres, M.A.M.M. van der Meijden, R. van der Pluijm, and B. Stouwie, "Modelling of Large Size Electrolyzer for Electrical Grid Stability Studies in Real Time Digital Simulation," in *Proc. of Energynautics 3rd International Hybrid Power Systems Workshop*, Tenerife, Spain, May 2018.
				X	L. Liu, "TSO2020-Activity 2: Modelling and Testing of Northern Netherlands Network in RTDS," TSO2020 internal report, Delft University of Technology, Delft, the Netherlands, June 2018.
			X		P.K.S. Ayivor, "Feasibility of Demand Side Response from Electrolysers to support Power System Stability," MSc. dissertation, Delft University of Technology, Delft, the Netherlands, July 2018. Available online at: repository.tudelft.nl
			X		V. García Suárez, "Exploitation of Power-to-Gas for Ancillary Services Provision," MSc. dissertation, Delft University of Technology, Delft, the Netherlands, August 2018. Available online at: repository.tudelft.nl
			X		F.A. Alshehri, "Ancillary Services from Hydrogen Based Technologies to Support Power System Frequency Stability," MSc. dissertation, Delft University of Technology, Delft, the Netherlands, September 2018. Available online at: repository.tudelft.nl
		X			J.L. Rueda Torres, "Control of large size electrolysers to support the stability electrical transmission systems," presentation, *2nd International Workshop DynPOWER Dynamic Stability Challenges of the Future Power Grids*, Winterthur, Switzerland, 17 September 2018
		X			P. Ayivor, J.L. Rueda Torres, and M.A.M.M. van der Meijden, "Modelling and Control of Large Size Electrolyzer for Electrical Grid Stability Studies in Real Time Digital Simulation," presentation, *2018 RTDS European User's Group Meeting*, Genk, 10-11 October 2018.
	X				P. Ayivor, J.L. Rueda Torres, and M.A.M.M. van der Meijden, "Modelling of Large Size Electrolyser for Electrical Grid Stability Studies - A Hierarchical Control," in *Proc. 17th Wind Integration Workshop,* Stockholm, Sweden, 17-19 October 2018.
				X	J.L. Rueda Torres, V. García Suárez, B.W. Tuinema, and M.E. Adabi, "TSO2020 Project – N3 Grid 2030/2040 – Technical Resilience Assessment," TSO2020 internal report, Delft University of Technology, Delft, the Netherlands, December 2018.

				X	B.W. Tuinema, M.E. Adabi, P.K.S. Ayivor, V. García Suárez, J.L. Rueda Torres, M.A.M.M. van der Meijden, and P. Palensky, "TSO2020 – Electrolyser Measurements Veendam-Zuidwending," TSO2020 internal report, Delft University of Technology, Delft, the Netherlands, March 2019.
		X			J.L. Rueda Torres, "Power to Gas – TSO2020 Activity 2," presentation, *Sustainable Energy Continues @TU DELFT,* Delft University of Technology, 22 May 2019.
	X				F.A. Alshehri, J.L. Rueda Torres, A. Perilla Guerra, and M.A.M.M. van der Meijden, "Generic Model of PEM Fuel Cells and Performance Analysis in Frequency Containment Period in Systems with Decreased Inertia," in *Proc. of 28th IEEE International Symposium on Industrial Electronics (ISIE19)*, Vancouver, Canada, 12-14 June 2019.
	X				B.W. Tuinema, P.K.S Ayivor, V. García Suárez, M.E. Adabi, L. Liu, J.L. Rueda Torres, and M.A.M.M. van der Meijden, "Exploitation of Power-to-Gas for Ancillary Services Provision in the Netherlands," in *Proc. of Cigré Symposium 2019*, Aalborg, Denmark, June 2019.
X					B.W. Tuinema, M.E. Adabi, P.K.S. Ayivor, V. García Suárez, L. Liu, A. Perilla, J.L. Rueda Torres, M.A.M.M. van der Meijden, and P. Palensky, "Development of an Electrolyser Model for Real-Time Simulation and Analysis of the Impact on Power System Stability," *submitted to IET Generation, Transmission & Distribution.*
X					F. Alshehri, V. García and J.L. Rueda, "Provision of Ancillary Services with PEM Hydrogen Technologies in Future Multi-Energy Sustainable Power Systems" Elsevier Heliyon, Vol. 5 no. 4, April 2019.
			X		N. Veera Kumar, "Real-time Simulation based Analysis of Fast Active Power Regulation Strategies to enhance Frequency Support from PE interfaced Multi-Energy Systems," MSc. dissertation, Delft University of Technology, Delft, the Netherlands, August 2019. Available online at: repository.tudelft.nl